Copyright is owned by the Author of the thesis. Permission is given for a copy to be downloaded by an individual for the purpose of research and private study only. The thesis may not be reproduced elsewhere without the permission of the Author.

A study on the physicochemical properties of defatted New Zealand green-lipped mussel protein concentrates (MPC) dispersions

A thesis presented in partial fulfilment of the requirements for the degree of Master of Food Technology

Massey University, Auckland, New Zealand.

Jingying Lin

2024

Abstract

This thesis investigated changes of physicochemical properties of mussel protein concentrates (MPC) dispersions at different pH affected by ultrasound treatment and the viscoelastic properties of heat-induced MPC gels with varying concentrations of different starches.

The first study evaluated the effect of pH (3,5,7,9) and ultrasound treatment (15 min) on the physicochemical and functional properties of desalted MPC, including particle size, solubility, zeta potential, emulsification, and gelation. Compared with control groups, it was found that the particle size of all samples at all pH decreased greatly after ultrasound treatment, as reflected in a 7~17 times reduction in D [3,2] and a 3~8 times reduction in D [4,3]. Ultrasound treatment also improved absolute values of zeta potential and made MPC dispersions more stable. In addition, ultrasound treatment increased the solubility of MPC dispersions at all pH values. The most significant increase in solubility was observed for samples at pH 3, from ~1.2% to ~57.4%; followed by pH 7 and pH 9 samples, from ~1% to ~20.8% and ~2% to ~18.7%, respectively; pH 5 showed the smallest change, from ~0.5% to ~0.8%, which was because it closed to the isoelectric point of MPC (pI~4.55). SDS-PAGE results showed that MPC composed of actin (43-46 kDa) and paramyosin (98–107 kDa), ultrasound treatment and pH changes did not result in significant changes in the mussel protein bands. All untreated and sonicated MPC samples were observed to form interconnection dense and fine gel network structures under confocal laser scanning microscopy (CLSM) after heat treatment, untreated MPC gels at pH 3 and pH 9 showed dense network structures compared to other gels. Also, ultrasound treatment led to finer and more homogeneous gel network structures. Microstructure images and rheological measurements of emulsions revealed that emulsions stabilized by sonicated MPC at pH 3 had the smallest oil droplet size with D [3,2] ~6.5 μm and D [4,3] ~12.7 μm, respectively. The gel strength (G'(1 Hz)) of pH 3 emulsion was the highest and reached ~502.3 Pa. Emulsion stabilized by sonicated MPC at pH 5 had the lowest G'(1 Hz) at ~107.9 Pa, the oil droplet was the greatest among all emulsions with D [3,2] ~20.4 μm and D [4,3] ~66.9 μm, respectively. This could be attributed to MPC dispersion at pH 5 having the lowest solubility and the greatest particle size. For heat induced MPC gels, ultrasound treatment declined the gel strength at all

pH values; gels without ultrasound treatment at pH 9 and pH 3 had the highest G'. The study may provide useful information for MPC applications in the food field.

The second study examined the viscoelastic properties of heat-induced defatted mussel protein gels with varying concentrations (0%, 2.5%, 5%, 10% w/w) of native rice starch (NRS), waxy rice starch (WRS), waxy corn starch (WCS), and waxy potato starch (WPS). CLSM images showed that a 10 w/w % mussel protein concentrate (MPC) sample cannot form a gel after heating at 90 ℃ for 30 min. When 5% starch was added to MPC samples, dense gel network structures were observed after heating, suggesting a crucial role of starch in MPC gelation. Rheological measurements indicated that starch addition can increase the strength of MPC gels. Both G' and G'' raised significantly in the protein-starch system when the starch concentration increased. Compared to the control (10% MPC without starch), in the presence of 10% starches, the G' of MPC-NRS, MPC-WRS, MPC-WCS, MPC-WPS gels increased ~120, ~32, ~50, ~185 times, respectively. MPC-WPS gel appeared the highest G' among all MPC-starch gels with a 10% starch addition. In the protein-starch system, the combination of MPC and starch resulted in a stronger gel, showing a greater effect than the sum of MPC and starch separately. Additionally, the pasting temperature of starch in the protein-starch system was higher compared to when it was in water.

Acknowledgement

Firstly, I would like to extend my heartfelt gratitude to my two supervisors, Dr. Zhi Yang and Dr. Hong (Sabrina) Tian, for their immense support throughout this year. Their invaluable suggestions and guidance have been crucial to my experimental process and thesis development. Without their assistance, completing my master's study on time would not have been possible.

Dr. Yang has been instrumental in teaching me hands-on experimental techniques, sharing numerous valuable papers, and providing insightful advice that has significantly enhanced my professional knowledge and practical skills.

Dr. Tian has meticulously helped refine the direction of my thesis and provided detailed feedback on my paper. I am especially grateful to Dr. Tian for her exceptional contribution to initiating this research concept and her invaluable engagement with the industry, which facilitated the provision of essential research materials.

Secondly, I would like to extend my deepest thanks to laboratory technicians Arthur Xu and Rachel Liu. Their patience, prompt responses, and assistance with booking and purchasing experimental materials have been invaluable. My experiment would not have gone so well without their help.

Finally, I would like to acknowledge my friends Jim, Sofea and Imman. Their persistent support and encouragement have been essential in lifting my spirits during times of difficulty.

Table of contents

Abstract I
Acknowledgement III
List of tables VII
List of figures VIII
List of abbreviations X
1. Chapter 1: Introduction 1
1.1. Overview of the research 1
1.2. Research objectives 3
1.3. Thesis structure 3
2. Chapter 2: Literature Review 5
2.1. Introduction of mussel 5
2.2. Chemical composition of mussel 7
2.2.1. Proteins 7
2.2.2. Lipids 9
2.2.3. Carbohydrates 10
2.3. Application of mussels in the food industry 10
2.4. Physical, chemical, and biochemical modifications of proteins 14
2.4.1. Ultrasound treatment 14
2.4.2. High pressure homogenization (HPH) 18
2.4.3. Ball milling treatment 18
2.4.4. pH 19
2.4.5. Enzymatic hydrolysis 22
2.4.6. TGase cross-linking 22
2.5. Physicochemical and functional characteristics of proteins 22
2.5.1. Particle size 23
2.5.2. Zeta potential 27
2.5.3. Solubility 31
2.5.4. Gelation 35

2.5.5. Emulsifying properties 46

3. Chapter 3: Effect of ultrasound treatment on desalted mussel protein concentrates (MPC): physicochemical and functional properties at different pH values 52

3.1. Introduction 53

3.2. Materials and methods 54

3.2.1. Materials 54

3.2.2. Preparation of mussel protein concentrates (MPC) 55

3.2.3. Ultrasound treatment of MPC dispersion 57

3.2.4. Determination of particle size distribution (PSD) and zeta potential 58

3.2.5. Determination of solubility 59

3.2.6. Sodium dodecyl sulphate polyacrylamide gel electrophoresis (SDS-PAGE) 59

3.2.7. Rheological measurements of heat-induced MPC gelation 60

3.2.8. Microstructure observation by using Confocal Laser Scanning Microscopy (CLSM) 61

3.2.9. Preparation of O/W emulsions stabilized by sonicated MPC 61

3.2.10. Determination of oil droplet size of the emulsions 62

3.2.11. Microstructure 62

3.2.12. Flowability of emulsions 62

3.2.13. Rheological properties of emulsions 63

3.2.14. Statistical analysis 63

3.3. Results and discussions 64

3.3.1. The influence of ultrasonication and pH on MPC particle size, zeta potential and solubility 64

3.3.2. SDS-PAGE 69

3.3.3. Viscoelastic properties of heat-induced gelation 70

3.3.4. CLSM 74

3.3.5. Effect of pH on oil droplet size and microstructure of sonicated MPC stabilized emulsions 76

3.3.6. Effect of pH on Rheological properties and viscosity of sonicated MPC stabilized emulsions 79

3.4. Conclusion 84

4. Chapter 4: Effect of incorporation of various starches on rheological and microstructural properties of heat-induced mussel protein concentrates gels 85
4.1. Introduction 86
4.2. Materials and methods 89
4.2.1. Materials 89
4.2.2. Sample preparation 89
4.2.3. Rheological measurements 90
4.2.4. Confocal laser scanning microscopy (CLSM) 91
4.2.5. Statistical analysis 91
4.3. Results and discussions 91
4.3.1. Gelation temperature and viscosity 91
4.3.2. Viscoelastic properties 97
4.3.3. Microstructures of MPC-starch mixture as revealed by CLSM 107
4.4. Conclusion 110
5. Chapter 5. Conclusion and future work 111
6. References 114
7. Appendices 129

List of tables

Table 1: Chemical composition (%) of mussels based on dry matter. 7

Table 2: Amino acid profile of mussel powder and fish powder. 9

Table 3: Application of mussels in food fields. 12

Table 4: Effects of ultrasound treatment on seafood proteins. 16

Table 5: The effect of pH on seafood proteins. 21

Table 6: The effect of ultrasound treatment on particle size of seafood protein dispersions 25

Table 7: The relation between zeta potential value and system stability (Cano-Sarmiento et al., 2018). 27

Table 8: The effect of ultrasound treatment on the absolute value of zeta potential of seafood protein dispersions. 29

Table 9: The effect of ultrasound treatment on the solubility of seafood protein dispersions 33

Table 10: Preparation methods of protein gels (K. Liu et al., 2021) 36

Table 11: The effect of ultrasound treatment on the gelling properties of seafood proteins 40

Table 12: The effect of adding starch on the gelling properties of seafood proteins. 44

Table 13: The effect of ultrasound treatment on emulsifying properties of seafood proteins 48

Table 14: Minerals content of desalted mussel powder. 56

Table 15: Amino acids composition of desalted mussel powder. 57

Table 16: Chemical composition (w/w, %) of starches. 89

Table 17: The pasting temperature of starches (10% w/w) in water and MPC solution. 97

List of figures

Figure 1: Probe ultrasonicator schematic illustration (Malek et al., 2023).....15

Figure 2: Heat-induced gel formation of myosin (Xie et al., 2024). 38

Figure 3: PSD (A), D [3,2] (B), D [4,3] (C) of mussel protein concentrates (MPC) dispersions at pH 7 depending on ultrasound treatment time. A significant difference (P<0.05) in the ultrasound time is shown by different letters above the columns.....66

Figure 4: PSD of MPC dispersions at various pH levels before (A) and after (B) ultrasound treatment. D [3,2] (C), D [4,3] (D), zeta potential (E), solubility (F) of MPC dispersions before and after ultrasound treatment as a function of pH changes. A significant difference (P<0.05) in ultrasound treatment and pH values is shown by different capital and lowercase letters above the columns, respectively.....67

Figure 5: SDS-PAGE of MPC under reducing condition. Lane 1- molecular weight marker; Lane 2-untreated MPC at pH 3; Lane 3-untreated MPC at pH 5; Lane 4-untreated MPC at pH 7; Lane 5-untreated MPC at pH 9; Lane 6-sonicated MPC at pH 3; Lane 7- sonicated MPC at pH 5; Lane 8- sonicated MPC at pH 7; Lane 9- sonicated MPC at pH 9. 70

Figure 6: During heat-induced gelation, G' (solid symbol) and G'' (open symbol) of untreated and sonicated MPC samples at different pH as a function of temperature and time. The blue curve represents the temperature change. Symbols are untreated MPC samples (■), sonicated MPC samples (●). 71

Figure 7: G' (solid symbol) and G'' (open symbol) as a function of frequency (A, C, E, G) and strain amplitude (B, D, F, H) for heat-induced MPC gels. Symbols are untreated MPC samples (■), sonicated MPC samples (●). G' (1 Hz) (I) and breaking stress (J) of untreated (control) and sonicated MPC gels as a function of pH values. A significant difference (P<0.05) in ultrasound treatment and pH values is shown by different capital and lowercase letters above the columns, respectively.....74

Figure 8: CLSM images of untreated and sonicated MPC samples before (sol) and after (gel) heating at 90 °C for 30 min. 76

Figure 9: Oil droplet size distribution (A), D [3,2] (B), D [4,3] (C) of sonicated MPC stabilized emulsions at various pH levels. A significant difference (P<0.05) in pH levels is shown by different letters above the columns.....78

Figure 10: Micrographs of emulsions stabilized by sonicated MPC dispersions. The scale bar shows 50 µm in length. Inset photos: emulsions upside down appearances.79

Figure 11: The dependence of G' (solid symbol) and G'' (open symbol) on frequency (A) and strain (B) amplitude for sonicated MPC stabilized emulsions at various pH levels. Symbols are pH 3 (■), pH 5 (●), pH 7 (▲), pH 9 (▼). G' (1 Hz) of sonicated MPC stabilized emulsions as a function of different pH levels (C). A significant difference (P<0.05) in pH levels is shown by different letters above the columns. 81

Figure 12: The viscosity of emulsions as a function of the shear rate (A) at various pH levels. Symbols are pH 3 (■), pH 5 (●), pH 7 (▲), pH 9 (▼). The "up" and "down" measurements are denoted by solid and open symbols, respectively. Viscosity of sonicated MPC stabilized emulsions as a function of various pH values when the shear rate is 1 s^{-1} (B). A significant difference (P<0.05) in pH levels is shown by different letters above the columns. 83

Figure 13: During starch gelatinization, viscosity for NRS (A), WRS (B), WCS (C), WPS (D) as a function of temperature. Symbols represents different concentrations (2.5%-10% w/w) of starch: 2.5% (■), 5% (●), 10% (▲). 93

Figure 14: Viscosity for 10% w/w MPC containing 2.5% (A), 5% (B), 10% (C) w/w different starches as a function of temperature. Starches are NRS (■), WRS (●), WCS (▲), WPS (▼). Solid samples and open samples represent MPC-starch mixture and pure starch, respectively. 10% w/w Pure MPC is (◆). 96

Figure 15: G' (solid symbols) and G'' (open symbols) for pure starches as a function of frequency (A, C, E, G) and strain amplitude (B, D, F, H). Figures are NRS (A, B), WRS (C, D), WCS (E, F), and WPS (G, H). Symbols are 2.5% starch (■), 5% starch (●), and 10% starch (▲). 99

Figure 16: G' (solid symbols) and G'' (open symbols) for MPC containing starches as a function of frequency (A, C, E, G) and strain amplitude (B, D, F, H). Symbols are MPC (■), MPC containing 2.5% starch (●), MPC containing 5% starch (▲), and MPC containing 10% starch (▼). Figures are MPC-NRS (A, B), MPC-WRS (C, D), MPC-WCS (E, F), and MPC-WPS (G, H). 100

Figure 17: G' at 1 Hz for pure starch (A) and MPC-starch samples (B), respectively. A significant difference (P<0.05) in starch type and starch concentration is shown by different capital and lowercase letters above the columns, respectively. 103

Figure 18: Breaking stress (A, B) and strain (C, D) for pure starch and MPC-starch samples, respectively. A significant difference (P<0.05) in starch type and starch concentration is shown by different capital and lowercase letters above the columns, respectively. 107

Figure 19: CLSM images of 10% w/w MPC containing 5% w/w different starches (NRS, WRS, WCS, WPS) before and after heat treatment (90 °C for 30 min). 109

List of abbreviations

CLSM	Confocal Laser Scanning Microscopy
DHA	Docosahaexanoic acid
DLS	Dynamic light scattering
EAI	Emulsifying Activity Index
ELS	Electrophoretic light scattering
EPA	Eicosapentaenoic acid
ESI	Emulsion Stability Index
HPH	High pressure homogenization
G''	Loss modulus
LVR	Linear viscoelastic region
MPC	Mussel protein concentrates
NRS	Native rice starch
PSD	Particle size distribution
TGase	Transglutaminase
SDS	Sodium dodecyl sulfate
SDS-PAGE	Sodium dodecyl sulphate polyacrylamide gel electrophoresis
SEM	Scanning electron microscopy
G'	Storage modulus
WCS	Waxy corn starch
WHC	Water-holding capacity
WPS	Waxy potato starch
WRS	Waxy rice starch

1. Chapter 1: Introduction

1.1. Overview of the research

Proteins are essential macromolecules for human and animal life, playing a vital role in maintaining health. They are critical components of cells, are involved in delivering oxygen to the body, and can provide energy for humans at critical times (Alberts, 2015). Therefore, it is important to intake enough protein. Seafood provides 17.3% of animal proteins, while land animals provide just 13.8%. Seafood contains all the essential amino acids required by humans, is easy to be digested and can be considered an excellent source of high-quality protein (Yada, 2018). In addition, seafood is rich in minerals (iodine, selenium, zinc, and iron), vitamins (A, B, D), and omega-3 fatty acids. These substances can improve cardiovascular health, reduce inflammation, and boost immunity (Miller et al., 2023; Yada, 2018).

The green-lipped mussel is a bivalve mollusk from New Zealand and is currently one of New Zealand's most iconic seafood. The commercial farming of green-lipped mussels began in the 1960s, and green-lipped mussel products are now exported worldwide in various forms (Alfaro, 2006). The registered trademark of green-lipped mussels in New Zealand is Greenshell^{TM} mussel (GSM); the annual export revenue of GSM in 2021 was more than NZD 303 million (Miller et al., 2023). In addition to the food forms of green-lipped mussels, they are also sold as freeze-dried powder and oil extract supplements (Powanda et al., 2015). The annual export revenue of powder and oil extracts in 2021 was NZD 13.4 million and 46 million, respectively (Miller et al., 2023).

Fresh whole green-lipped mussel comprises 1.6-2.2% fat and 12-14% protein, and dried whole mussel comprises 6-12% fat and 36-67% protein (Miller & Tian, 2018). The green-lipped mussel protein is rich in essential and non-essential amino acids. The lipids in green-lipped mussels are high in omega-3 fatty acids, accounting for about 40%

of total fatty acids (Powanda et al., 2015). In general, powder is mainly dried from the green-lipped mussel's muscle and soft tissue parts. The muscle and soft tissue are usually freeze-dried and milled into powders, while the oil extract is derived from the lipid parts (Miller et al., 2023). However, there are some by-products produced during shellfish processing. For example, out of every ton of mussels, approximately 660 kg are directly consumed in food forms by humans, while the remaining portion is discarded (Naik & Hayes, 2019; Vareltzis & Undeland, 2012). Another example, when harvest 1 ton live blue mussels (*Mytilus edulis*), about 27% of mussels are discarded as by-products due to small, broken, or dead during mussel processing (Vareltzis & Undeland, 2012). The proteins found in green-lipped mussel by-products possess both nutritional and economic value. Researching these proteins can mitigate environmental pollution and resource wastage, while also generating economic benefits and facilitating broader utilization of green-lipped mussels by-products.

The functional properties of natural seafood proteins often fall short of the stringent demands in processing, as these proteins are sensitive to heat. Improper storage or the use of inappropriate processing techniques can accelerate protein degradation and compromise quality. Ultrasound treatment, however, represents a non-thermal technology capable of modifying the functional properties of seafood proteins by altering their structure while minimizing impacts on their nutritional composition and flavor. Ultrasound treatment is environmentally friendly, highly efficient, and widely used to study the effects on protein techno-functional properties. Some recent studies have looked the influence of ultrasound treatment on proteins from some other mussel species, such as blue mussel (*Mytilus edulis*) proteins, including actomyosin (Yan et al., 2022), myofibrillar protein (Yu, Li, et al., 2022) or sarcoplasmic protein (Zou et al., 2020). For example, Yu, Li, et al. (2022) discovered that ultrasound treatment at 600 W for 16 min decreased the particle size (from ~48.64 μm to ~20.6 μm) and increased the solubility (from ~11.1% to ~33.4%), increased the absolute zeta potential value (from ~56.24 mV to ~79.92 mV), making the protein solution more stable.

Gelation has been one of the most crucial functional properties of proteins. The most typical example of seafood protein gelation is surimi. Starch plays a vital role in surimi production due to its ability to enhance the strength of the surimi gel and increase its water-holding capacity (Hunt et al., 2009). Furthermore, some previous studies found that ultrasound treatment could improve gelling properties of seafood proteins, such as shrimp myofibrillar protein (Li et al., 2023), grass carp myofibrillar protein (Wen et al., 2017). Protein emulsification is essential for making salad dressings, mayonnaise, and other sauces. Many studies have proven that ultrasound treatment can enhance seafood proteins′ emulsifying properties, including shrimp myofibrillar protein (Li et al., 2023), silver carp myofibrillar protein (Hong et al., 2024). However, there have been no reports on the ultrasound treatment of green-lipped mussel proteins and the effect of adding starch on the gelation of green-lipped mussels.

1.2. Research objectives

The objectives of this research were:

- To study the influence of pH and ultrasound treatment on the physicochemical and techno-functional properties of mussel protein concentrates (MPC), including particle size, zeta potential, solubility, gelation, and emulsification.
- To investigate the changes in microstructure and rheological properties of heat-induced MPC gels containing different starch types and concentrations.

1.3. Thesis structure

Chapter 1: Introduction

Chapter 2: Literature review

Chapter 3: Effect of ultrasound treatment on desalted mussel protein concentrates (MPC): physicochemical and functional properties at different pH values

Chapter 4: Effect of incorporation of various starches on rheological and

microstructural properties of heat-induced mussel protein concentrates gels
Chapter 5: Conclusion and future work
Chapter 6: References

2. Chapter 2: Literature Review

2.1. Introduction of mussel

Seafood, mainly composed of fish, shellfish, and crustaceans, occupies a vital role in the global diet because it provides a wealth of minerals, vitamins, essential fatty acids and high-quality protein, and is closely related to human health, including reducing inflammation and improving cardiovascular function (Nollet & Toldrá, 2010; Park, 2014).

Bivalve mollusks (oysters, clams, and mussels) have great potential to replace traditional meat, and their aquaculture causes far less environmental pollution than traditional animal husbandry (Gawel et al., 2023). Mussels have wedge-shaped shells pointed at the front, broad, and rounded at the back. Marine mussels prefer to inhabit the interflow and middle intertidal zones in temperate seas, while freshwater mussels generally live in mineral-rich rivers, lakes, and other areas (McGevin, 2010). Many creatures are predators of mussels, including but not limited to starfish, seabirds, ducks, geese, and baboons. In addition, people worldwide have been eating mussels for thousands of years. In Europe, mussels are usually served with bread, wine, and chips. Mussels can be steamed, boiled, fried, and grilled in various ways in China (Strayer, 2008).

Green-lipped mussel (*Perna canaliculus*) is a shellfish native to New Zealand. The green-lipped mussel can live for many years in the wild, and its shell can grow to 20 cm or more. Fertilization occurs outside the body, with the larval stage drifting for three weeks to six months before settling on hard surfaces as young mussels. It can move slowly by attaching and separating byssus for a better living position (Buchanan,2001).

Green-lipped mussels are economically important to New Zealand, where they have been farmed since the 1960s and have significantly expanded. In 2021, the annual

income from exporting green-lipped mussels to the international food market exceeded NZD 303 million (Miller et al., 2023). In New Zealand, green-lipped mussels are mainly farmed with ropes. Mussels are tied to ropes, suspended from a backbone of ropes supported by large plastic floats secured by concrete anchors screwed into the seabed. When the spats are transferred to mussel farms around the country, the algae covering the spats are fixed and suspended off the backbone ropes. When the algae rot, only the mussels are left. This method of breeding green-lipped mussels is currently the most used in New Zealand, but the subsequent spats loss rate is as high as 50% (Alfaro et al., 2001). Unlike other mussels in appearance, the green-lipped mussel has a dark brownish-greenish outer shell with turquoise edges that resemble lips. The green-lipped mussel has only one adductor (Alfaro, 2006).

For green-lipped mussel, fresh whole mussel meat contains 76–82% moisture, 1.6–2.2% fat, 2–3% ash, 3–6% carbohydrate and 12–14% protein; dried whole mussel meat is composed of <5% moisture, 6–12% fat, 2–25% ash, 10–25% carbohydrate and 36–67% protein (Miller et al., 2023). The approximate composition of mussels varies seasonally and is related to habitat and water temperature (Miller & Tian, 2018; Miller et al., 2023). In addition to being eaten by humans as seafood, green-lipped mussels are sold worldwide as health supplements in powder and oil extracts. The annual export revenue of powder and oil extracts in 2021 was NZD 13.4 million and 46 million, respectively (Miller et al., 2023). Regarding nutrition values, green-lipped mussels are nutrient-rich, high in micronutrients, vitamins, protein, and polyunsaturated fatty acids. The omega-3 fatty acids are beneficial to the heart function and the brain. Local Maori commonly eat green-lipped mussels to relieve osteoarthritis, allergies, and asthma (Miller et al., 2023). Current clinical studies have proved that green-lipped mussel extracts can improve osteoarthritis and relieve pain, regulate metabolism to reduce the risk of cardiovascular disease, relieve asthma symptoms, improve inattention (Konieczny et al., 2021; Miller et al., 2023).

2.2. Chemical composition of mussel

Table 1 lists the chemical composition of different kinds of mussels. Mussels from different places, species, and seasons have slightly different compositions. These mussels are a good source of proteins (34.26%-52.7%) and carbohydrates (20.38%-52.72%).

Table 1: Chemical composition (%) of mussels based on dry matter.

Mussel variety	**Crude protein**	**Lipid**	**Ash**	**Moisture**	**Carbohydrate**	**References**
Green-lipped mussel (*Perna canaliculus)*	49.5	9.05	16.74	4.33	20.38	(Vijaykrishnaraj et al., 2015)
Blue mussel (*Mytilus edulis*)	52.7	7.45	7.4	3.9	27.71	(Zhang et al., 2013)
Freshwater mussel (*Sinanodonta woodiana*)	34.26	2.03	6.97	10.44	52.72	(Konieczny et al., 2021)

2.2.1. Proteins

Mussels contain various proteins, including myofibrillar protein, sarcoplasmic protein, and stromal protein (Zou et al., 2020). Myofibrillar protein mainly comprises myosin, paramyosin, and actin (Binsi et al., 2006). According to Konieczny et al. (2021), protein bands of actin (43-46 kDa) and paramyosin (98-107 kDa) accounted for a large proportion at 63%. Myosin only accounts for 4.55% of total protein. They also observed

protein bands over 250 kDa could be due to presence of some protein aggregates and heavy myosin.

Amino acids are the basic units of protein synthesis and are essential for human and animal life and health activities. Amino acids can be involved in energy metabolism, signalling in the nervous system, synthesis of hormones and enzymes, repair of cells, and more (Wu, 2013). **Table 2** compares the amino acid composition of commercial fish powder and different kinds of mussel powder. This commercially available fish powder is rich in essential and non-essential amino acids (Konieczny et al., 2021). The amino acid content in mussel powders is comparable to, and in some cases even higher than that found in commercial fish powder. Three branched-chain amino acids, including isoleucine, leucine, and valine, are essential for muscle protein synthesis and energy metabolism (Konieczny et al., 2021; Wu, 2013). Therefore, mussels can be an excellent source of essential and non-essential amino acids.

In addition, mussels are also rich in taurine compared to other meat products. Laidlaw et al. (1990) reported the taurine content per 100 g of meat or seafood products based on wet matter. The taurine content of raw beef, pork, white fish, shrimp, mussel, and squid was ~43 mg, ~61 mg, ~151 mg, ~39 mg, ~655 mg, ~356 mg, respectively. Taurine is essential for human health. Taurine has been reported to reduce obesity and help control blood sugar levels; it can also protect the cardiovascular system and reduce the risk of atherosclerosis, improve neurodevelopment and prevent liver disease (Minkyung et al., 2022).

Table 2: Amino acid profile of mussel powder and fish powder.

Amino acid (mg per 100g protein)	**Fish powder**	**Freshwater mussel (*Sinanodonta woodiana*)**	**Freshwater pearl mussel (*Hyriopsis cumingii*)**	**Green-lipped mussel (*Perna canaliculus)***
Alanine	42.8	49.2	54.8	30-43.8
Arginine	37.2	77.6	82.9	44.3-64.1
Aspartic acid	61.1	94.8	102.5	70.2-78.6
Glutamic acid	91.8	123.9	145.6	84.9-105
Histidine	13.4	25	19.3	12.8-15.2
Isoleucine	30.2	44.1	28.6	26.2-31.6
Leucine	50.3	77.3	73.9	29.3-42.1
Lysine	50.3	76	88.9	47.9-91.6
Methionine + Cystine	22.5	34.3	128.2	23.9-28.8
Phenylalanine + Tyrosine	44.6	76.4	88	47-56.4
Proline	27.1	49	34.1	23.8-35.2
Serine	28	43	52.3	31-34.8
Threonine	27.7	42.3	43.7	31-37.9
Tryptophan	-	-	4.1	8-9.3
Valine	-	-	14.1	23.9-29.1
References	(Konieczny et al., 2021)	(Konieczny et al., 2021)	(Liu et al., 2009)	(Powanda et al., 2015)

2.2.2. Lipids

Green-lipped mussel lipid extracts are mainly composed of ~60% phospholipids, ~5.75% sterols, ~12% free fatty acids, ~22% triglycerides, 0.25% sterol esters (Ulbricht et al.,

2009). The sterols and fatty acids composition and content of green-lipped mussels are affected by the seasonality, the water conditions in which they grow, and the floating organisms they eat because mussels are filter-feeders (Murphy et al., 2003). Green-lipped mussels generally contain about 90 fatty acids, including polyunsaturated, monounsaturated, and saturated fatty acids, with polyunsaturated fatty acids being the most abundant. For example, omega-3 fatty acids account for about ~40% of the total fatty acids content. The total content of eicosapentaenoic acid (EPA) and docosahaexanoic acid (DHA) accounts for ~84% of the omega-3 fatty acids (Powanda et al., 2015). Omega-3 fatty acids, a type of polyunsaturated fatty acid essential for human health. It can significantly decrease the risk of cardiovascular disease, among which EPA and DHA can lower triglyceride levels in the blood, decrease the risk of atherosclerosis, and reduce the occurrence of arrhythmias (Powanda et al., 2015). An adequate intake of DHA promotes brain development and retinal health in children (Stewart et al., 2012)

2.2.3. Carbohydrates

Carbohydrates are usually composed of small oligosaccharides, glycogen, and bio-glycans. Glycogen has been the focus of many studies (Naik & Hayes, 2019). The glycogen content in mussels varies with sex, environment, season, and dietary habits. The glycogen content in blue mussels (*Mytilus edulis*) was highest in summer and lowest in spring. This trend is the opposite of protein content (Li et al., 2010). Different organic solvents can extract carbohydrates from mussels, lyophilization and dialysis can separate the sugar components (Grienke et al., 2014).

2.3. Application of mussels in the food industry

The New Zealand green-lipped mussel trademark is Greenshell^{TM} mussel (GSM), mainly sold as freeze-dried powder or oil extract supplements. GSM is thought to have

many benefits for human health, and it can relieve osteoarthritis, reduce muscle soreness, and improve attention deficit hyperactivity disorder in children. Also, people take GSM to treat asthma and allergies (Matthew et al., 2023). Konieczny et al. (2021) found that mussels could be applied for pet food due to their higher taurine content. Mussel protein hydrolysate also could be used as a flavouring agent for instant noodles or as a marine ingredient for gluten-free bread (Breternitz et al., 2017; Vijaykrishnaraj et al., 2015). Mussel proteins, lipids or freeze-dried powders can be applied to many aspects of the food field. **Table 3** lists some applications of mussels in food fields.

Table 3: Application of mussels in food fields.

Mussel variety	Mussel fraction used	Applications	Highlights	References
Green-lipped mussel (*Perna canaliculus*)	Lipids	Nutraceutical products (powder, oil extract)	● Rich in Omega-3 fatty acid, vitamin B_{12}, and minerals, including phosphorus, iodine, iron, and selenium.	(Matthew et al., 2023)
Green-lipped mussel (*Perna canaliculus*)	Defatted mussel protein concentrates	Wheat-purple rice flour biscuit	● Higher content in ash (~6%), fiber (~52.9%), and protein (~26.36%); lower content in total fat (~5.64%). ● The predicted glycemic index (pGI) and in vitro starch digestibility decreased by ~6.18% and ~18.95%.	(Klunklin & Savage, 2018)
Mussel (*Perna perna*)	Mussel protein hydrolysate	Powder flavoring for instant noodles as microcapsule.	● Without particle collapse, agglomeration, and segregation.	(Breternitz et al., 2017)
Green mussel	Mussel protein	Gluten free bread with a	● As an alternative natural flavoring agent.	(Vijaykrishnaraj et al.,

(*Perna canaliculus*)	hydrolysate	mussel flavor.	● Can be eaten by celiac patients. ● Improve the volume and texture of the bread.	2016)
Green-lipped mussel (*Perna canaliculus*)	Freeze-dried powders	Extemporaneous oral veterinary paste	● Simple oral paste formulation and good stability. ● Suitable for large animals. ● Simple and safe operation.	(Juliano et al., 2016)
Freshwater mussel (*Sinanodonta woodiana)*	Mussel protein concentrates	Pet food powder	● High content in taurine. Good emulsification and gel performance	(Konieczny et al., 2021)
Blue mussel (*Mytilus edulis*)	Mussel myofibrillar protein	Emulsifier	● As a nature emulsifier.	(Cha et al., 2019)

2.4. Physical, chemical, and biochemical modifications of proteins

Protein is an essential part of many food ingredients and is important in food quality and stability. Protein structure and their characteristics determine its applications in the food industry. Generally, natural seafood protein cannot meet the high requirements for its function in the food processing field (Wu et al., 2019). Protein surface activity, hydration, and its structure affect protein functional properties (Mirmoghtadaie et al., 2016). Physical, chemical, and biochemical modifications result in changes in the functional properties of the protein. Many physical modifying techniques are used to improve the structure, physicochemical properties (particle size, solubility, zeta potential) and functional properties (emulsification, gelation, foaming) of seafood proteins. These techniques include and not limit to the ultrasound treatment, high-pressure homogenization (Mirmoghtadaie et al., 2016). Chemical modifications to proteins to change their properties are also commonly used in food science, such as oxidation, etherification, esterification, and changing pH (Glazer & Gould, 1976). In addition, enzymatic hydrolysis and TGase crosslinking are popular as protein modification methods (Mirmoghtadaie et al., 2016).

2.4.1. Ultrasound treatment

Ultrasound is an acoustic wave whose frequency exceeds the upper limit of human ear hearing, and its frequency range is mainly 20 kHz-10 MHz, which is a longitudinal wave (Gallo et al., 2018). When ultrasound propagates in the medium, it can produce cavitation effect and mechanical effect, so it is widely used in many fields, such as the medical field (Moshrefi & Nabki, 2021), food processing field (Gallo et al., 2018), environmental protection field (Qaderi et al., 2024).

Compared with the traditional heat treatment food processing method, ultrasound is a

non-heat treatment processing technology that is very environmentally friendly. Ultrasonic technology mainly uses high-frequency sound waves to make physical or chemical changes in food to meet the needs of consumers (Gallo et al., 2018). Ultrasound can be mainly used in food processing, such as enzymatic and microbial Inactivation, extraction, food emulsification and homogenization, fermentation, and antifoaming action (Bhargava et al., 2021). The use of ultrasound in food processing can be divided into two parts: to replace traditional technology and to assist traditional technology (Tao & Sun, 2015). The ultrasonic processor comprises a generator, transducer, control system, booster, and horn. The ultrasonic processor's schematic representation is shown in **Figure 1**.

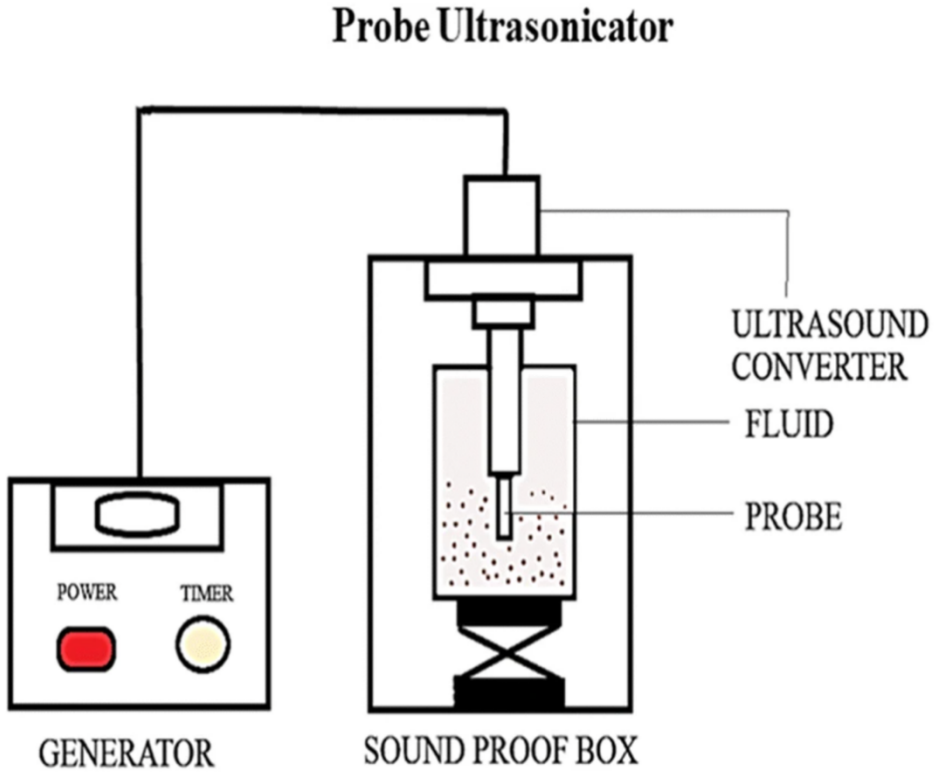


Figure 1: Probe ultrasonicator schematic illustration (Malek et al., 2023).

Many previous studies focused on the impact of ultrasound treatment on the physicochemical and functional properties of seafood proteins. **Table 4** provides a summary of these effects on seafood proteins.

Table 4: Effects of ultrasound treatment on seafood proteins.

Protein types	Ultrasound treatment	Highlights	References
Fish myofibrillar protein	20 kHz 750 W 40% and 60% amplitudes 5, 10, 15 min	● Ultrasound treatment (40%, 15 min) increased solubility and surface hydrophobicity. ● The solubility, surface hydrophobicity, and emulsifying properties reduced with increasing amplitude.	(Malek et al., 2023)
Mussel protein concentrates	20 kHz 200, 400, 600 W 18, 36 min	● Changed the structure of mussel protein (including secondary, tertiary, quaternary). ● Decreased particle size, water holding capacity, improved solubility, absolute zeta potential value, and oil holding capacity.	(Yu, Wu, et al., 2018)
Shrimp myofibrillar protein	20 kHz 400 W 0, 5, 10, 15 min	● Decreased the α-helix content from ~19.98% to ~13.75%, increased β-sheet and β-turn content from ~63.3% to ~71.98%, increased active sulfhydryl group content from ~3.99 μmol/g to ~5.31 μmol/g after ultrasound treatment for 15 min. ● Decreased particle size, increased solubility, and absolute zeta potential value.	(Li et al., 2023)

		• Improved water holding capacity of gel from ~78.1% to ~85.4%.	
Shrimp myofibrillar protein	20 kHz 100, 300, 500 W 60 min	• Increased the carbonyl content, increased free radicals from ~6368.50 to ~12116.33, increased free amines from ~14.30 nmol/mg to ~16.62 nmol/mg. • Decreased α-helix, increased β-sheet. • Total sulfhydryl group content decreased from ~18.49 μmol/g to ~12.79 μmol/g, increased surface hydrophobicity from ~6.33 to ~30.76 μg. • Increased the gel strength from ~0.25 N to ~0.38 N.	(Li et al., 2022)
Tuna myofibrillar protein	280 W for 0, 6, 12, 18, 24 min 0, 160, 280, 400 W for 12 min	• Decreased particle size from ~782.26 nm to ~619.77 nm at 280 W for 24 min.	(Liu et al., 2022)
Scallop myofibrillar protein	20 kHz 200 W 0-15 min	• Increased EAI and ESI.	(Yu, Sun, et al., 2022)
Mussel myofibrillar protein	20 kHz 0, 150, 300, 450, 600 W 16 min	• Increased surface hydrophobicity from ~134.41 to ~161.50. • Increased the α-helix and β-turn content. • Decreased β-sheet content.	(Yu, Li, et al., 2022)

2.4.2. High pressure homogenization (HPH)

Homogenization refers primarily to the physical process of transforming large, dispersed particles into small particles (Martínez-Monteagudo et al., 2016). It was initially applied in the dairy production process to improve the stability of milk (José et al., 2020). The homogenizer with operating pressure in the range of 50-300MPa is called HPH (Martínez-Monteagudo et al., 2016). HPH does not affect food nutrition values and sensory properties, and it mainly uses high pressure and high-speed liquid shearing to process foods (Karabulut et al., 2024). The protein solution is pushed into a narrow, high-pressure unit by a high-pressure pump, after which the sample is homogenized through a high-speed homogenizing valve, during which the sample experiences a sudden release of pressure and an increase in flow rate, resulting in a significant change in its physical properties (Francesca & Rosalba, 2016).

HPH is popular in food processing, which has high efficiency and low cost (Wu et al., 2019). Yu, Cha, Wu, Xu, et al. (2018) investigated the influence of HPH at 0-100 MPa for 3 cycles on the structure and functional properties of mussel (*Mytilus edulis*) myofibrillar protein. They found that HPH decreased particle size significantly and changed mussel myofibrillar protein's secondary, tertiary, and quaternary structure. Wu et al. (2019) investigated the influence of HPH at 0-120 MPa on the functional properties of oyster myofibrillar protein. The particle size distribution of homogenized protein dispersion became narrow, and the particle size was smaller than non-homogenized samples. After HPH at 120 MPa, the absolute zeta potential and solubility increased from ~22.5 mV to ~34 mV, from ~40.5% to ~81.1%, respectively. Also, HPH improved the emulsifying properties of oyster myofibrillar protein.

2.4.3. Ball milling treatment

Ball milling is a mechanical process, and the basic principle is to use the ball in the ball mill to grind the sample; the ball usually moves or rotates at a controlled speed. When the grinding ball hits or friction with the sample, it will cause the sample particle size to decrease and the surface to become smooth (Wang et al., 2018). Ball milling treatment can change the material's crystal structure, microstructure, and surface properties. For proteins, ball milling treatment reduces particle size and improves functionality, which affects its application in the food field (Bangar et al., 2023).

Many studies provide reference values for ball milling processing of seafood proteins. For instance, Yu, Cha, Wu, Fan, et al. (2018) discovered that after ball milling treatment for 20 min, the α-helix content decreased from ~11.5% to ~9.1%, free sulfhydryl content increased from ~13.51 mol/10^4g to ~14.87 mol/10^4g. Ball milling treatment decreased the mean particle size from ~900 nm to ~250 nm and decreased the solubility from ~74.89% to ~53.1%. The reduction in solubility can be attributed to the formation of insoluble protein aggregates after ball milling treatment (Yu, Cha, Wu, Fan, et al., 2018). Wang et al. (2018) studied changes in the physicochemical properties of pacific oyster protein influenced by ball milling treatment for 0-20 min. They found that ball milling treatment changed protein's secondary structure and decreased particle size to less than 20 μm.

2.4.4. pH

pH has a significant effect on proteins, but pH affects differently on different protein sources. In general, pH can affect the solubility, conformational change, and stability of proteins (Gao et al., 2018). The isoelectric point (pI) is the pH of the protein without a net charge. The zeta potential value is positive when pH is below the protein's pI, and the zeta potential value is negative when the pH is above pI.

pH affects the solubility of proteins, and in the case of seafood proteins, they are more sensitive to pH. Most proteins have very low solubility near the pI, and solubility increases as they move away from the pI (Yada, 2018). When near the pI, the electrostatic repulsion between protein molecules is very low, resulting in proteins more likely to gather to form a precipitate, but when away from the pI, the protein surface with more net charges, increasing the electrostatic repulsion between protein molecules, making it easier to dissolve (Thawornchinsombut & Park, 2004). **Table 5** shows some examples of pH affecting seafood proteins.

Table 5: The effect of pH on seafood proteins.

Protein sources	pH	Isoelectric point (pI)	Highlights	References
Sarcoplasmic protein from striped catfish	2-12	pH 5	● The solubility was the lowest at pH 5 with ~15.1 mg/mL. Solubility increased when far away from pI. ● Easier to enhance hydrophobic interactions at pH 2-4, unfold and expose hydrophobic residues at pH 10-12.	(Tadpitchayangkoon et al., 2010)
Pacific whiting muscle protein	2-12	pH 5.5	● The solubility was the highest at pH 2 and pH 12, compared to low solubility at pH 5-10.	(Thawornchinsombut & Park, 2004)
Pearl mussel meat protein isolate	2-12	pH 5	● The solubility was the lowest at pH 5 with ~8.8% and reached the maximum at pH 11 (~87.4%) and pH 3 (~79.6%). ● The foaming ability was the best at pH 11, with ~300%.	(Liu et al., 2009)

2.4.5. Enzymatic hydrolysis

Enzymatic hydrolysis involves using enzymes to divide protein molecular chains into peptides or free amino acids. Usually, this method can improve the solubility of proteins because peptides or amino acids are more soluble than protein molecules. According to Noman et al. (2018), after 6 hours of papain enzymatic hydrolysis, the viscera protein hydrolysate from Chinese sturgeon (*Acipenser sinensis*) had better foaming capacity (~76.67%) and higher solubility (~98.74%). In addition, proteins become easier for humans to digest and absorb after hydrolysis. But sometimes, the hydrolyzed product can be accompanied by a little bitter taste (Liaset et al., 2000).

2.4.6. TGase cross-linking

Transglutaminase (TGase) is an enzyme that can catalyze the formation of covalent cross-linking between protein molecules. It is widely used in surimi and meat products. For example, Zhang and Chang (2023) found that TGase at 0.5 units/g catalyzed the cross-linking reaction between catfish by-product protein molecules to form a strong 3D network structure, the deformation and hardness of surimi gels improved by ~71% and ~218%, respectively .

2.5. Physicochemical and functional characteristics of proteins

Protein is a polymer compound composed of one or more polypeptide chains, and amino acids are the basic units of proteins. Protein has a primary, secondary, tertiary, and quaternary structure, and its molecular structure determines its functional properties (Petsko & Ringe, 2003). Due to its unique physical, chemical, and functional properties, protein has important research value in food processing. Many methods have been used to measure and characterize protein particle size, isoelectric point, solubility,

emulsification, and gelation.

2.5.1. Particle size

Particle size is used to characterize the size of proteins and is essential for understanding solubility, stability, and other properties. The smaller the protein particle, the higher its solubility (Yu, Li, et al., 2022). Because small particles are subject to less resistance, diffusion speed is faster (Arakawa & Timasheff, 1984). And smaller particles provide more surface area and are easier to interact with water molecules (Wang & Roberts, 2018). In addition, the particle size of proteins is influenced by various factors, including pH and ionic strength (Boulet et al., 2000). When the pH of the protein solution is close to the pI, the net charge on the protein surface decreases, resulting in protein aggregation and, therefore, larger particle size near the isoelectric point.

Light scattering and microscopy are used to measure particle size. Dynamic light scattering (DLS), being fast and non-destructive, is popular for measuring protein particle size, and its principle is to calculate the diameter of the particles by measuring the rate of Brownian motion of the particles in solution (Berne & Pecora, 1976). In addition, scanning electron microscopy (SEM) can be used to observe the details of the particle surface. The principle is to use an electron beam to scan the sample's surface and form a high-resolution image (Viacheslav, 2012).

Table 6 shows the effect of ultrasound treatment on the particle size of different seafood proteins. Numerous studies have proved that ultrasound treatment can reduce the particle size of seafood protein dispersions due to shear forces during ultrasonication processing. However, too long ultrasound treatment time or too high ultrasonic power may increase protein particle size (Ding et al., 2021; Zou et al., 2020).

Yan et al. (2022) investigated the influence of different ultrasonic power (0-600 W) for

16 min on the particle size of mussel actomyosin. They found that the particle size reduced from ~110 μm to ~20 μm with ultrasonic power increased from 0 to 300 W. This result may be attributed to the cavitation caused by ultrasound treatment, which is accompanied by strong shear forces that can break hydrogen bonds and electrostatic interactions between proteins, thereby breaking up protein aggregates and causing them to disperse into small particles. However, the particle size increased to ~50 μm as the ultrasonic power increased to 600 W. They thought that too high ultrasonic power increased the speed at which proteins collide, causing dispersed protein aggregates to come together again to form larger particles. Zou et al. (2020) found a significant decrease in mussel sarcoplasmic protein particle size after ultrasound treatment at 600 W for 10 min, from ~1081.33 nm to ~151.67 nm. However, the particle size increased to ~286.33 nm when the ultrasound treatment duration exceeded 30 min.

Table 6: The effect of ultrasound treatment on particle size of seafood protein dispersions.

Protein types	Ultrasound treatment	Particle size	References
Mussel protein concentrates	20 kHz 200, 400, 600 W 18, 36 min	Decreased significantly after ultrasound treatment.	(Yu, Wu, et al., 2018)
Actomyosin from mussel	20 kHz 0, 150, 300, 450, 600 W 16 min	Decreased from ~110 μm to ~20 μm at 300 W, increased to ~50 μm at 600 W.	(Yan et al., 2022)
Myofibrillar protein from mussel	20 kHz 0, 150, 300, 450, 600 W 16 min	Decreased significantly after ultrasound treatment.	(Yu, Li, et al., 2022)
Sarcoplasmic protein from mussel	20 kHz 600 W 0, 5, 10, 20, 30 min	Decreased from ~1081.33 nm to ~151.67 nm for 10 min, increased to ~286.33 nm.	(Zou et al., 2020)
Mantle protein from scallop	0, 100, 200, 300, 400, 500 W 15 min	Decreased from ~386.77 nm to ~247.1 nm.	(Ding et al., 2021)

Myofibrillar protein from shrimp	20 kHz 400 W 0, 5, 10, 15 min	Decreased from ~945.4 nm to ~179.5 nm.	(Li et al., 2023)
Scallop protein	200, 400 W 0, 5, 10, 15 min	The particle size distribution became narrow.	(Yu, Sun, et al., 2022)

2.5.2. Zeta potential

Zeta potential is a vital physical parameter to characterize the surface charge of proteins and a key index to reflect the stability of colloidal dispersions (Yan et al., 2022). **Table 7** shows the direct relation between zeta potential value and system stability. In general, if the absolute zeta potential value of the protein solution is higher, the solution is more stable. Conversely, if the absolute zeta potential value is very low, the protein particles are more inclined to aggregate.

Table 7: The relation between zeta potential value and system stability (Cano-Sarmiento et al., 2018).

Zeta potential (mV)	**0–10**	**± 10–20**	**± 20–30**	**± 30**
System	very unstable system	relatively stable system	moderately stable system	highly stable system

Electrophoretic light scattering (ELS) and electroacoustic are two different methods of measuring zeta potential. A zetasizer, which mainly uses ELS to measure zeta potential, is a commonly used instrument in food technology. The main principle is measuring the moving speed of charged particles in solution in the electric field according to the Henry equation to calculate the potential (Lunardi et al., 2021).

Table 8 shows the effect of ultrasound treatment on the absolute value of zeta potential of seafood protein dispersions. Ultrasound treatment can improve the absolute zeta potential value. For instance, Yu, Li, et al. (2022) found that ultrasound treatment increased the absolute zeta potential value of mussel myofibrillar protein (from ~56.24 mV to ~79.92 mV). They believed that ultrasound treatment broke up protein aggregates, which exposed hydrophobic groups and increased the protein's surface

charge. Li et al. (2023) also came to a similar conclusion. They studied the influence of ultrasound treatment at 400 W for 15 min on the myofibrillar protein from shrimp. They found that ultrasound treatment improved the absolute zeta potential value from ~5.79 mV to ~8.4 mV. Ultrasound treatment decreased myofibrillar protein's particle size, causing these particles to be more evenly dispersed in the solution and have more charges on the surface.

Table 8: The effect of ultrasound treatment on the absolute value of zeta potential of seafood protein dispersions.

Protein types	Ultrasound treatment	Zeta potential (the absolute value)	References
Mussel protein concentrates	20 kHz 200, 400, 600 W 18, 36 min	Increased after ultrasound treatment.	(Yu, Wu, et al., 2018)
Actomyosin from mussel	20 kHz 0, 150, 300, 450, 600 W 16 min	Increased from ~17.2 mV to ~41 mV at 300 W, decreased to ~36 mV at 600 W.	(Yan et al., 2022)
Myofibrillar protein from mussel	20 kHz 0, 150, 300, 450, 600 W 16 min pH 7	Increased from ~56.24 mV to ~79.92 mV.	(Yu, Li, et al., 2022)
Sarcoplasmic protein from mussel	20 kHz 600 W 0, 5, 10, 20, 30 min pH 7	Increased from ~10 mV to ~24 mV.	(Zou et al., 2020)

Scallop protein	200, 400 W 0, 5, 10, 15 min pH 7	Increased from ~19.62 mV to ~30.28 mV at 200 W for 5 min, to ~54.61 mV at 400 W for 15 min.	(Yu, Sun, et al., 2022)
Myofibrillar protein from shrimp	20 kHz 400 W 0, 5, 10, 15 min pH 7	Increased from ~5.79 mV to ~8.4 mV.	(Li et al., 2023)

2.5.3. Solubility

Solubility affects gelation, emulsification, and foaming properties (Liu et al., 2022). There are many factors affecting protein's solubility, including pH, temperature, and ionic strength. In addition, solubility is directly influenced by the protein source and can vary greatly for different proteins (Grossmann & McClements, 2023). For most protein dispersions, the solubility is lowest at the isoelectric point. However, the solubility increases when away from the isoelectric point.

Various methods are used to measure the solubility of proteins, among which is Bradford Assay, the most sensitive protein measurement method at present. It was first proposed by Bradford in 1976. It has become the premier method of protein quantification in universities and laboratories. The method is convenient, fast, sensitive, and less interfered with by some commonly used reagents. However, there are other disadvantages: it is susceptible to SDS detergent, and the standard curve will be slightly nonlinear (Gebauer, 2001). The principle of this method is that the dye Coomassie Blue G250 is combined with the protein basic amino acid and aromatic amino acid residues in an acidic solution, and the color depth of the compound formed is proportional to the protein concentration. Therefore, the protein content of the solution can be calculated by measuring the absorbance of the solution at 595nm (Bradford, 1976). Generally, a standard absorbance-versus-protein concentration curve is plotted before the experiment, and then the protein content in the solution is calculated according to the standard curve. The protein solubility equation is shown below:

$$(\%)\text{Protein Solubility} = \frac{\text{Protein content in the supernatant}}{\text{Total protein content}} \times 100 \quad (1)$$

Many previous studies investigated the solubility of seafood proteins affected by ultrasound treatment, listed in **Table 9**. Ultrasound treatment can increase the solubility, but too long treatment time or too high power may decrease the solubility (Li et al.,

2023). Ding et al. (2021) studied the influence of ultrasound treatment at 0-600 W for 15 min on the mantle protein from scallops. They found that ultrasound treatment at 400 W increased the solubility from ~14% to 42.5%. Ultrasound treatment could cause changes in protein molecular structure and expose the internal hydrophilic groups inside the protein, leading to the transformation of insoluble protein aggregates into soluble proteins (Ding et al., 2021). In addition, ultrasound treatment decreased the particle size of the protein, increased the contact area between the protein and water, and improved the interaction between them, which was also conducive to the increase of solubility. However, Ding et al. (2021) found that as the ultrasonic power increased to 600 W, the solubility decreased to ~34%. High ultrasonic power may cause excessive protein denaturation. The speed at which the protein particles collide too quickly may result in the formation of some insoluble protein aggregates and a reduction in solubility (Ding et al., 2021).

Table 9: The effect of ultrasound treatment on the solubility of seafood protein dispersions.

Protein types	Ultrasound treatment	Solubility	References
Mussel protein concentrates	20 kHz 200, 400, 600 W 18, 36 min	Increased greatly after ultrasound treatment; the solubility increased with the increase of power.	(Yu, Wu, et al., 2018)
Actomyosin from mussel	20 kHz 0, 150, 300, 450, 600 W 16 min	Increased from ~38.5% to ~57.1% after ultrasound treatment at 300 W, decreased to ~40% at 600 W.	(Yan et al., 2022)
Myofibrillar protein from mussel	20 kHz 0, 150, 300, 450, 600 W 16 min	Increased from ~11.1% to ~33.4% after ultrasound treatment at 600 W for 16 min.	(Yu, Li, et al., 2022)
Sarcoplasmic protein from mussel	20 kHz 600 W 0, 5, 10, 20, 30 min	Increased from ~63% to ~81% after ultrasound treatment at 600 W for 20 min, then decreased to ~61% for 30 min.	(Zou et al., 2020)
Mantle protein from scallop	100, 200, 300, 400, 500, 600 W	Increased from ~14% to 42.5% after ultrasound treatment at 400 W, decreased to 34% at 600 W.	(Ding et al., 2021)

	15 min		
Scallop protein	200, 400 W	Increased from ~14% to ~40% after ultrasound	(Yu, Sun, et al., 2022)
	0, 5, 10, 15 min	treatment at 400 W for 15 min.	
Myofibrillar protein from shrimp	20 kHz	Increased from ~2.04 mg/mL to ~3.88 mg/mL after	(Li et al., 2023)
	400 W	ultrasound treatment for 15 min.	
	0, 5, 10, 15 min		

2.5.4. Gelation

Under certain conditions, proteins interact to form a 3D network structure and capture water called gelation. For seafood proteins, collagen and gelatin can be used to produce cold-set gels, where hydrophilic interactions dominate, so this kind of gel is reversible and transparent; heat-set gels, made from myofibrillar protein, are irreversible and opaque because hydrophobic and cross-linked interactions caused by protein aggregation dominate (Yada, 2018).

There are many methods to prepare gels. **Table 10** summarizes different gelation methods for proteins and their advantages and disadvantages. Heat-induced gelation is simple and safe, and only the heating conditions need to be controlled, so it is widely used to prepare gels (K. Liu et al., 2021).

Table 10: Preparation methods of protein gels (K. Liu et al., 2021).

Gelation method	Description	Advantages	Disadvantages
Heat-induced gelation	Heat causes protein molecules to unfold and interact to form gels.	● Simple and safe ● Heat only	● Required precise temperature ● Energy-consuming
Cold-induced gelation	Prepare gels at low temperature.	● Energy-saving ● Cost-effective ● Wide adaptability	● Time-consuming ● Required additional conditions (salt, acid, cross-linking agent)
pH-induced gelation	Adjust the pH of solution and induce protein molecules to interact to form gels.	● Safe ● Economical	● Required precise pH values ● May affect taste
Ion-induced gelation	Add specific salt ions to induce the cross-linking of proteins to form gels.	● Good viscoelasticity of formed gels ● environmental protection	● Required precise salt ion concentration ● May affect taste
Enzymatic Cross-Linking	Covalent cross-linking between protein molecules is catalyzed by enzymes such as TGase to form gels.	● Mild reaction condition ● Good stability of formed gels.	● Required precise enzymes concentration ● High cost

According to Naik and Hayes (2019), mussel protein comprises ~11.39% matrix proteins, ~17.19% myofibrillar proteins and ~48.4% sarcoplasmic proteins. Sarcoplasmic proteins are water-soluble and globular (Naik & Hayes, 2019). The gelation process of sarcoplasmic protein is as follows: When the temperature begins to rise and exceed its deformation temperature, the protein structure unfolds, exposing hydrophobic groups and active sites, and these proteins form aggregates through hydrophobic interactions, electrostatic interactions, and hydrogen bonds. As the temperature increases, these protein aggregates form a more stable 3D network structure through stronger interactions (such as disulphide bonds), eventually forming a gel (Jafarpour & Gorczyca, 2009; Park, 2014).

However, sarcoplasmic proteins have been removed during the preparation of most surimi gels because they are readily soluble in water, so it does not involve the gelation of sarcoplasmic proteins (Park, 2014). For the gelation of seafood proteins, most studies focused on the gelation mechanism of myofibrillar proteins (Amiri et al., 2018; Li et al., 2023). Myofibrillar protein is a salt-soluble protein with fibrous structures, and its heat-induced gelation mechanism is entirely different from that of globular protein. Myosin protein plays a vital role in the gelation of meat products because actin cannot form gels (Sun & Holley, 2011). The heat-induced gel formation of myosin is shown in **Figure 2**. When the temperature increases, the myosin light chain de-helixes and its head (S1 region) attract each other through hydrophobic and electrostatic interactions, forming a preliminary aggregate. At this point, the head of myosin forms a spherical aggregate, and the tail of myosin radiates outward. When the temperature increases, the myosin tail (S2 and light chain regions) folds and crosslinks with other tails. The denatured myosin aggregates form stable network structures through disulphide, hydrogen, and hydrophobic interactions (Park, 2014; Xie et al., 2024).

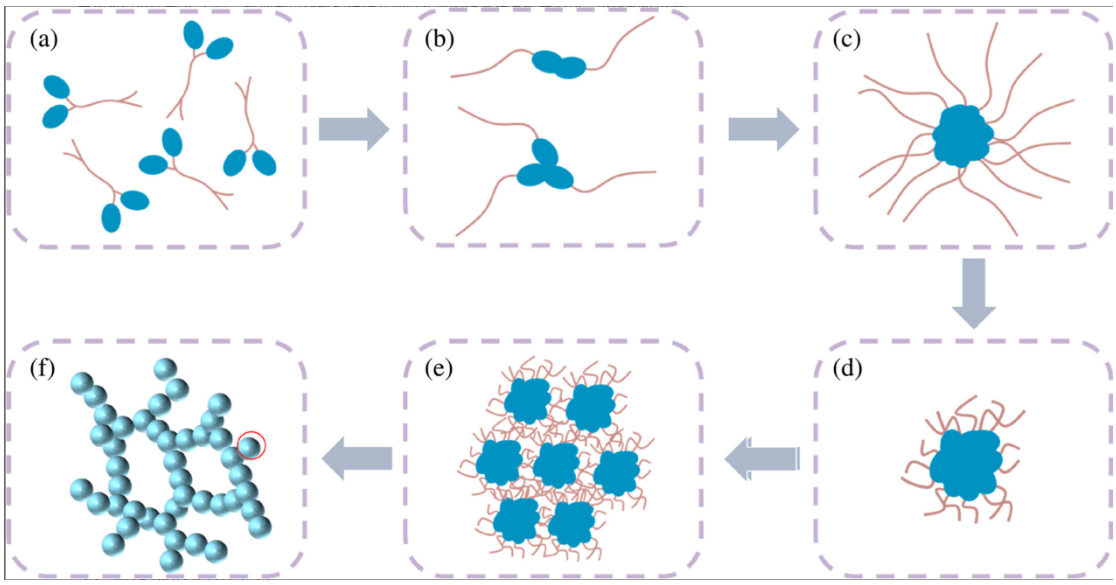


Figure 2: Heat-induced gel formation of myosin (Xie et al., 2024).

Many factors can affect the gelling properties of proteins during heat induction, including heating rate, ionic strength, pH, protein concentration, physical modifications (such as ultrasound treatment, HPH), the addition of Transglutaminase and polysaccharides (Sun & Holley, 2011). The gel strength is highly influenced by the protein concentration. The minimum gel concentration of proteins is the critical concentration of the proteins at the time of gel formation. In other words, proteins cannot form a 3D network structure below this concentration (Konieczny et al., 2021). Gel strength is generally believed to increase with increasing protein concentration (Sun & Holley, 2011). pH also affects the gelling properties of myofibrillar proteins. The gel performance of myofibrillar protein is the worst near the isoelectric point due to zero net charge on the protein surface and the lowest solubility (Park, 2014). The optimum pH for heat-induced myofibrillar protein gelation is 6 (Xie et al., 2024). The gelation of myofibrillar protein is affected by ionic strength because the protein is salt-soluble. According to Wu et al. (2023), the hardness of myofibrillar protein gels from sea bass increased from ~9.3 N to ~15.5 N as the ionic strength increased from 0 to 0.6 mol/L, then decreased to ~13 N as the ionic strength increased to 1 mol/L. Compared to a faster heating rate, a slow heating rate can cause proteins to form stronger 3D network

structures (Xie et al., 2024). In addition, physical modifications such as ultrasound treatment can improve the gel strength of proteins. Adding starches can also improve the gel performance of proteins, especially when widely used in preparing surimi gels (Campo & Tovar, 2008).

Table 11 shows some examples of the effect of ultrasound treatment on the gelling properties of seafood proteins. Ultrasound treatment changes the structures and interactions of seafood proteins. In general, ultrasound treatment can improve the gelling capacity of proteins. Li et al. (2023) studied the effect of ultrasound treatment at 400 W for 15 min on the gel properties of shrimp myofibrillar protein. They found that ultrasound treatment changed protein conformation, resulting in the improvement of gel properties, which was reflected in an increase of WHC from ~78.1% to ~85.4% as ultrasound treatment time increased from 0 to 15 min. SEM images showed that ultrasound treatment resulted in more uniform and denser myofibrillar protein gel 3D network structures. However, recent studies have also shown that physical modification technologies may not affect the gel properties of proteins. Janssen et al. (2024) found that homogenization at 50 MPa for 2 cycles did not affect the final linear storage moduli of the fava bean protein and pea protein heat-induced gels. However, homogenization led to a reduction in the particle size of these two proteins.

Table 11: The effect of ultrasound treatment on the gelling properties of seafood proteins.

Protein types	Ultrasound treatment	Gelling properties	References
Silver carp surimi	40 kHz 300 W 10 min	● Increased the breaking force. ● The chewiness, gumminess, and hardness of surimi gels increased by ~5.7%, 6.6%, and 7.2%. ● Improved microstructures, reduced pore diameter, and formed a uniform network. ● Increased water-holding capacity (WHC).	(Gao et al., 2021)
Shrimp myofibrillar protein	20 kHz 400 W 15 min	● Improved WHC from ~78.1% to 85.4%. ● Increased adhesiveness, hardness, gumminess. ● Increased storage modulus (*G′*), a stable and clear 3D network structure was observed.	(Li et al., 2023)
Myofibrillar protein from bay scallop	550 W 60 min	● Scanning Electron Microscope (SEM) images showed a dense and fine network structure. ● Increased the gel strength from ~0.33 to ~0.51 N.	(Liu et al., 2024)

		• Increased WHC from ~59.2% to ~83%.	
Myofibrillar protein from grass carp	20 kHz 0-800 W 20 min	• WHC increased from ~73.97 to ~78.26. • The whiteness increased from ~56.77 to ~63.86. • Some big aggregates and irregular pores were observed before ultrasound treatment, but silky fiber structure and uniform and small pores were observed on the gels surface after ultrasound treatment.	(Wen et al., 2017)

Adding starch to seafood protein can improve the gel strength of the mixture. A typical example is the addition of starch during the preparation of surimi (Xie et al., 2024). Adding starch to surimi to enhance its gel properties is a common technique, and the process involves starch gelatinization and protein gelation, which are different processes (Hunt et al., 2010). **Figure 2** illustrates the process of myosin gelation in detail. For starch gelatinization, the water absorption of starch granules is reversible at low temperatures. With the increase in temperature, starch granules absorb water and swell, the internal hydrogen bonds are gradually broken, and the crystal structure of starch is destroyed. Then amylose and amylopectin are dispersed into water, resulting in a sharp increase in the viscosity of the solution, which is the most apparent change in the process of starch gelatinization (Ai & Jane, 2015). The interaction between protein particles and starch granules greatly affects the rheological properties and texture of mixture gels (Hunt et al., 2010). When starch is added to surimi, starch granules absorb water and swell as temperature increases. The gelatinized starch forms hydrogen bonds and hydrophobic interactions with the proteins. The starch granules fill the gaps in the gel network, resulting in an increase in surimi's gel strength. Adding starch also increases the bound water content and decreases the free water content in the gel, thus improving the WHC of gel (Hunt et al., 2009; Ratnayake & Jackson, 2008). For a protein-starch system, types of starch, concentrations of starch, types of protein, and the ratio of amylose to amylopectin affect the strength of mixture gels (Campo & Tovar, 2008; Hunt et al., 2009).

Table 12 lists some recent examples of the effect of starches on the gel properties of seafood proteins. For example, Luo et al. (2020) investigated the influence of adding 0-20% potato starch on the gel properties of hairtail surimi. The addition of potato starch significantly changed the gel properties of surimi. The strength and WHC of surimi gels increased with the increasing starch concentration, reaching the maximum value when the starch concentration was 16%. Weak internal structure and high amylopectin content for potato starch led to a low gelatinization temperature and strong granule swelling capacity. In the process of heat-induced surimi gelation, after the

gelatinization and expansion of potato starch, its water absorption increased, and great pressure was exerted on the protein matrix, increasing the gel strength of the surimi-potato starch mixture gels. Huang et al. (2024) studied the effect of 0-14% tapioca starch on the quality of *Nemipterus virgatus* surimi gels. They found that after adding 12% tapioca starch, the hardness, gel strength, and WHC of surimi gels increased by ~24 N, ~17.48 N, ~89.01%, respectively. The addition of tapioca starch changed the microstructure of surimi gels. The scanning electron microscope (SEM) images showed that after adding 12% starch, a more uniform and compact gel network microstructure was observed. Surimi gel without starch showed a loose and rough surface.

Table 12: The effect of adding starch on the gelling properties of seafood proteins.

Protein types	Starch types and concentrations	Highlights	References
Hairtail surimi	Potato starch 4%, 8%, 12%, 16%, 20%	● Optimal concentration of starch addition: 16% ● Adding starch improved the hardness, chewiness, cohesiveness, and springiness of surimi gels. ● The strength and WHC of surimi gels increased significantly as the potato starch concentration increased from 0 to 16%, then decreased slightly when the starch concentration reached 20%.	(Luo et al., 2020)
***Nemipterus virgatus* surimi**	Tapioca starch 0-14%	● As the tapioca starch concentration increased from 0 to 12%, the chewiness, gumminess, springiness, hardness, gel strength, WHC of surimi gels improved largely, from ~6.66 to ~21.36, ~8.64 to ~15.32, ~0.77 to ~1.41, ~12.61 N to ~24 N, ~7.59 N to ~17.48 N, ~75.4% to ~89.01%, respectively. ● The addition of 14% tapioca starch decreased the whiteness of surimi gels from ~71.1 to ~61.75. ● More uniform and compact gel network structures were observed after adding	(Huang et al., 2024)

		tapioca starch.	
Myosin from hairtail	Corn starches	● Adding different kinds of corn starches improved the gel strength of myosin. ● The gel quality of myosin containing high amylose corn starch was the greatest due to high content amylose.	(Mi et al., 2021)
Alaska Pollock surimi	Modified cassava starches	● Adding all starches increased the whiteness of surimi gel. ● Hydroxypropylated cassava starch had high viscosity at low temperature, led to a reduction in gel strength.	(Kong et al., 2016)

2.5.5. Emulsifying properties

The emulsion is a dispersion system in which one liquid (dispersed phase) is dispersed in the form of tiny droplets (0.1-100 μm) in another immiscible liquid (continuous phase). There are two common types of emulsions: O/W emulsion (such as salad dressing, cream, and milk) and W/O emulsion (such as butter) (Lam & Nickerson, 2013). Protein is amphiphilic and can be used as an emulsifier to prepare emulsions. The emulsification properties of proteins are affected by their physicochemical properties, such as particle size, surface charge, and surface hydrophobicity. Physical and chemical modifications, including ultrasound treatment, HPH, and pH, can improve proteins' physicochemical and functional properties. In general, the emulsifying property of protein is the worst when close to the isoelectric point. This can be explained by at the isoelectric point, the net charge on the protein surface is zero, the protein is easy to aggregate, and the low solubility is not conducive to the adsorption of protein molecules on the oil-water interface, thus affecting the emulsification property.

Table 13 lists the effect of ultrasound treatment on the emulsifying properties of seafood proteins. For instance, Yu, Li, et al. (2022) studied the effect of ultrasound treatment at 0-600 W for 16 min on the emulsifying properties of mussel myofibrillar protein (MMP). For emulsions stabilized by MMP, as the ultrasonic power increased from 0 to 600 W, the mean oil droplet size decreased from ~8.11 μm to ~5.21μm, the absolute value of zeta potential increased from ~20.35 mV to ~31.78 mV. Microstructure images showed that emulsions stabilized by sonicated MMP (450 W) had smaller, more uniform oil droplets and oil droplets tightly distributed. Ultrasound treatment reduced the particle size of protein dispersion, resulting in faster adsorption of the protein at the oil-water interface and emulsions with small oil droplets. Ultrasound treatment also destroyed the protein structure, exposing more negative charges. These proteins containing negative charges on the surface would be adsorbed to the oil surface, thus preventing flocculation, and increasing the stability of the

emulsion. However, too high, or too long ultrasound treatment may decrease the emulsifying capacity of proteins, which could be attributed to excessive deformation and aggregation of proteins (Deng et al., 2023; Hong et al., 2024).

Table 13: The effect of ultrasound treatment on emulsifying properties of seafood proteins.

Protein types	Ultrasound treatment	Highlights	References
Mussel myofibrillar protein	20 kHz 0-600 W 16 min	● Ultrasound treatment at 600 W reduced the mean oil droplet size from ~8.11 μm to ~5.21μm and increased the absolute value of the zeta potential from ~20.35 mV to ~31.78 mV. ● The absorb protein significantly increased from ~12.5% to ~36% with the increase of ultrasonic power from 0 to 450 W, suggesting that the stability of the emulsion increased. ● Ultrasound treatment at 450 W improved the Emulsifying Activity Index (EAI) and Emulsion Stability Index (ESI) of the emulsion.	(Yu, Li, et al., 2022)
Scallop myofibrillar protein	20 kHz 200, 400 W 0, 5, 10, 15 min	● Emulsion stabilized by sonicated protein at 400 W had higher EAI. ● ESI of emulsion stabilized by sonicated protein at 400 W increased significantly as the ultrasound time increased from 0 to 15 min.	(Yu, Sun, et al., 2022)

		● Ultrasound treatment improved the emulsifying properties, as reflected in smaller oil droplets, higher storage and loss moduli, higher protein adsorption at the interface, and a more stable emulsion.	
Shrimp myofibrillar protein	20 kHz 400 W 0, 5, 10, 15 min	● Ultrasound treatment for 15 min increased EAI from ~45.54 m^2/g to ~78.82 m^2/g, increased ESI from ~84.26% to ~94.39%. ● Ultrasound treatment for 15 min led to a more homogeneous, smaller oil droplet emulsion.	(Li et al., 2023)
***Neosalanx taihuensis* myofibrillar protein**	0-600 W 60 min	● Ultrasound treatment at 600 W for 60 min increased by EAI and ESI ~1.52-fold and ~3.32-fold, respectively. ● Emulsion stabilized by sonicated protein showed smaller oil droplets and a more homogeneous microstructure.	(Deng et al., 2023)
Silver carp myofibrillar protein	40 kHz 0-520 W 30 min	● With the increase of ultrasonic power, the size of emulsion droplets decreased, and the distribution became more uniform. ● Interfacial adsorbed protein increased from ~74.01% to ~84.56%, interfacial tension reduced from ~7.92 mN/m to ~6.02 mN/m, as ultrasonic power increased from 0 to 390 W.	(Hong et al., 2024)

Shrimp myofibrillar protein	20 kHz 100, 300, 500 W 60 min	● Improved emulsification performance, increased EAI from ~35.48 m^2/g to ~62.01 m^2/g, increased ESI from ~71.40 min to ~166.75 min.	(Li et al., 2022)

This literature review includes an introduction to the New Zealand green-lipped mussel, proximate analysis for fresh and dried mussels, and amino acid composition for other species of mussel powder. It also introduces some modification techniques for seafood proteins. Some studies were performed on the effect of ultrasound treatment on the structure, physicochemical, and functional properties of mussel proteins or the effect of starch on heat-induced surimi gels. However, there is limited research on the effect of the treatments on the structure, physicochemical, and functional properties of proteins of green-lipped mussels.

The purposes of this thesis are:

- To study the effect of pH and ultrasound treatment on the structure, physicochemical, and functional properties of desalted MPC dispersions
- To study the change in the microstructure and rheological properties of heat-induced defatted MPC gels containing different concentrations and types of starches.

3. Chapter 3: Effect of ultrasound treatment on desalted mussel protein concentrates (MPC): physicochemical and functional properties at different pH values

Keywords: Mussel protein concentrates; Ultrasonication; emulsion; gelation; Microstructures

3.1. Introduction

The burgeoning world population alongside increasing cravings for meat and seafood have led to the expansion of aquaculture. The growing demand for animal protein has also driven the mussel farming industry in recent years. The main species of aquaculture in New Zealand are Green-lipped mussel (*Perna canaliculus*), Chinook salmon (*Oncorhynchus tschawytscha)*, and Pacific oysters (*Crassostrea gigas*), and Green-lipped mussels account for a large proportion of aquaculture. In 2019, 97,462 metric tons of Green-lipped mussels were harvested, which was much higher than other two species. New Zealand is one of the most essential mussel producers worldwide. The export revenue of Green-lipped mussels in 2019 was NZ $336 million (Stenton-Dozey, 2021). New Zealand government projects annual aquaculture revenues to reach NZ$3 billion by 2030 (Stenton-Dozey, 2021). The green-lipped mussel, also known as Greenshell™ mussel, is a shellfish endemic to the coast of New Zealand. The green-lipped mussel is so versatile that it can be eaten directly as a food or as a dietary supplement. Green-lipped mussel extract except shell contains about 56-61% crude protein, 9.6-12% carbohydrate, and 10-10.8% lipids in its dried form. It is abundant in vitamins and omega-3 fatty acids, making it an indispensable part of the local Maori people's diet (Abshirini, 2022; Ulbricht et al., 2009).

Proteins have been widely used and studied in the food industry because of their rich nutritional values and safety considerations (Chen et al., 2006). Proteins also play an important role in the production of functional foods (Yu, Wu, et al., 2018). Green-lipped mussel contains various proteins, including myofibrillar protein, sarcoplasmic proteins and stromal proteins (Zou et al., 2020). It could be used as a reliable source of protein for all these purposes.

Various techniques are applied in food processing to enhance protein functionality, including heat treatment, high-pressure processing (HPP), ultrasound treatment, and enzymatic hydrolysis (Xue et al., 2018). These methods are used to modify the

solubility, foaming, gelation, and other physicochemical properties of protein. Ultrasound, a non-heat technology, is quite popular and famous in food processing due to safety, high efficiency, economy, and environmental friendliness (Bangar et al., 2022). Most current studies focus on plant-based, animal, and dairy products. Recently, several researches have studied the effects of ultrasound treatment on fish and shellfish proteins, such as myofibrillar protein from frozen shrimp (Li et al., 2023), fish myofibrillar protein (Rajasekaran et al., 2023). Various studies revealed that ultrasonic processing promoted proteins' physicochemical, technical, and functional properties, such as enhancing the gel strength, and extending emulsions' storage stability, improving the emulsifying and water-holding capacity (Ma et al., 2019; Rajasekaran et al., 2023). For example, Yu, Wu, et al. (2018) studied the influence of different ultrasound treatment power and time on mussel (*Mytilus edulis)* protein isolate, they found that ultrasound can improve solubility, water retention capacity, emulsion stability and rheological characteristics; minimize the particle size and make the dispersion more stable.

However, there is no available information about the application of ultrasound treatment to modify the physicochemical and techno-functional properties of proteins from Green-lipped mussels. The primary purpose of this research is to study how ultrasound treatment affects the structure, physicochemical, and techno-functional characteristics of mussel proteins. In addition, considering the significant application of heat-induced gel and emulsification in food technology, this paper also investigates the influence of ultrasonic processing on the heat-induced gelation and emulsification of mussel protein.

3.2. Materials and methods

3.2.1. Materials

Defatted mussel powder was donated by Sanford Ltd (New Zealand). It composed of

48.6% crude protein, 4% fat, 14.3% carbohydrate, 29.1% ash, and 4% moisture. Chemicals for Bradford protein assay, Bradford agent and standard protein solution; and other chemicals for preparing samples, including sodium azide (≥99%), hydrochloric acid (HCl, 37%), sodium hydroxide (NaOH, ≥98%), were bought from Sigma-Aldrich (St. Louis, MO, USA). Various chemicals essential for conducting SDS-PAGE, such as 4× Laemmli sample buffer, Mini-PROTEIN TGX gels (Cat.# 4561083, Bio-Rad), were all purchased from Bio-Rad (Hercules, CA, USA). Soybean oil used for preparing emulsions was bought in a local supermarket (PAKnSave, Albany) in Auckland. RO water was used to prepare samples in this study. All these chemicals, unless specified otherwise, were of analytical grade.

3.2.2. Preparation of mussel protein concentrates (MPC)

In this research, defatted mussel powder provided by Sanford Ltd (New Zealand) was a by-product of commercial oil extraction. The treatment of the raw defatted mussel powder was mainly divided into three steps: The first step was screening and filtration. About 100 g of untreated defatted mussel powder with uneven particle size and high salt content was passed through a 500-micron sieve, and powder with particle size less than 500 μm was collected. This step is to remove large particles. The second step was desalting by centrifugation. Defatted mussel powder with particle size less than 500 μm obtained in the first step was dissolved in RO water; the weight ratio of powder to RO water was about 1:5, then these samples were centrifuged by a centrifuge (Sigma 6-16KS Osterode am Harz, Germany) at 10000 g for 10 min at 20 ℃. An EC meter (HI98304, HANNA instruments, UK) was used to measure the electric conductivity of the supernatant after centrifugation, compared the electric conductivity of RO water and that of supernatant after each centrifugation until the supernatant was no longer cloudy and the electric conductivity of final supernatant was below 120 μS/cm. Centrifugation was performed at the same condition 6 times in total to remove more salt in this step. The third step was freeze-dried. Put the wet powder obtained in the

second step in a freezer at -20 ℃ for about a week and then put it in a freeze dryer (model 7753034, Labconco, USA) for seven days to remove excess moisture and obtain a dry powder. A mortar and pestle were used to grind powder, then stored in an airtight container with parafilm and in the desiccator to avoid absorbing moisture for further use. Kjeldahl method was used to determinate crude protein content of desalted mussel powder, it contained 69.5% crude protein. The nutrition lab of Massey University (Palmerston North, New Zealand) conducted the mineral test (**Table 14**), and amino acid composition (**Table 15**) analysis of desalted mussel protein concentrates (MPC).

Table 14: Minerals content of desalted mussel powder.

Minerals (mg/kg)	**Desalted mussel powder**
Calcium	11900
Magnesium	1220
Potassium	310
Sodium	<300
Phosphorus	6000
Iron	1610
Chromium	7.7
Copper	8.1
Iodine	32
Manganese	40
Selenium	2.1
Zinc	97
Chloride	<100
Arsenic	6.0
Cadmium	0.47
Lead	0.83

Table 15: Amino acids composition of desalted mussel powder.

Amino Acids (mg/100 mg)	Desalted mussel powder
Aspartic Acid	7.92
Threonine	3.38
Serine	3.46
Glutamic Acid	7.79
Proline	2.49
Glycine	3.04
Alanine	2.62
Valine	3.41
Isoleucine	3.05
Leucine	4.21
Tyrosine	2.64
Phenylalanine	3.26
Histidine	1.14
Lysine	5.55
Arginine	4.69
Cysteine	0.97
Methionine	2.15

3.2.3. Ultrasound treatment of MPC dispersion

Desalted mussel powder was dispersed in RO water containing 0.02% w/w sodium azide to prepare 5 w/w % MPC dispersion. The 5% MPC dispersion was stirred gently at room temperature over weekends to make it fully hydrated. Then the dispersion was divided into 4 parts, the pH was adjusted to 3, 5, 7, 9, using 1M and 2M HCl and 1M NaOH. The dispersions were stirred for 6 hours, checked pH, and adjusted to target pH regularly until pH was stable. MPC dispersion at pH 7 was used as an example to

investigate the optimal ultrasonication duration of MPC. Then a 10 g MPC sample at pH 7 was treated by a 20 kHz ultrasonic processor (JY92-IIN, Ningbo Scientz Biotechnology Co., Ltd, China) furnished with 6mm probe under 2s on/2s off mode at 34 W for 0, 1, 5, 10, 15, 20, 30 min. All MPC solutions were put in the combined ice water bath during ultrasound treatment to avoid sample denaturation caused by excessive temperature, ice water was changed regularly to ensure the temperature below 20 ℃. Based on the subsequent results, ultrasonication for 15 min was the optimal condition. Therefore, MPC dispersions at pH 3, pH 5, pH 7, and pH 9 were sonicated (20 kHz, 34 W/10 g sample) for 15 min for further studies. The control group is MPC dispersions at different pH (3, 5, 7, 9) without ultrasound treatment. Calorimetry was used to calculate the ultrasonic intensity (Jambrak et al., 2008).

3.2.4. Determination of particle size distribution (PSD) and zeta potential

A Mastersizer 3000 (Malvern Instruments Ltd, Malvern, UK) was used to measure the particle size distribution, D [4,3] and D [3,2] of MPC dispersions at pH 3, 5, 7, 9 before and after ultrasound treatment. D [4,3] and D [3,2] are the mean particle diameter based on volume and surface area, respectively (Surh et al., 2006).

$$D[4,3] = \frac{\sum n_i d_i^4}{\sum n_i d_i^3} \quad (2)$$

$$D[3,2] = \frac{\sum n_i d_i^3}{\sum n_i d_i^2} \quad (3)$$

where n_i represents the number of particles with diameter d_i. The refractive index of mussel protein solution was 1.33 (C. Liu et al., 2021). A Zetasizer (Nano-ZS, Malvern Instruments Ltd., UK) was used to measure the zeta potential of MPC dispersions at pH 3, 5, 7, 9 before and after ultrasound treatment. pH-adjusted RO water was used to dilute MPC samples from 5% to 0.1%. All samples were measured in triplicates at 20 ℃ and calculated the average and standard deviation.

3.2.5. Determination of solubility

To obtain more precise results and minimize errors, the solubility of MPC dispersion was measured on the day of the end of ultrasound treatment. A standard absorbance-versus-protein concentration curve was generated by plotting the concentration of standard protein solution (mg/mL) as the x-axis and the absorbance value at 595 nm as the y-axis in advance. MPC samples were centrifuged at 5000 g for 15 min at 20 ℃ by a centrifuge (Thermofisher 3000, MO, USA). Collected supernatants after the centrifugation step. Bradford method was used for determination of the protein content in the supernatant.

The supernatants were diluted with pH-adjusted RO water to various concentrations to achieve an absorbance within the 0.2 to 0.5 range. Then, samples were transferred to cuvettes, the absorbance of these samples at 595 nm was determined by a spectrophotometer (Shimadzu 2000, Kyoto, Japan). Protein solubility was determined according to the following formula. Each sample was determined in duplicate, the mean and standard deviation were calculated.

$$(\%)\text{Protein Solubility} = \frac{\text{Protein content in the supernatant}}{\text{Total protein content}} \times 100 \quad (4)$$

3.2.6. Sodium dodecyl sulphate polyacrylamide gel electrophoresis (SDS-PAGE)

SDS-PAGE was carried out using the reducing condition to investigate the difference in mussel protein composition before and after ultrasound treatment at pH 3, 5, 7, 9 (Liu et al., 2009). 5% MPC dispersion was diluted to 0.2 v/v % using 2 w/w % SDS solution, then incubated overnight at room temperature. 25 µl 0.2% MPC sample was thoroughly mixed with 1.5 µl β-mercaptoethanol and 12 µl 4× Laemmli sample buffer, then boiled for 20 min. 10ul of boiled samples were loaded into the well of Mini-

PROTEIN TGX Gel (Bio-Rad Laboratories, USA). Electrophoresed at 130 v in the running buffer for about 45 mins, the gel was stained using staining solution under shaking for 45 min and then destained about 3-4 times. Checked the color of the solution in the container regularly and stopped destaining until it became clear, not blue. A standard protein marker (Precision Plus Protein Dual Xtra Standards) (Catalog # 161–0377, Bio-Rad, USA) between the range of 10 and 250 kDa was used to identify different molecular weights of the mussel protein. ChemiDoc touch imaging system (Bio-Rad, USA) was used to scan the gel.

3.2.7. Rheological measurements of heat-induced MPC gelation

Heat-induced (90 ℃ for 30 min) method was used to form MPC gel. A stress-controlled rheometer (DHR-3, TA instruments, New Castle, DE, USA) fitted with a parallel plate geometry (40 mm diameter, 1 mm gap) was used to perform rheological measurements. 10 w/w % untreated MPC dispersions and 5 w/w % sonicated MPC dispersions at different pH levels were prepared according to 3.2.3 procedure. For 10 w/w % sonicated MPC dispersions, put 5 w/w % sonicated MPC dispersions at pH 3, 5, 7, 9 into the freezer for 3 days and a freeze dryer (model 7753034, Labconco, USA) was used to get dried sonicated MPC powder. Different pH powders and corresponding pH buffers were mixed in a radio of 1:9. The reason can be that 10 w/w % of the MPC solution was very viscous, and ultrasound direct treatment may not achieve the desired effect.

About 1.5 mL MPC dispersion was placed on the rheometer plate using a dropper; some dispersion was added or removed to ensure it fitted the geometry. Soybean oil was dripped around the sample to prevent it from evaporating during measurements. The rheological analysis was performed as following: (1) at first, the 10% MPC dispersion was heated from 20 ℃ to 90 ℃ at 2 ℃/min, MPC samples were kept at 90 ℃ for 30

min before being cooled down from 90 ℃ to 20 ℃ at 2 ℃/min, then holding at 20 ℃ for 15 min. during the above measurements, the strain and frequency were held at 1% and 1 Hz, respectively; (2) subsequently, a frequency sweep measurement was carried out with a consistent 1% strain, while the frequency ranged from 0.01 to 10 Hz; (3) finally, a strain sweep measurement was carried out with a consistent 1 Hz, while the strain ranged from 0.01% to 1000%.

3.2.8. Microstructure observation by using Confocal Laser Scanning Microscopy (CLSM)

CLSM was used to observe microstructures of MPC dispersions before and after ultrasound treatment and compare MPC dispersions and gels after heat treatment. First, about 50 µl MPC sample was mixed with 10 µl fast green dye (Sigma Aldrich, USA) in the Eppendorf tube, shaken gently and waited for 2 min to make samples fully dyed. Then, mixture samples were transferred to the microscopy slide with a single cavity and covered with a glass coverslip. Glass slides with MPC samples were incubated in an oven at 90 ℃ for 30 min for those gel samples. All samples were sealed with nail polish to avoid evaporation. A confocal laser scanning microscope equipped with a 100 × oil immersion objective lens was used to observe the microstructure characteristics of MPC dispersions and gels. All acquired images were processed by Image J software (USA).

3.2.9. Preparation of O/W emulsions stabilized by sonicated MPC

Ultrasonicated MPC dispersions at different pH levels were mixed with soybean oil in a 3:7 ratio (v/v) using a high shear mixer (T10 basic ULTRA-TURRAX®, IKA Corp., Staufen, Germany) fitted with a 10 mm probe (S10N-10 G, IKA, Germany). The

mixtures were then homogenized at 20,000 rpm for 5 min. The oil volume fraction of all emulsions was 70%. Emulsions were stored at room temperature; all measurements were duplicated and finished in 2 days.

3.2.10. Determination of oil droplet size of the emulsions

A Mastersizer 3000 (Malvern Instruments Ltd, Malvern, UK) was used to measure the oil droplet size of emulsions with or without 1% SDS solution. The refractive index of soybean oil and ultrasonicated MPC dispersions were 1.47 and 1.33 respectively (Cha et al., 2019). An appropriate amount of 1% sodium dodecyl sulfate (SDS) solution was added to emulsions; this step aimed to break up oil droplet flocculation (McClements, 2016).

3.2.11. Microstructure

The microstructures of all emulsions stabilized by sonicated MPC were observed by an optical microscope (Olympus BX53, New Zealand) equipped with a camera (Olympus DP74, New Zealand). An appropriate emulsion was dropped onto a microscope slide and covered with a cover slide. Observations were conducted at a magnification of 40× (Campana & Moksness, 1991).

3.2.12. Flowability of emulsions

The freshly made emulsions at different pH levels were photographed on the workbench and recorded simultaneously. The yellow plastic bottle containing the emulsion was turned upside down and photographed again to record its flowability.

3.2.13. Rheological properties of emulsions

Rheological measurements were conducted using the same rheometer mentioned in this study. During the measurements, the rheometer recorded the storage modulus (G') and loss modulus (G''). A spatula was used to transfer the emulsion onto the bottom plate. The emulsion sample was trimmed properly, soybean oil was dripped around the emulsion to prevent evaporation during the process. The steps for measuring MPC emulsion rheological properties were performed as following: (1) first of all, a 30 min time sweep measurement was carried out at 1 Hz and 1% strain; (2) then, a frequency sweep measurement was performed with a consistent 1% strain, while the frequency ranged from 0.01 to 10 Hz; (3) finally, a strain sweep measurement was carried out with a consistent 1 Hz, while the strain ranged from 0.01% to 1000%.

Then, new MPC emulsions were used to conduct the viscosity measurement, and the steps as followed: (1) first, a time sweep measurement was carried out at constant of 1% Hz and 1% strain for 30 min; (2) secondly, the shear rate increased from 0.1 to 1000 s^{-1}; (3) thirdly, the shear rate decreased from 1000 to 0.1 s^{-1}. All measurements were conducted at 20 ℃. Origin Pro software (OriginLab, USA) was used to plot the figure of the viscosity as a function of the shear rate and calculate the area between up measurements and down measurements, which can estimate the degree of thixotropy of emulsions stabilized by ultrasonicated MPC.

3.2.14. Statistical analysis

All experiments were measured in duplicate. The results were expressed as the mean ± standard deviation of at least two experiments. Minitab Software (Minitab 2021, USA)

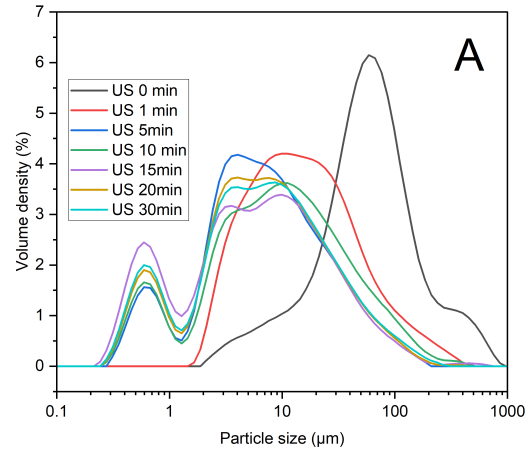
was used to conduct a one-way analysis of variance (ANOVA). Significant differences between samples were assessed using Tukey's test with a significance level of $P < 0.05$. Origin Pro Software (Origin Pro 2024b, USA) was used to plot figures. Image J Software (Fiji, USA) was used to analyze CLSM images.

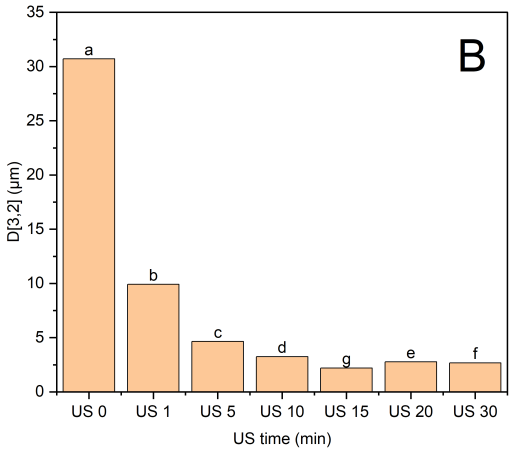
3.3. Results and discussions

3.3.1. The influence of ultrasonication and pH on MPC particle size, zeta potential and solubility

Particle size is one of the essential indicators of protein products. D [4,3] and D [3,2] are the mean diameters of the particle size based on volume-weighted and area-weighted mean results, respectively. The pre-experiment showed that ultrasound treatment for 15 min can notably diminish the D [3,2] and D [4,3] of MPC dispersion, from ~30.7 μm to ~2.2 μm, from ~98.7 μm to ~16 μm, respectively (**Figure 3 B and C**). As the ultrasound time increased from 0 to 15 min, the particle size first reduced greatly before becoming stable. However, with excessively extended ultrasound time, the MPC particle size increased slightly. This finding agreed with other studies. Zou et al. (2020) found a narrower particle size distribution (PSD) and smaller mean particles of mussel sarcoplasmic protein after ultrasound at 600 W for 10 min, from ~1081.3 nm to ~151.7 nm. Their study also suggested that when ultrasound time was further extended to 30 min, the mean particle size of mussel sarcoplasmic protein would increase to ~286.3 nm. It has been widely reported that ultrasound can reduce protein particles, including plant, dairy, and animal proteins. The reduction of particle size can be explained by the shock wave, shear force, cavitation effect generated during the ultrasonic process. These forces disrupt non-covalent interactions (including hydrogen bonding, hydrophobic and electrostatic interactions), promote the disintegration of protein aggregates, and decrease particle size (Ma et al., 2019; Yu, Li, et al., 2022).

Nevertheless, extended ultrasonic processing would lead to excessive protein denaturation, intensifying molecules' propensity towards random aggregation (Zou et al., 2020). Therefore, the MPC sample treated with ultrasonication for 15 min was chosen for subsequent research.





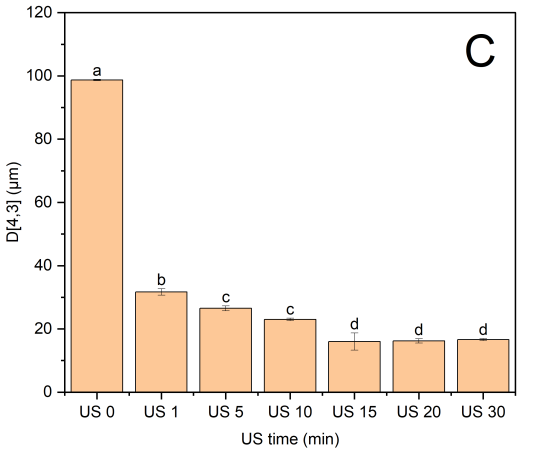


Figure 3: PSD (A), D [3,2] (B), D [4,3] (C) of mussel protein concentrates (MPC) dispersions at pH 7 depending on ultrasound treatment time. A significant difference (P<0.05) in the ultrasound time is shown by different letters above the columns.

Figure 4 A and B showed the PSD of 5% MPC dispersions at different pH (3, 5, 7, 9) before and after ultrasound treatment for 15 min. The untreated group exhibited a considerably large particle size and only had a single peak, this meant that these particles had similar size and exhibited a relatively uniform distribution. The PSD of the ultrasonication group was bimodal, it implied that each sample had two groups of particles with distinct size ranges after ultrasound treatment. Particles were mainly distributed between 10 and 100 μm for the control group, while some particles of the ultrasonication group were less than 1 μm. As shown in **Figure 4 C and D**, D [3,2] and D [4,3] of all untreated MPC samples considerably less than those of sonicated samples. Changes in D [3,2] and D [4,3] also proved that ultrasound treatment decreased the particle size significantly. In addition, pH also affected the PSD, D [3,2] and D [4,3] of MPC dispersion. For the untreated group, samples at all pH showed the similar PSD. However, for sonicated group, the PSD was different at various pH, many small particles (between ~0.1μm and ~1 μm) and some large particles (between ~2 μm and ~300 μm) were formed at pH 3; more medium-sized particles (between ~1 μm and ~10 μm) were formed at pH 5. D [3,2] and D [4,3] results also indicated this. pH 3 had the smallest D [3,2] and the largest D [4,3]; pH 5 was the opposite. pH 7 and pH 9 showed the same trend in PSD, D [3,2] and D [4,3].

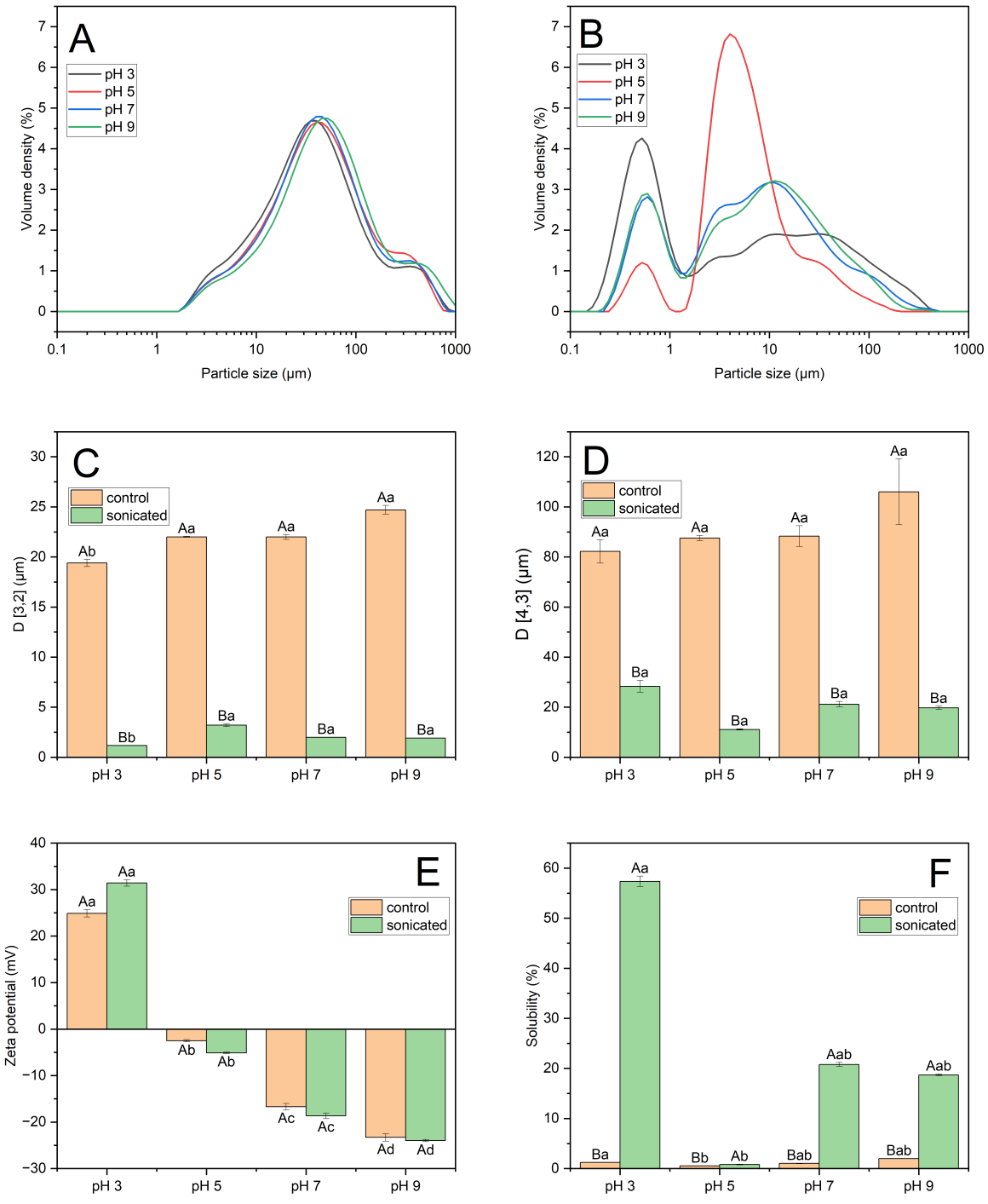


Figure 4: PSD of MPC dispersions at various pH levels before (A) and after (B) ultrasound treatment. D [3,2] (C), D [4,3] (D), zeta potential (E), solubility (F) of MPC dispersions before and after ultrasound treatment as a function of pH changes. A significant difference (P<0.05) in ultrasound treatment and pH values is shown by different capital and lowercase letters above the columns, respectively.

The zeta potential is an essential indicator to assess the stability of a colloid system, representing the degree of mutual repulsion or attraction between particles (Grisham & Nanda, 2020). If a system has a high absolute value (above 30 mV), it could be considered as a stable system. Conversely, a small absolute zeta potential value (0~10 mV) indicates an increased tendency for aggregation or coagulation, the system could be considered as an unstable system (Cano-Sarmiento et al., 2018). **Figure 4 E** revealed that the absolute zeta potential values of all MPC samples increased after ultrasound treatment. This implied that after ultrasound treatment, the particles of all MPC samples became smaller, and all MPC dispersion systems became more stable. The result coincided with the tendency of the particle size obtained from the Mastersizer 3000. On the one hand, the zeta potential of MPC samples at pH 3 was positive, indicating that pH 3 MPC samples contained more positively charged particles than negatively charged ones; on the other hand, other MPC samples exhibited a negative zeta potential, including pH 5, pH 7, pH 9. **Figure 4 E** also showed that the isoelectric point (pI) of MPC was between pH 4 and pH 5. Previous studies proved that the isoelectric point of mussel was close to pH 5. Liu et al. (2009) found that the isoelectric point of freshwater pearl mussel (*Hyriopsis cumingii)* protein isolate was pH 5.

It is essential to determine the solubility of proteins when studying physicochemical properties of proteins because the solubility of proteins impacts various critical functional properties, including foaming, emulsification, gelation, texture, color, and viscosity (Jambrak et al., 2008). From **Figure 4 F**, untreated MPC dispersion at all pH values showed very low solubility. The solubility of the sonicated group improved noticeably except for pH 5 samples when compared to the untreated group. The reason why ultrasonication increases protein solubility can be summarized as follows: The intense physical force of the ultrasound disrupts protein aggregates and some bonds, helps unfold the protein structure and expose hydrophilic amino acids. Ultrasound leads to a reduction in protein particles, increases the surface area of the protein in contact

with water and encourages water-protein interactions. In addition, ultrasound treatment changes some insoluble protein aggregates into soluble protein aggregates when the protein particles decrease (Li et al., 2023; Nazari et al., 2018; Yu, Li, et al., 2022). In addition, earlier findings suggested that pH values affected the protein's solubility; proteins had low solubility when the pH value was around the isoelectric point (Liu et al., 2009). Taking the sonicated group as an example, the solubility of the pH 3 sample was the highest at ~56.3%, almost 3 times that of pH 7 (~20.8%) and pH 9 (~18.7%). The solubility of pH 7 and pH 9 was very similar. However, for pH 5 sonicated samples, the solubility was very low at ~0.8%. The reason was that pH 5 was around the isoelectric point of MPC (Surasani et al., 2018). As the pH value near the isoelectric point, the solubility was at its lowest level, but once the pH was away from pI, the solubility would be increased (Liu et al., 2009; Tang, 2007; Zhao et al., 2013).

3.3.2. SDS-PAGE

The protein profile of MPC before and after ultrasound treatment at different pH levels was identified by reducing SDS-PAGE. As **Figure 5** shows, a protein band was seen in the top loading well, which indicates that there were proteins with molecular weights greater than 250 kDa. This may comprise myosin-heavy chains and some protein aggregates (Konieczny et al., 2021). The results indicated that ultrasound treatment and pH changes did not lead to apparent alterations of the mussel protein bands. The finding agreed well with the research performed by Yu, Wu, et al. (2018). They concluded that the protein profile of the mussel did not alter with the increasing ultrasound treatment intensity and duration. Moreover, there were two visible protein bands in **Figure 5**, the protein bands at 43 kDa and 100 kDa could be considered actin (43–46 kDa) and paramyosin (98–107 kDa), respectively, according to previous mussel studies (Konieczny et al., 2021; Liu et al., 2009; Yu, Wu, et al., 2018). The protein bands on SDS-PAGE were a little light which could be due to low solubility and large aggregate

of mussel protein (López et al., 2002).

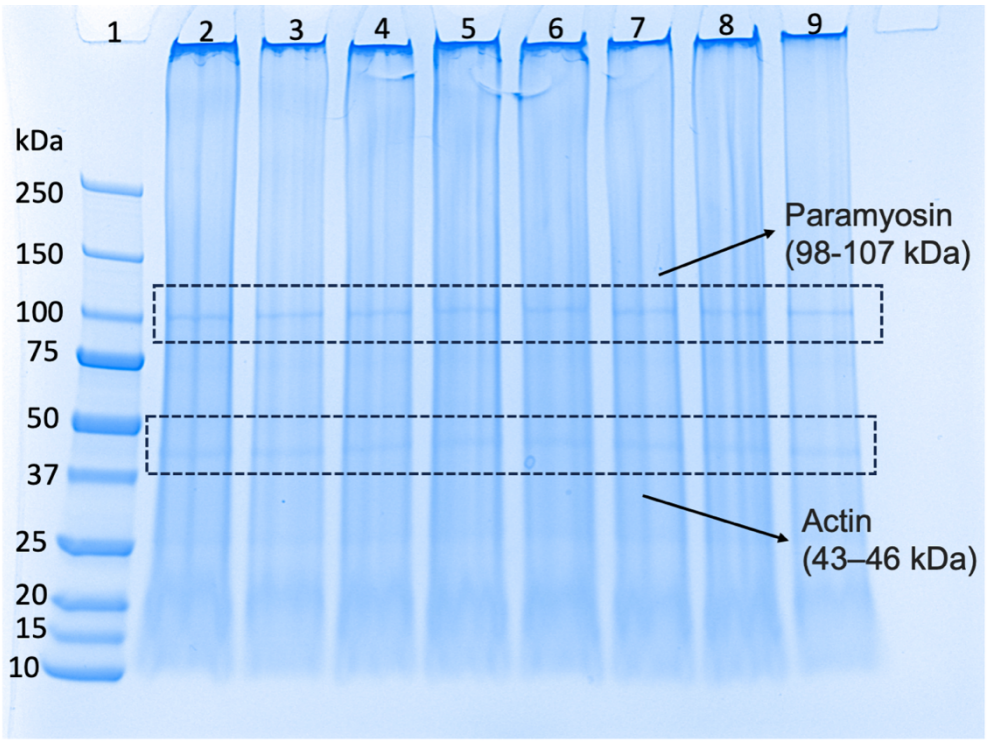


Figure 5: SDS-PAGE of MPC under reducing condition. Lane 1- molecular weight marker; Lane 2-untreated MPC at pH 3; Lane 3-untreated MPC at pH 5; Lane 4-untreated MPC at pH 7; Lane 5-untreated MPC at pH 9; Lane 6-sonicated MPC at pH 3; Lane 7- sonicated MPC at pH 5; Lane 8- sonicated MPC at pH 7; Lane 9- sonicated MPC at pH 9.

3.3.3. Viscoelastic properties of heat-induced gelation

Figure 6 illustrates the curves of storage modulus (G') and loss modulus (G'') of the MPC as well as the temperature at different pH levels (3, 5, 7, 9) before and after ultrasound treatment with time. For all samples, G' and G'' consistently increased during the stage of the temperature ramp (20 ℃ to 90 ℃), temperature holding (90 ℃ for 30 min), and temperature decrease (90 ℃ to 20 ℃). This was agreed well with other studies, Ding et al. (2012) studied rheological properties of actomyosin from grass carp and yellowcheek carp during heat gelation, they found that G' increased first as the temperature increasing, then decreased and reached a valley at 45 ℃ or 49 ℃,

respectively. *G′* continued to increase during subsequent temperature ramp and decrease. The initial increase in *G′* may be due to the separation of the light and heavy subunits of myosin at low temperatures, which led to the formation of association between myosin filaments to form a loose network structure (Benjakul et al., 2001; Ding et al., 2012). The myosin protein molecular chains unfolded when the temperature kept rising and was higher than its denaturation temperature. Their internal hydrophobic groups were exposed, forming some hydrogen bonds and intermolecular hydrophobic interactions, then the protein molecules began to aggregate slowly and formed a new 3D network structure (Ding et al., 2012). When the temperature was constant at 90 °C, the aggregation rate between proteins accelerated, leading to a more elastic gel being formed. During the stage of temperature cooling, the formed gel network structure became more compact due to hydrogen bonds (Park, 2014).

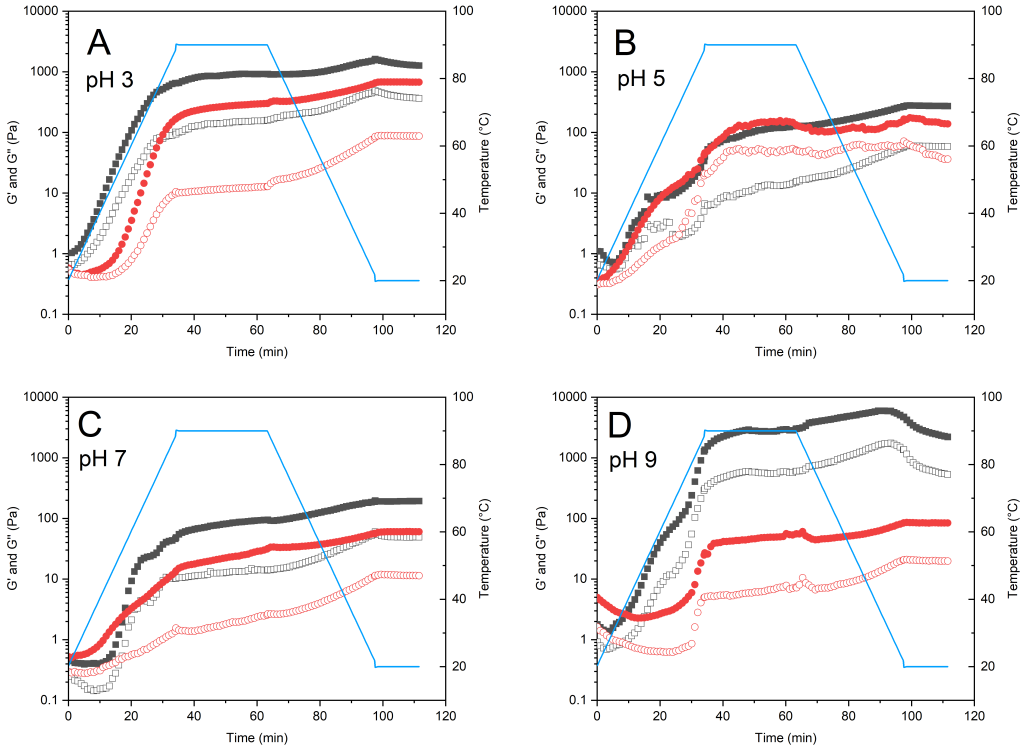


Figure 6: During heat-induced gelation, *G′* (solid symbol) and *G″* (open symbol) of untreated and sonicated MPC samples at different pH as a function of temperature and time. The blue curve represents the temperature change. Symbols are untreated MPC samples (■), sonicated MPC samples (●).

After the sample was cooled from 90 ℃ to 20 ℃, it was held at 20 ℃ for 15 min to reconstruct the gel network. Then frequency sweep and strain sweep were performed to test the small deformation and large deformation rheological behavior of MPC gels. The dependence of viscoelasticity of the MPC gels with frequency is shown in **Figure 7**. For all MPC samples, G' was always higher than G'' during the whole frequency range, but the ratio of G' and G'' was less than 10 times, G' and G'' increased mildly with frequency increasing, showing an elastic behavior, and could be seen as weak gels (Khokhlov & Osada, 2002). To compare the gel strength of MPC before and after ultrasound treatment and at different pH values, the G' at 1 Hz was also plotted. Overall, ultrasound treatment reduced the gel strength of MPC. For untreated samples, G' of MPC gel at pH 9 was the largest among all pH, about ~1999.7 Pa, followed by G' at pH 3 (~1291.5 Pa). Both G' at pH 5 (~131.4 Pa) and pH 7 (~67.4 Pa) were very low. All G' values at pH 3, pH 5, pH 7, and pH 9 decreased after ultrasound treatment. Furthermore, the reduction of G' at pH 9 was the most obvious, from ~1999.7 Pa to ~74.5 Pa. Interestingly, most studies reported that ultrasound treatment improved the gel strength of proteins, such as myofibrillar protein (Amiri et al., 2018), soybean protein (Cui et al., 2019), chicken protein (Zhang et al., 2021), which was the opposite of the conclusion reached in this experiment. Although there are very limited reports on the reduction of protein gel strength by ultrasound treatment, there is a study has reported that another treatment does not increase protein gel strength. Janssen et al. (2024) found that homogenization did not affect the final G' for faba bean protein and pea protein gels during heat-induced gelation. Different protein source may lead to different results (gel strength increase or decrease).

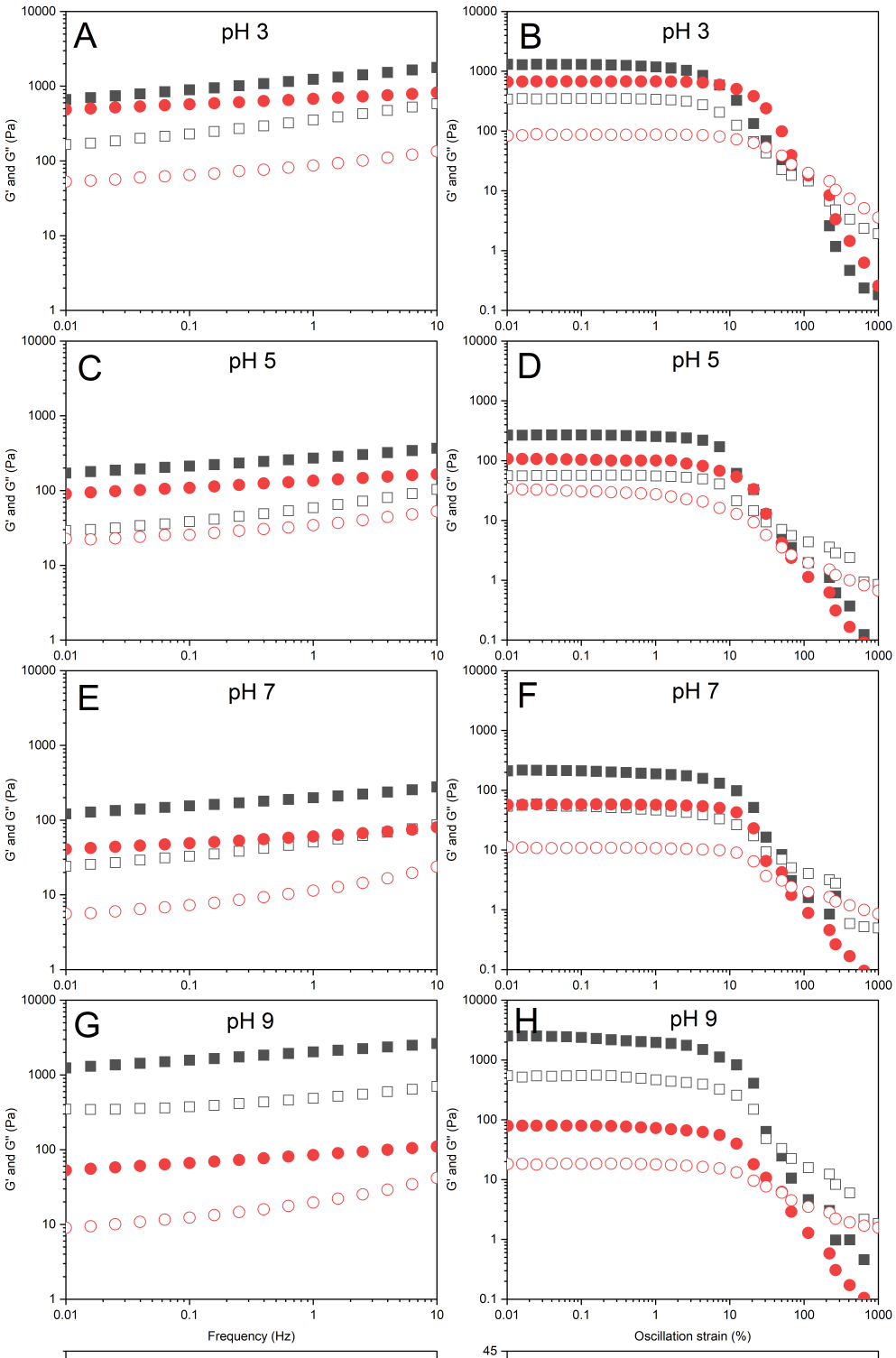

A
pH 3
B
pH 3
C
pH 5
D
pH 5
E
pH 7
F
pH 7
G
pH 9
H
pH 9
G' and G'' (Pa)
Frequency (Hz)
Oscillation strain (%)
I
control
sonicated
G' at 1 Hz (Pa)
Aa
Ba
Aa
Ba
Aa
Ba
Aa
Ba
pH 3
pH 5
pH 7
pH 9
J
control
sonicated
Breaking stress (Pa)
Aab
Bab
Ab
Bb
Ab
Bb
Aa
Ba
pH 3
pH 5
pH 7
pH 9

Figure 7: G' (solid symbol) and G'' (open symbol) as a function of frequency (A, C, E, G) and strain amplitude (B, D, F, H) for heat-induced MPC gels. Symbols are untreated MPC samples (■), sonicated MPC samples (●). G' (1 Hz) (I) and breaking stress (J) of untreated (control) and sonicated MPC gels as a function of pH values. A significant difference (P<0.05) in ultrasound treatment and pH values is shown by different capital and lowercase letters above the columns, respectively.

The strain sweep of MPC gels is shown in **Figure 7**, where G' and G'' were plotted relative to the applied strain amplitude. For all MPC samples, they showed similar trends. Within the linear viscoelastic region (LVR), G' was always higher than G''; no matter how the strain changed, G' and G'' did not change with the applied strain, and all MPC gel samples suggested a linear viscoelastic behavior. However, once the critical value of LVR was exceeded, G' and G'' reduced greatly, with G' dropping more rapidly, resulting in the intersection of G' and G'', which was of great significance in gelation studies, and the corresponding stress of this point (G'=G'') was referred to as the breaking stress (Yang et al., 2022). The breaking stress result was consistent with G' at 1 Hz. Ultrasound treatment decreased the breaking stress. Untreated MPC gel at pH 9 had the highest breaking stress, suggesting it could withstand higher stress than other samples without being damaged. Then, with further increase in the applied strain, G'' was higher than G', indicating that the gel was severely disrupted. The large deformation rheological behavior was consistent with the small deformation rheological behavior.

3.3.4. CLSM

CLSM was employed to compare the microstructures of MPC at different pH levels before and after ultrasound and heat treatment (**Figure 8**). The protein stained by Fast Green appeared as green, while the voids in between the protein particles appeared as black. Some protein aggregates were due to large particle size and low solubility for all untreated MPC dispersions. Moreover, it can be observed that the untreated MPC dispersion at pH 5 had the largest particles, this was because proteins were more likely

to aggregate around the isoelectric point (Li et al., 2020). For MPC dispersions, ultrasound treatment decreased the protein particle size. Previous MPC dispersion particle size results also proved this. Compared to MPC dispersions, all MPC gels at different pH levels after heat treatment showed interconnected protein network structures. In general, after heat treatment, proteins are denatured, exposing more internal hydrophobic groups, and protein-protein interactions are enhanced, leading to cross-linking of proteins and forming a dense network structure (Luo et al., 2021). For untreated gels, there were big black voids in pH 5 and pH 7 samples images but small black voids in pH 3 and pH 9 samples, suggesting untreated pH 3 and pH 9 gels had denser protein gel network structures than pH 5 and pH 7 gels. This was consistent well with the rheological measurements. In addition, heat-induced MPC gels after ultrasound treatment exhibited more homogeneous and delicate microstructures than untreated samples. Previous studies also indicated that the protein gel network became uniform after ultrasound treatment, such as chicken plasma protein (Zou et al., 2021), myofibrillar protein (Wen et al., 2017).

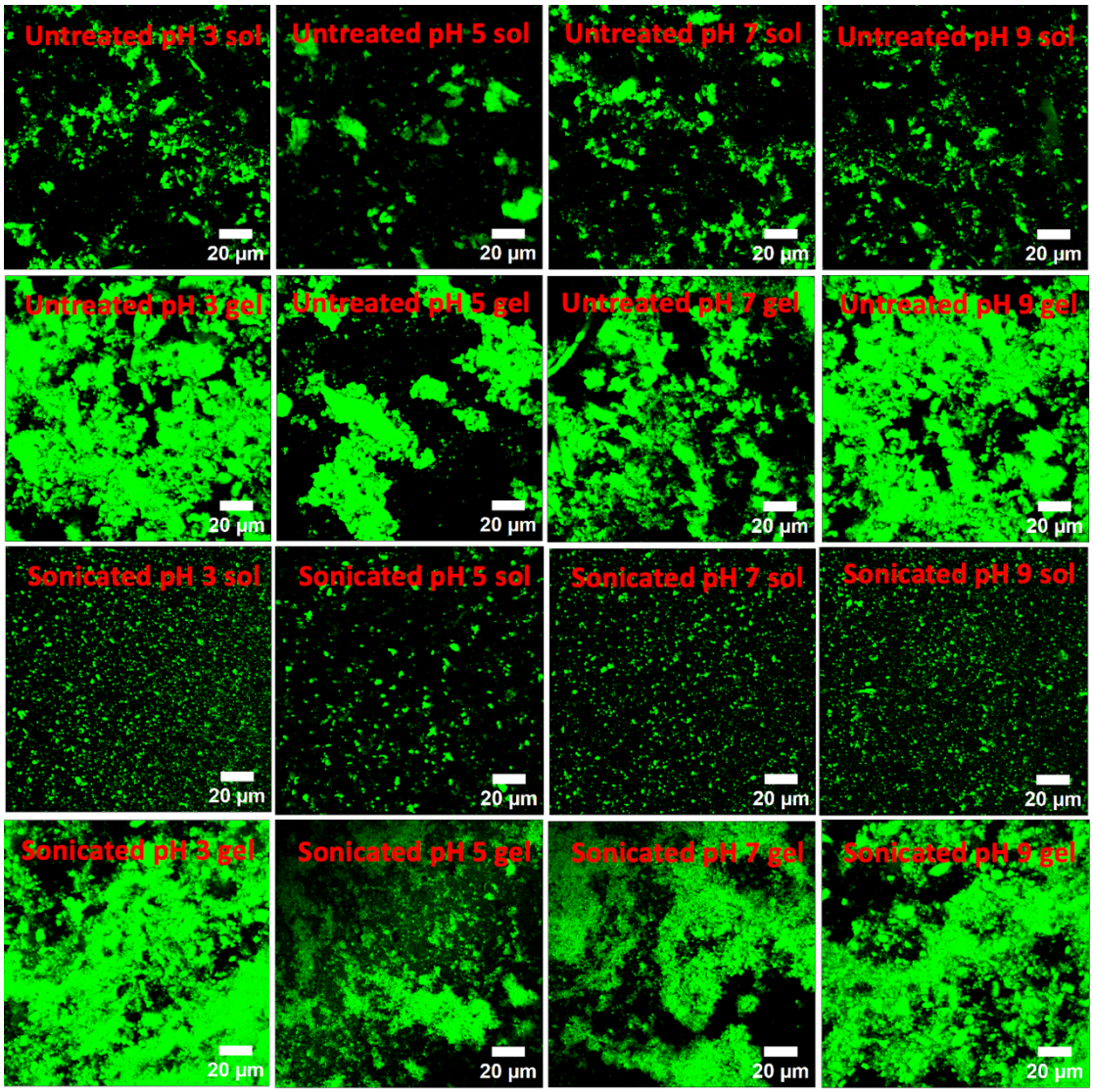


Figure 8: CLSM images of untreated and sonicated MPC samples before (sol) and after (gel) heating at 90 ℃ for 30 min.

3.3.5. Effect of pH on oil droplet size and microstructure of sonicated MPC stabilized emulsions

All untreated MPC samples cannot formed highly concentrated O/W emulsions (oil volume fraction = 70% v/v) because of large particle size and poor solubility (Yang & Cheng, 2023); oil and water were always separate. Ultrasonication was used to reduce the particle size of MPC dispersion before emulsification. **Figure 9** shows the oil

droplet size of the emulsion. In general, the oil droplet size strongly correlates with pH values and MPC particles when the oil volume fraction is fixed (70%). MPC emulsion at pH 5 had the largest oil droplet size, followed by pH 7 and pH 9, while the oil droplet size of the emulsion at pH 3 was the smallest. For example, the oil droplet size D [3,2] of MPC emulsions was ~20.4 μm, ~14.3 μm, ~13.3 μm, and ~6.5 μm at pH 5, pH 7, pH 9, pH 3, respectively. High solubility of protein solution facilitates protein diffusion at the oil-water interface, small protein particles could be efficiently adsorbed at the oil-water interface, resulting in the formation of smaller, more stable emulsion oil droplets (Yu, Wu, et al., 2018). Emulsion stabilized by sonicated MPC dispersion at pH 3 had the best emulsification performance due to the smallest protein particles and the highest solubility. However, emulsion stabilized by MPC dispersion at pH 5 had the largest oil droplet size due to protein aggregates and poor emulsification around the isoelectric point (Hu et al., 2023; Li et al., 2020). Usually, the smaller the oil droplet size of the emulsion, the more stable the emulsion is (Yu, Li, et al., 2022).

Figure 10 shows the microstructures of all emulsions under a light microscope. pH 3 emulsion had the smallest oil droplets with between ~3 μm and ~40 μm among all emulsion samples, and it was tightly packed and evenly distributed across the entire visual perspective. However, emulsion at pH 5 showed giant oil droplets, suggesting a poor emulsification capability when close to the isoelectric point. This was consistent with the previous oil droplet size result in **Figure 9**. Li et al. (2020) studied the effect of pH (3, 5, 7, 9) on oil droplet size of emulsion stabilized by Antarctic krill protein, they found that emulsion at pH 3 had the smallest oil droplets with ~17.6 μm, followed by pH 7 and pH 9, whereas emulsion at pH 5 had the largest oil droplets with ~26.6 μm. the isoelectric point of Antarctic krill protein was around pH 5. There was less net charge at the protein surface when closed to the isoelectric point (pH 5), protein tended to aggregate due to increased hydrophobic interactions, resulting in large oil droplets. However, there were many net positive or negative charges at the protein surface under pH 3, 7, 9. These charges inhibited protein aggregates, leading to small oil droplets and stable emulsion (Li et al., 2020).

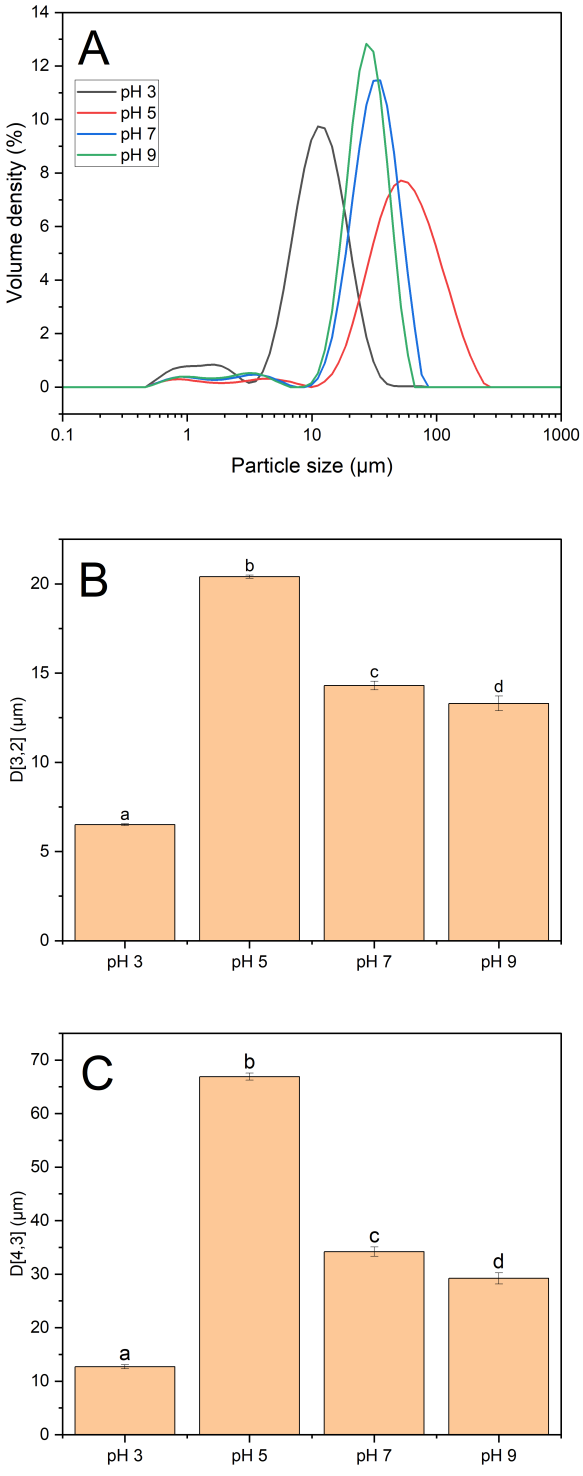


Figure 9: Oil droplet size distribution (A), D [3,2] (B), D [4,3] (C) of sonicated MPC stabilized emulsions at various pH levels. A significant difference (P<0.05) in pH levels is shown by different letters above the columns.

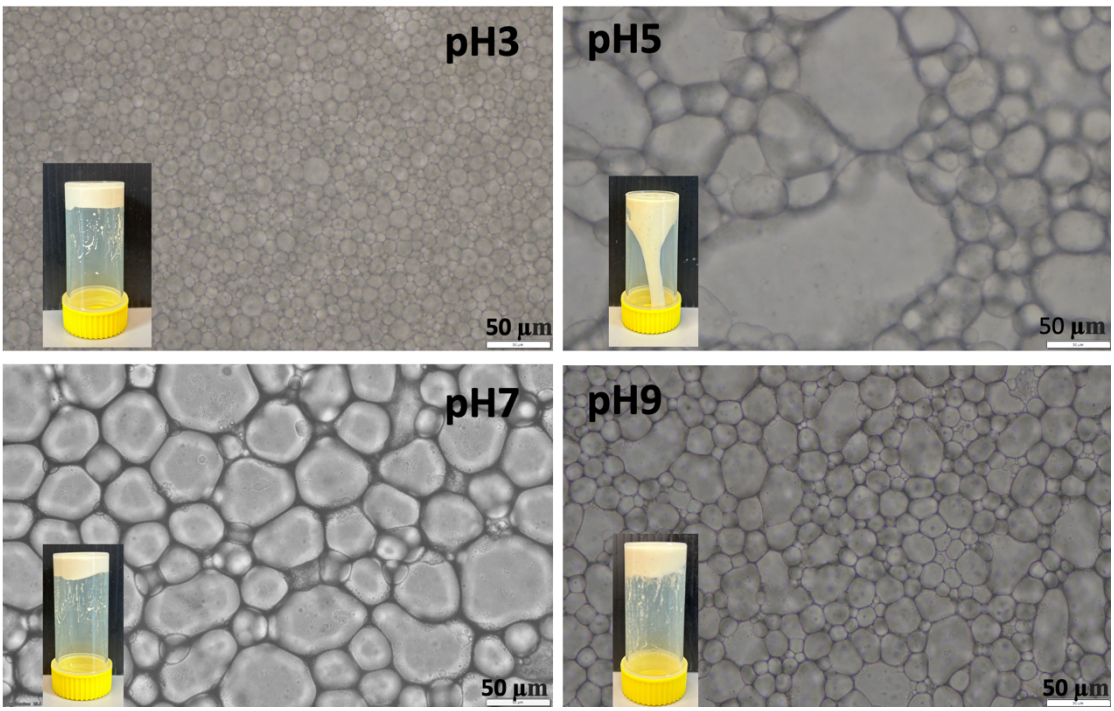


Figure 10: Micrographs of emulsions stabilized by sonicated MPC dispersions. The scale bar shows 50 µm in length. Inset photos: emulsions upside down appearances.

3.3.6. Effect of pH on Rheological properties and viscosity of sonicated MPC stabilized emulsions

It is vital to study the rheological properties of stabilized emulsion for various reasons. The rheological characteristics of emulsion products are directly related to sensory characteristics and the shelf life of emulsions. A variety of useful information could be obtained from rheological measurements. **Figure 11 A** shows the relationship between frequency and storage modulus (G') and loss modulus (G'') at different pH levels (3, 5, 7, 9). For all emulsion samples at different pH levels, G' remained essentially parallel to G'' and G' was always higher than G'', exhibiting an elastic behavior (Oldroyd, 1953). This indicated that emulsions behaved more like solids than liquids. G' and G'' of all emulsions varied little with frequency over the entire frequency range, suggesting that all emulsions had stable structures and may have maintained their structures under various oscillatory shear forces and were not easily damaged. Emulsion at pH 3 had the

highest G' and G'', followed by pH 9 and pH 7, pH 5 had the lowest G' and G''. pH 3 emulsion sample could be considered as a strong gel because G' was almost 10 times as large as G''. pH 7 and pH 9 emulsion samples could be considered as weak gels. The G' at 1Hz is displayed in **Figure 11 C** to compare the viscoelasticity of all emulsions at different pH levels. pH affected the rheological properties of MPC stabilized emulsions, G' of the emulsion at pH 3 was the largest at ~502.3 Pa, followed by emulsions at pH 9 and pH 7 (~250.8 and ~229 Pa, respectively), the emulsion at pH 5 presented the lowest value of G' at ~107.8 Pa. This was consistent with invert test results in **Figure 10**. When the bottle was inverted, the MPC emulsion at pH 5 flowed rapidly, while the emulsion at pH 3 did not flow, the emulsion at pH 7 and pH 9 flowed slowly at an imperceptible speed.

For all emulsion samples, G' and G'' did not vary with a small range of strain amplitude in the LVR, and G' was always higher than G'', exhibiting elastic behaviors. As the strain raised and exceeded the limit of the LVR, G' significantly declined, showing that the internal structure of the emulsions began to collapse. However, for all emulsions, G'' initially increased before slowly decreased with increasing strain, which may be attributed to energy dissipation (Menut et al., 2012). In this range, although the gel was broken, G' was still dominant and higher than G'', which meant that the sample exhibited a solid state. G' dropped considerably faster than G'' with further increasing strain, therefore G' intersected with G'', which marked the transition from elastic behavior to viscous behavior of the sample. Beyond this point, G'' was higher than G', and the gel network of emulsions disintegrated and behaved as a fluid state.

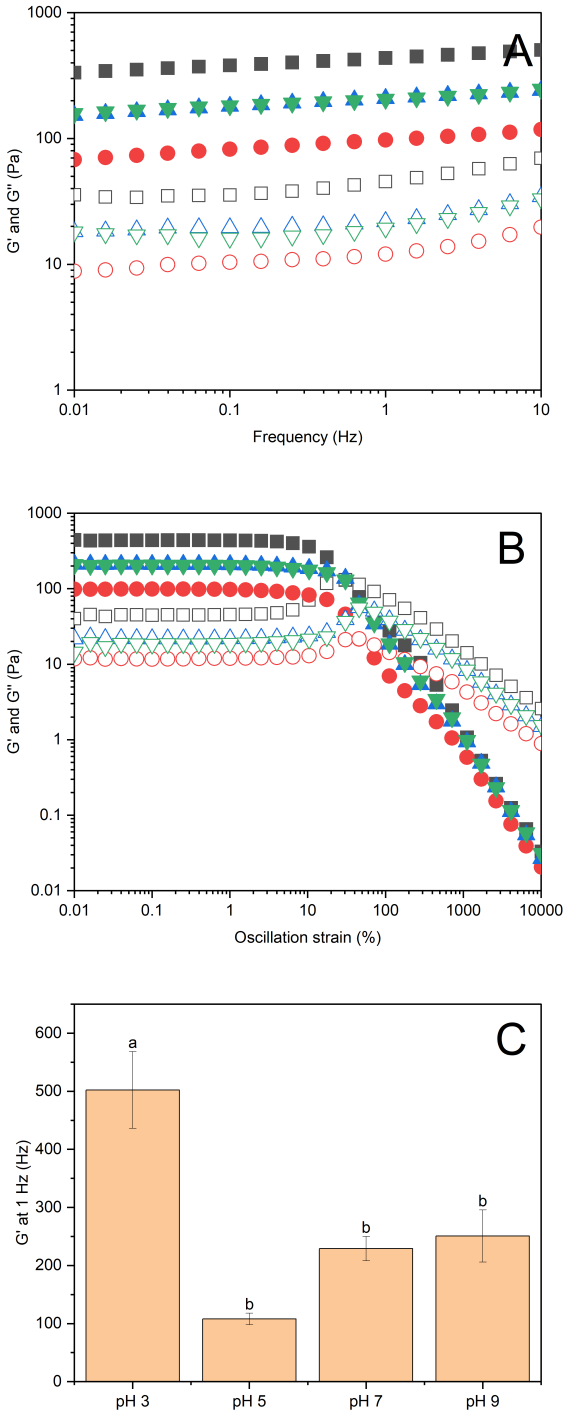


Figure 11: The dependence of *G´* (solid symbol) and *G"* (open symbol) on frequency (A) and strain (B) amplitude for sonicated MPC stabilized emulsions at various pH levels. Symbols are pH 3 (■), pH 5 (●), pH 7 (▲), pH 9 (▼). *G´* (1 Hz) of sonicated MPC stabilized emulsions as a function of different pH levels (C). A significant difference (P<0.05) in pH levels is shown by different letters above the columns.

Figure 12 A shows the viscosity of emulsions stabilized by sonicated MPC measured at various pH levels as a function of the shear rate. For all emulsions, the viscosity decreased with increasing shear rate, which indicated the typical shear thinning behavior of non-Newtonian fluids. The effect of pH on viscosity was evident at lower shear rates, while at higher shear rates, the difference between pH values was reduced. The up and down viscosity sweep was conducted for all emulsions, the result suggested a hysteresis loop. This was because the viscosity of the emulsion changed over time, and its hysteresis effect in the process of increasing and decreasing the shear rate can reflect the thixotropy of the emulsion (Grecco Zanotti & Gonçalves dos Santos, 2019). The areas of the up and down curve at varied pH were calculated by Origin Pro software as follows: pH 3 (~163074.8), pH 5 (~52220.7), pH 7 (~76078.1), pH 9 (~69910.7). The area varied greatly at different pH levels. The area of emulsion at pH 3 was the largest, which suggested that pH 3 samples had the most thixotropic properties among all emulsions (Luo et al., 2021). This may be because the emulsion at pH 3 had the strongest gel strength, protein-protein interactions were strong, and the 3D cross-linking network was tight. Hence, the emulsion at pH 3 was easier to reorganize its structure after shearing. However, the area of emulsion at pH 5 reduced a lot compared to pH 3, which indicated that the thixotropy of emulsions was lower at pH 5, making it difficult to reorganize the structure of emulsions during shearing. Emulsions at pH 7 and pH 9 showed a similar area; this may be because these emulsions have a somewhat looser protein structure than the pH 3 sample, but at the same time, they have stronger protein interactions to reorganize the structure than the pH 5 sample. To compare the flow behaviors of emulsion at different pH, **Figure 12 B** shows the viscosity of emulsion when the shear rate is 1 s^{-1}. Emulsion at pH 3 had the largest viscosity, followed by pH 9 and pH 7, the viscosity of emulsion at pH 5 was the smallest.

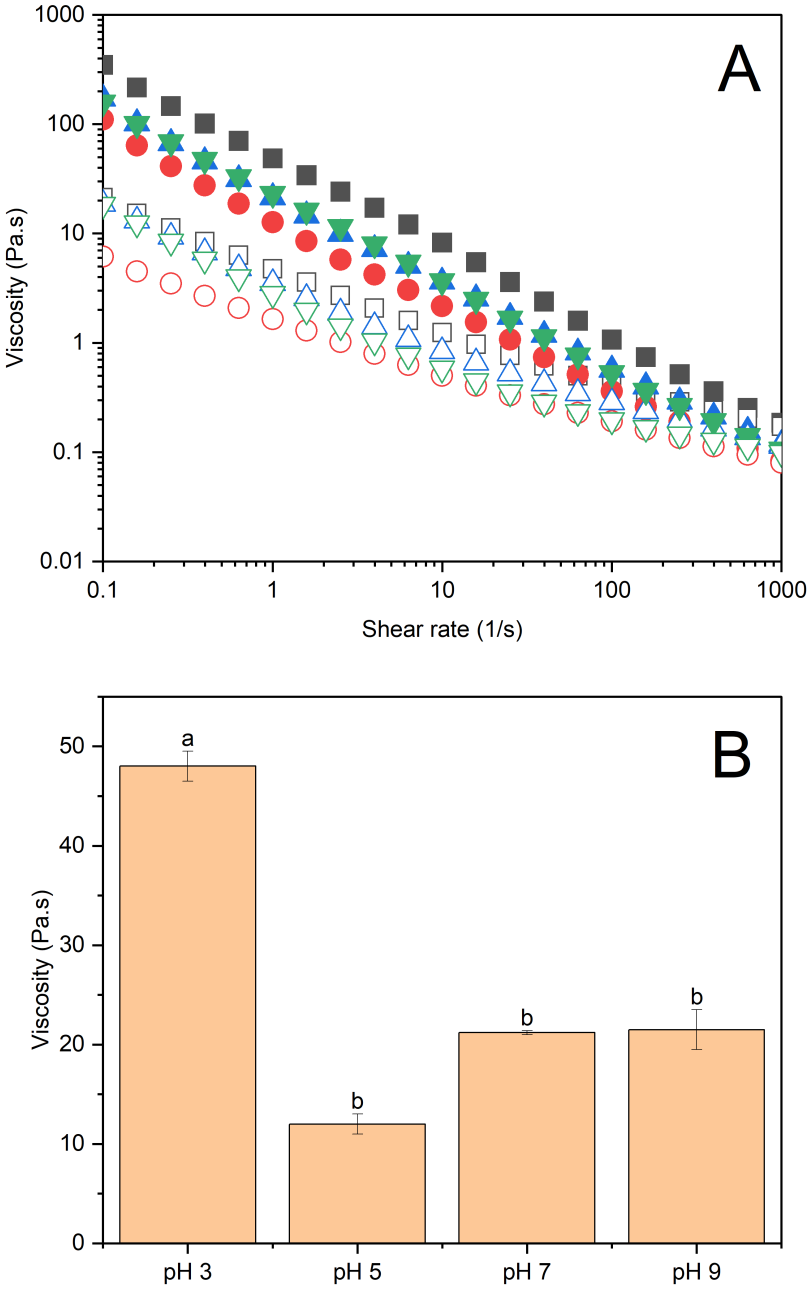


Figure 12: The viscosity of emulsions as a function of the shear rate (A) at various pH levels. Symbols are pH 3 (■), pH 5 (●), pH 7 (▲), pH 9 (▼). The "up" and "down" measurements are denoted by solid and open symbols, respectively. Viscosity of sonicated MPC stabilized emulsions as a function of various pH values when the shear rate is 1 s^{-1} (B). A significant difference (P<0.05) in pH levels is shown by different letters above the columns.

3.4. Conclusion

This study investigated the effect of ultrasound treatment and pH changes on the physicochemical and functional properties of mussel protein concentrates. The MPC dispersion at pH 3 had the highest solubility and the smallest particles; the solubility of pH 5 dispersion was very low, and the particle size was the largest around the isoelectric point. pH affected MPC stabilized emulsion, emulsion at pH 3 showed the smallest oil droplet size and packed close; the oil droplet of emulsion stabilized by sonicated pH 5 dispersion was the greatest and accumulated very loosely. In addition, rheological measurements of MPC gels showed that ultrasound treatment reduced the gel strength. Heat-induced gels prepared by untreated MPC at pH 9 showed the highest gel strength.

The study's findings could contribute to the development of mussel-flavored sauces, promote mussel protein as an alternative to meat, and advance the creation of high-protein foods.

Furthermore, the impact of other techniques on the physicochemical and functional properties of mussels, such as high-pressure processing, could be explored in future studies. Additionally, enzymes could be introduced to investigate variations in mussel gel strength.

4. Chapter 4: Effect of incorporation of various starches on rheological and microstructural properties of heat-induced mussel protein concentrates gels

Keywords: Mussel protein concentrates; Starch; Gelation; Viscoelastic properties; Microstructures

4.1. Introduction

Significant pressure will be placed on traditional meat resources as human demand for animal protein continues to rise. It has been reported that the daily animal protein requirement per capita is expected to increase from 6 g in 1961 to 25 g by 2050 (Surasani et al., 2018). Many researchers have focused on seafood to meet the human demand for animal protein. One of the best sources of seafood protein is mussels. Regarding nutrition values, green-lipped mussels are nutrient-rich, high in micronutrients, vitamins, protein, and polyunsaturated fatty acids (Miller et al., 2023). Green-lipped mussels are farmed shellfish unique to New Zealand (Abshirini, 2022). Aquaculture of this species was developed in the 1960s (Miller et al., 2023), and New Zealand is now a major exporter of green-lipped mussels (Abshirini, 2022). In addition to being sold as a fresh or frozen food product, one of the most common uses for green-lipped mussels is as dietary supplements for people, such as mussel powder and oil extracts, or pet food ingredients for dogs and cats (Konieczny et al., 2021). Mussels contain various proteins, including myofibrillar protein, sarcoplasmic protein, and stromal protein (Zou et al., 2020). Myofibrillar protein mainly comprises myosin, paramyosin, and actin (Binsi et al., 2006). Until now, research on the physicochemical and techno-functional properties of New Zealand green-lipped mussel proteins has been very limited (Jayaprakash & Perera, 2020).

Gelation, a crucial protein property, is indispensable in producing surimi and sausage. Heat-induction is simple and safe, and only the heating conditions need to be controlled, so it is widely used to prepare gels of different seafood proteins (K. Liu et al., 2021). For example, during the preparation of surimi, the myofibrillar proteins unfold, interact, and form a 3D network structure under heating conditions (Hunt et al., 2009). Mussel protein has great potential as a raw material for surimi because mussels contain many delicate flavors (Fukuda et al., 2006). However, the gel properties of native invertebrate proteins such as mussels are poor (Binsi et al., 2006). There are some methods to increase the gel strength, such as adding enzyme, polysaccharides (starch, non-starch)

(Xie et al., 2024). Dong et al. (2020) found that adding 0.3% microbial transglutaminase significantly increased the gel strength of *Scomberomorus niphonius* surimi, more than doubling its original gel strength. Zhang et al. (2023) found that adding 1% konjac glucomannan increased the gel strength of fish myofibrillar protein. Although adding non-starch polysaccharides or enzyme can improve the gelling property of seafood proteins, there are some limitations. Non-starch polysaccharides usually require specific processing steps, including pH regulation and ion addition, and different types of non-starch polysaccharides may interact differently with proteins. In addition, enzymes are expensive and very sensitive to reaction time and temperature (Han & Li, 2024; Xie et al., 2024). Starch, by contrast, is available, cost-effective, and easy to add (Xie et al., 2024). Therefore, different types of starch could be used to enhance the gel qualities of mussel protein.

A common source of starch is wheat, potatoes, corn, and rice. When heated, starch granules absorb water and expand in volume. As the temperature rises, the structure of starch granules begins to change and gradually dissolves in water, forming a 3D gel network structure called starch gelatinization (Ai & Jane, 2015; Kumar et al., 2017). The gelatinization temperature of starch varies with the size of starch granules and the type of starch (Ai & Jane, 2015). Starches from different crops contain different proportions of amylose to amylopectin (Hunt et al., 2010). Amylose and amylopectin are very different in molecular structure, chemical reaction, and characteristics (Leloup et al., 1991). Amylose is a straight structure composed of α-glucan chains, and its spatial structure is a spiral. Although amylopectin is also composed of α-glucan chains, from the perspective of spatial structure, its molecules are dendritic branch structures, and each branch is also curled in a spiral shape (He et al., 2024). Starch with high amylose content usually forms a hard and brittle gel and leads to a higher gel strength; starch with high amylopectin content usually forms a soft and elastic gel and leads to a lower gel strength (Hunt et al., 2010). Native rice starch (NRS) has about 18%-28% amylose content and 72%-82% amylopectin content. However, for waxy rice starch (WRS), waxy potato starch (WPS) and waxy corn starch (WCS), they contain almost 97%-100%

amylopectin content (Trivedi, 2006). These starches differ in amylose and amylopectin content, resulting in their different behavior in gel formation. In addition, the swelling capacity, hydration characteristics, particle structure, gelatinization temperature of starch, will also influence the strength of the formed gel (Hsieh et al., 2019).

The effects of adding starch to surimi gels have been investigated in earlier research. For example, Mi et al. (2021) found that hairtail (Trichiurus haumela) myosin gels containing corn starch had higher gel strength than pure myosin. Kong et al. (2016) investigated that when starches were added to Alaska Pollock surimi, the swelling initiation temperature and starch viscosity may affect the surimi's gel strength. In protein-starch systems, the interaction of protein particles and starch granules is affected by different factors, including the starch type and concentration (Hunt et al., 2009). When starch is added to surimi, the starch can act as a filler through gelatinization to form special structures that fill the gel network and absorb water, leading to a denser 3D surimi gel network structure. Even though research has indicated that starch helps strengthen surimi gel, different starches may lead to varying degree of improvement in gel strength. When adding potato starch to surimi, the surimi gel strength increases greatly than adding other starches, this is because potato starch has a lower gelatinization temperature, larger granules, and a higher water absorption capacity. The internal structure of corn starch is stronger than that of potato starch, and its swelling capacity is weaker in the surimi-starch system, so the strengthening ability of surimi gel is much smaller than that of potato starch (Liu et al., 2014). NRS, WRS, WCS, and WPS varies in different amylose and amylopectin content, gelatinization characteristics, interactions with mussel proteins, resulting in different effect on the mussel protein gel strength (Trivedi, 2006). Starch can be used as a filler to enhance the protein gel's strength, but excessive starch addition may also compresses the protein matrix and disrupt the network structure, reduce the gel performance (Fan et al., 2017; Hunt et al., 2010). However, there was less research about the impact of various starch types and concentrations on the mussel gels.

This study aims to investigate the effects of adding different concentrations (2.5%, 5%, 10% w/w) of various starches (NRS, WRS, WCS, WPS) on the viscoelastic properties of heat-induced mussel protein concentrates (MPC) gels. This work explores the changes in gel strength and microstructures of MPC gels after starches were added and protein-starch interactions formed. The results will provide valuable insights into the practical application of different starches in enhancing the properties of mussel protein gels, thereby contributing to the creation of premium mussel protein rich products.

4.2. Materials and methods

4.2.1. Materials

Defatted mussel powder was supplied by Sanford Ltd (New Zealand), which provided the approximate composition of the powder. It consisted of 4% fat, 29.1% ash, 48.6% crude protein, 14.3% carbohydrates, and 4% moisture (w/w). All starches used in the experiments, including NRS, WRS, WCS, and WPS, were purchased from Ingredion Inc. (USA). **Table 16** shows the chemical composition of four kinds of starches. The data was provided by Ingredion Inc.

Table 16: Chemical composition (w/w, %) of starches.

	Carbohydrate	**Protein**	**Fat**	**Ash**
NRS	91.4	< 0.1	< 0.1	0.17
WRS	87.2	< 0.5	< 0.1	0.4
WCS	88.3	0.1	< 0.1	< 0.1
WPS	99.4	< 0.1	< 0.1	0.1

4.2.2. Sample preparation

Desalted mussel protein solution (10% w/w) was prepared by mixing desalted mussel powder in 0.02% sodium azide solution at room temperature; a magnetic stirrer was used to stir gently for two days to make the mussel solution fully hydrated. In this experiment, the concentration of desalted mussel powder in the mixture solution always remained consistent at 10% w/w. For example, for 10% w/w mussel-10% w/w starch mixture solution, 6 g starch was mixed with 10% w/w 60 g mussel solution; and for 10% w/w mussel-5% w/w starch mixture solution, 3 g starch was mixed with 10% w/w 60 g mussel solution. In other words, the amount of mussel solution (water) was constant no matter how much starch was mixed with the mussel dispersion. Sample preparation procedure was conducted using the Noisuwan et al. (2009) method specified. This ensures that changes in rheological measurements are not influenced by the amount of water but by the concentration of the starch.

4.2.3. Rheological measurements

The stress-controlled rheometer (DHR-3, TA instruments, New Castle, DE, USA) fitted with a starch cell geometry (diameter: 37 mm) was employed to conduct rheological measurements. The starch cell geometry, consisting of a cup and a paddle mixer, could control temperature precisely and stir the mixture solution at a constant speed simultaneously. This can prevent starch sediment during rheological measurements (Noisuwan et al., 2009).

Rheological measurements were conducted according to the method provided by Noisuwan et al. (2009): (1) Firstly, mussel and starch mixture dispersion was transferred into the cup and heated at 50 ℃ for 3 min under a constant shear rate of 1.67 1/s to avoid the starch sediment; (2) secondly, the sample was heated from 50 ℃ to 90 ℃ at 2 ℃/min under a constant shear rate of 1.67 1/s; (3) thirdly, the paddle mixer stopped stirring (shear rate was 0) when the sample reached 90 ℃ and was immediately cooled down to 25 ℃ at 2 ℃/min; (4) once the temperature decreased to 25 ℃, a frequency sweep measurement was performed at a constant 1% strain, while the

frequency varied from 0.01 to 10 Hz; (5) finally, a strain sweep measurement was conducted at a consistent frequency of 1 Hz, while the strain ranged from 0.01% to 1000%.

4.2.4. Confocal laser scanning microscopy (CLSM)

CLSM was operated following the method demonstrated by Noisuwan et al. (2009), with some modifications. A confocal microscope (Leica TCS SP5, Leica Microsystems) fitted with a 100 mm oil immersion objective lens was used to conduct confocal laser scanning microscopy and compare microstructural characteristics of mussel dispersions by adding different starches before and after heat treatment. Mixture samples were evenly mixed with 1% fast green dye; each sample, after dyeing, was transferred into a glass slide with a cavity and covered with a glass coverslip. For these gelation samples, all glass slides containing dyed samples were incubated in an oven at 90 ℃ for 30 min. Then, samples were removed from the oven and cooled to room temperature; after about 30 min, these samples were observed under the CLSM. Image J Software (Fiji, USA) was used to analyze CLSM images.

4.2.5. Statistical analysis

All experiments were measured in duplicate. The results were expressed as the mean ± standard deviation of at least two experiments. Minitab Software (Minitab 2021, USA) was used to conduct a one-way analysis of variance (ANOVA). Significant differences between samples were assessed using Tukey's test with a significance level of $P < 0.05$.

4.3. Results and discussions

4.3.1. Gelation temperature and viscosity

When starch is added to cold water, although the starch granules absorb a small amount of water, leading to a slight expansion in volume, the structure of the crystalline portion of the starch granules does not change, and the starch granules slowly settle into the bottom without stirring. At this stage, the starch solution exhibits a very low viscosity (Ratnayake & Jackson, 2008). However, as the temperature of the starch suspension gradually rises, the starch granules absorb more water, and these water molecules gradually enter the starch granules' crystalline regions (Schirmer et al., 2015). Continuous heating causes the starch granules to swell and eventually destroy the granules as they can no longer absorb the excess water. The apparent viscosity increases significantly and peaks (Ai & Jane, 2015). Afterwards, some of the starch molecules may be degraded, leading to a slight reduction in viscosity. These molecules are dispersed in water to produce a gel or paste (Ratnayake & Jackson, 2008).

Figure 13 shows NRS, WRS, WCS, and WPS gelatinization properties. All starches exhibited a low viscosity below 60 °C, indicating that gelatinization had not yet begun. As the temperature increased, the viscosity increased significantly and reached peak, then the highly swollen starch granules were easily broken under stirring, resulting in a reduction in viscosity (Hsieh et al., 2019). The peak apparent viscosity increased as the starch concentration increased for the same starch source. This could be explained by the more vital intermolecular forces between starch granules and less available free water as the starch concentration increased (Ai & Jane, 2015). The peak apparent viscosity was closely related to starch intrinsic properties, such as starch granules size and amylopectin and amylose content (Ratnayake & Jackson, 2008). WPS had the highest peak apparent viscosity and significantly higher than other starch sources. This was consistent with other studies. Hsieh et al. (2019) studied pasting properties of 6% w/w waxy starches in water. The peak viscosity of waxy potato, waxy maize, and waxy rice starch was ~1482, ~879, ~704 BU (Brabender Units), respectively. They concluded that the pasting viscosity of potato starch (regardless of genotype) always significantly higher than that of other starches. It could be explained by negatively charged phosphate ester in potato starch, which can promote starch granules to swell. In contrast, other

starches had smaller granules and less water absorption, so the gelatinization temperature was higher, and the viscosity was lower.

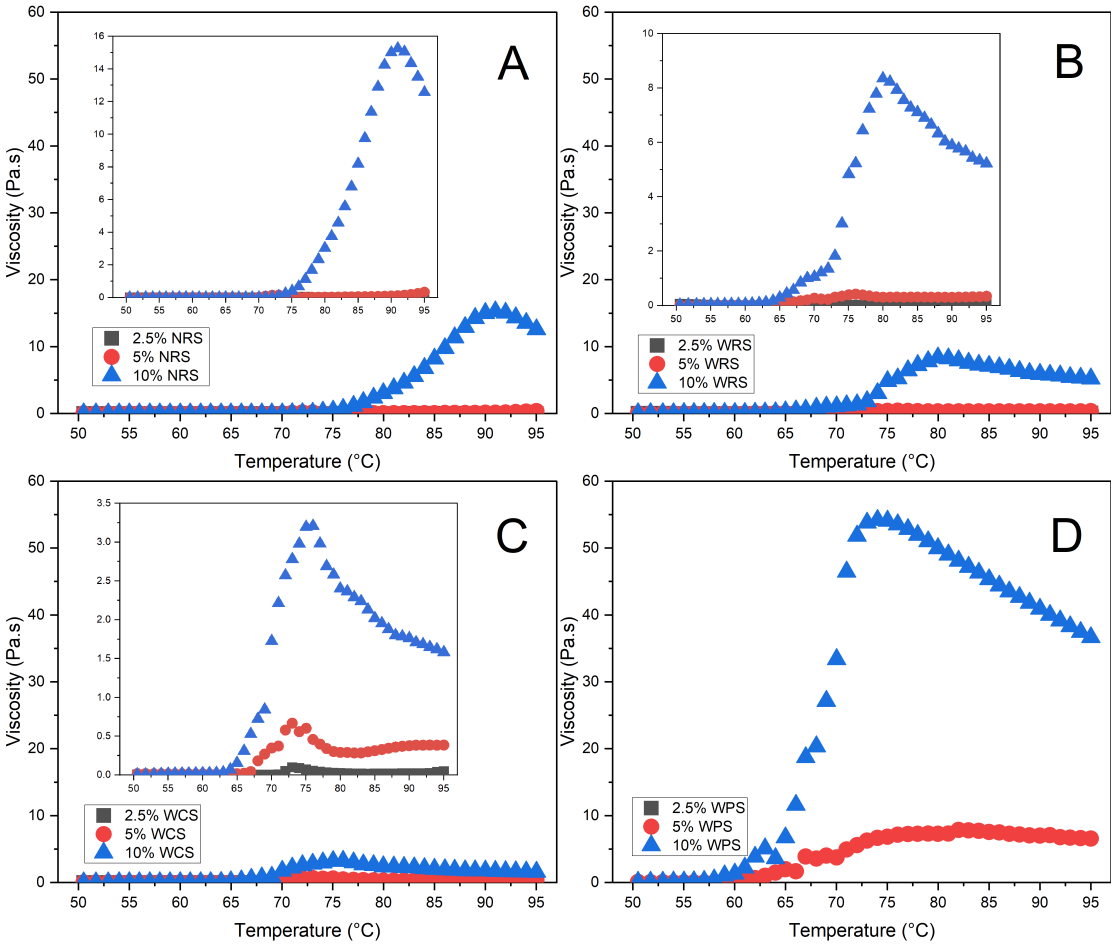
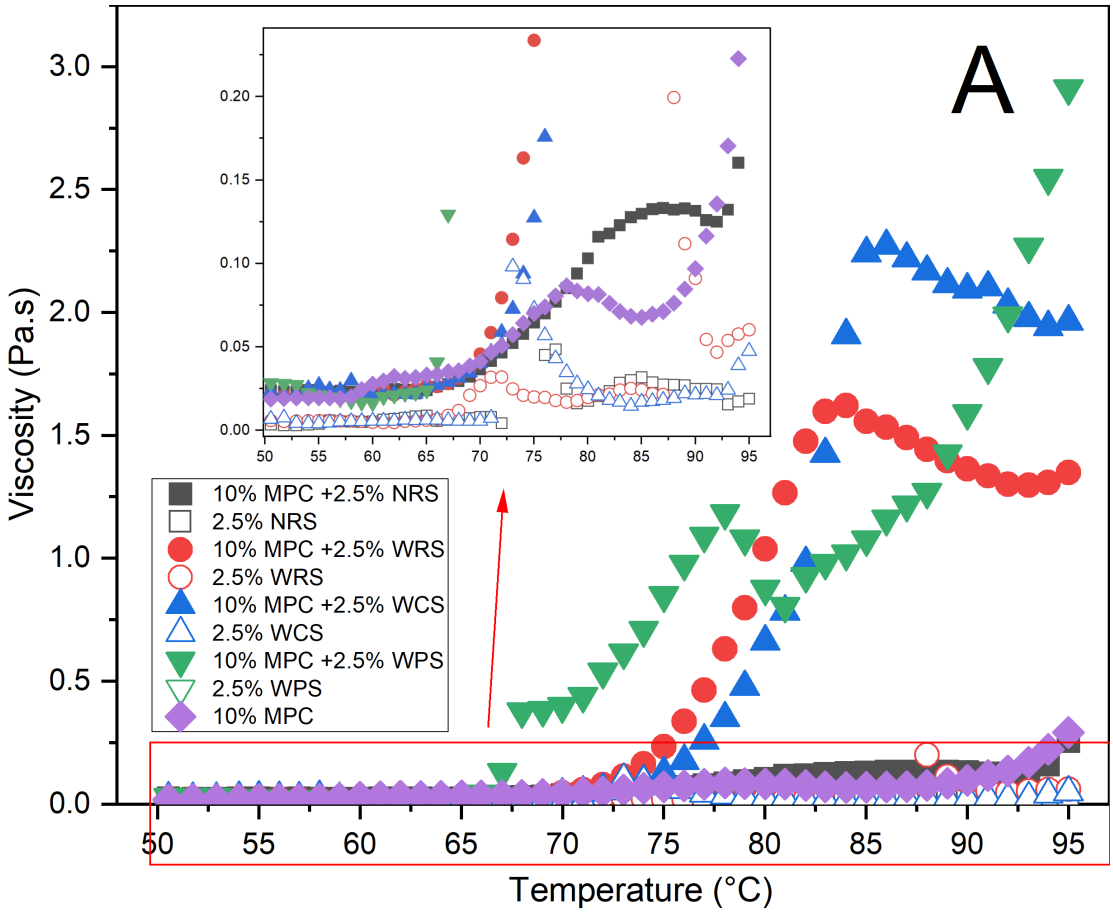
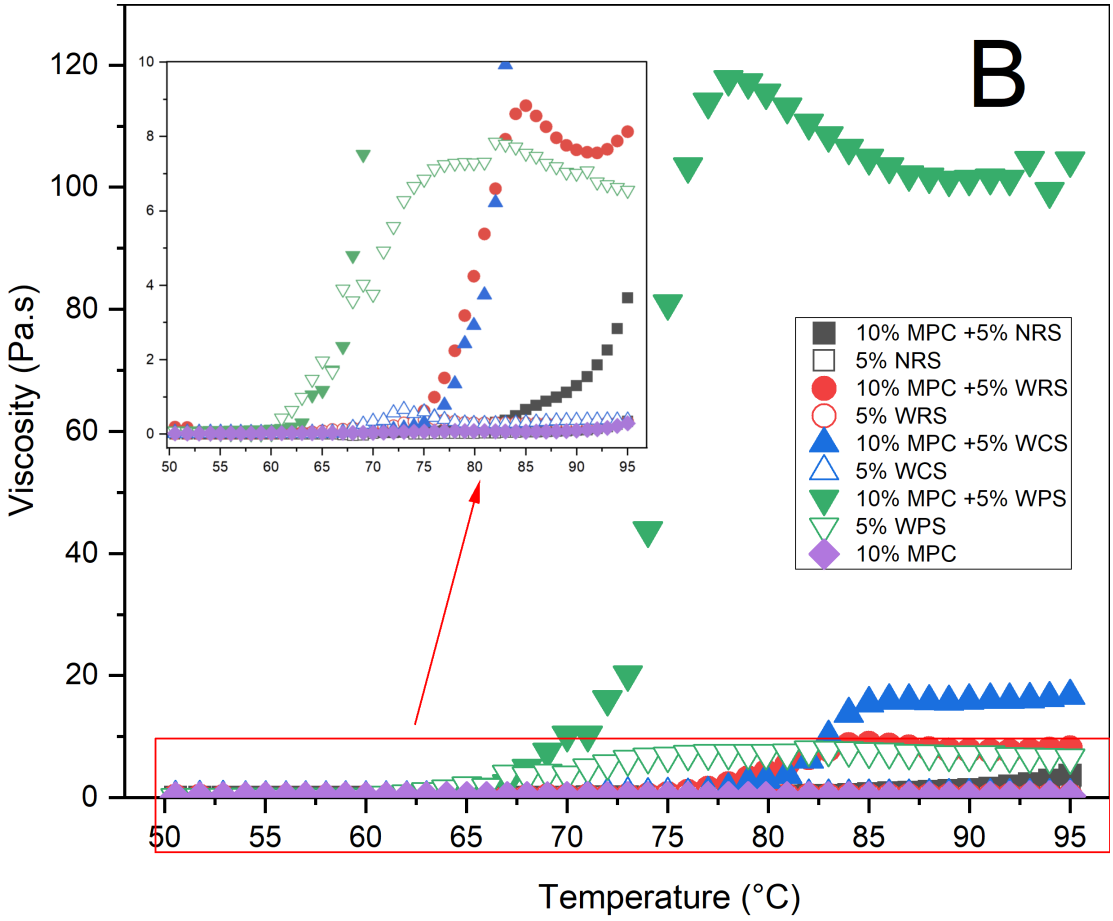


Figure 13: During starch gelatinization, viscosity for NRS (A), WRS (B), WCS (C), WPS (D) as a function of temperature. Symbols represents different concentrations (2.5%-10% w/w) of starch: 2.5% (■), 5% (●), 10% (▲).

Figure 14 compares the viscosity of MPC, starch, MPC-starch mixtures as a function of temperature under heat conditions. Compared with pure starch and protein-starch mixtures, the increase in viscosity of pure protein was almost imperceptible (**Figure 14**). For protein-starch mixtures, the swelling of starch granules, the leaching of amylose and amylopectin molecules resulted in a significant rise in viscosity of protein-starch mixtures (Noisuwan et al., 2007). Therefore, for protein-starch mixture samples, the point at which viscosity sharply increases (transition temperature) could be

considered the starch pasting temperature in MPC solution (Shim & Mulvaney, 2001). All protein-starch samples showed very low viscosity between 50 ℃ and 65 ℃, indicating that starch gelatinization had not yet begun in protein-starch solution. The viscosity of most protein-starch mixtures rose and then dropped when the temperature rose from 65 °C to 95 °C, which was in line with the pure starch group. Adding starch enhanced the apparent viscosity of MPC samples. When adding 2.5%-10% w/w starch, the MPC-WPS group exhibited the highest viscosity, which was much larger than other groups. According to Hsieh et al. (2019), the granules of WPS were larger, there were negatively charged phosphate esters in WPS granules, resulting in repelling between WPS chains and swelling of starch granules and a large increase in viscosity. Pure WPS group also showed the highest apparent viscosity among all pure starches, it acted as a filler in MPC-WPS sample, so the gelatinization of WPS resulted in a sharp rise in the viscosity of the MPC-WPS sample (Hsieh et al., 2019; Hunt et al., 2009). The peak apparent viscosity for protein-starch systems was higher than the linear sum of single MPC and single starch groups. This may be because of the synergy between protein and starch, resulting in the mixture's viscosity being much higher than that of pure MPC and pure starches. As the added starch concentration rose, MPC-starch samples' apparent viscosity increased. However, when high-concentration (10% w/w) starch was added to the MPC samples, all mixtures showed the highest peak apparent viscosity except for MPC-WPS. WPS had great swelling capacity, it could significantly increase the viscosity of MPC-starch mixtures at low-concentration (5% w/w), but when adding high-concentration (10% w/w) WPS, granules may compete for water, which reduced their ability for swell further and the apparent viscosity of MPC-WPS mixtures (Singh et al., 2003).


A
Viscosity (Pa.s)
Temperature (°C)
10% MPC +2.5% NRS
2.5% NRS
10% MPC +2.5% WRS
2.5% WRS
10% MPC +2.5% WCS
2.5% WCS
10% MPC +2.5% WPS
2.5% WPS
10% MPC


B
Viscosity (Pa.s)
Temperature (°C)
10% MPC +5% NRS
5% NRS
10% MPC +5% WRS
5% WRS
10% MPC +5% WCS
5% WCS
10% MPC +5% WPS
5% WPS
10% MPC

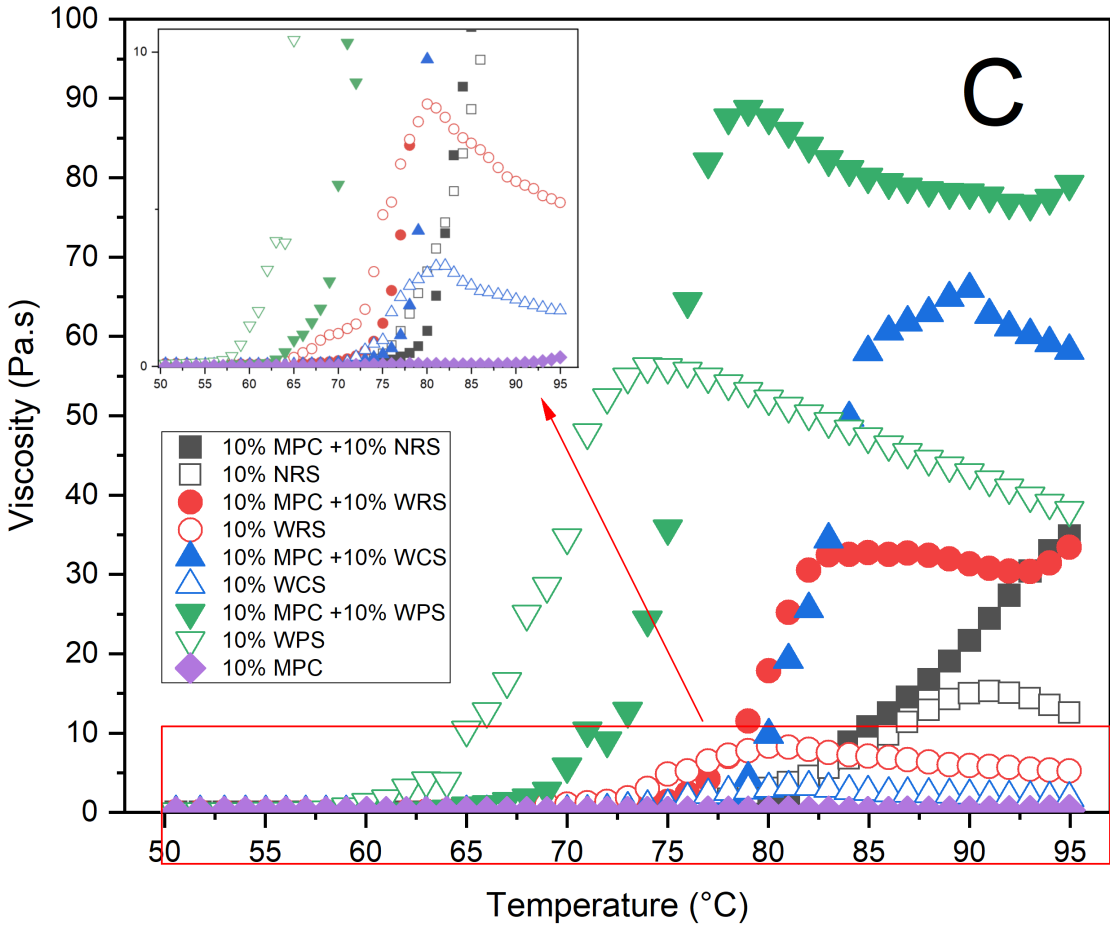


Figure 14: Viscosity for 10% w/w MPC containing 2.5% (A), 5% (B), 10% (C) w/w different starches as a function of temperature. Starches are NRS (■), WRS (●), WCS (▲), WPS (▼). Solid samples and open samples represent MPC-starch mixture and pure starch, respectively. 10% w/w Pure MPC is (◆).

The starch pasting temperature in the seafood protein-starch system was higher than in water (Wu et al., 1985). **Table 17** shows the pasting temperatures of starches (10% w/w) in water and MPC solution. The pasting temperature of 10% w/w WPS in water was ~61.5 °C, but it increased to ~69.5 °C when 10% w/w WPS was added to 10% w/w MPC solution. NRS, WRS, and WCS also followed this trend. Protein gelation can bind the water in the gel network, thus limiting the water utilization of starch gelatinization (Hunt et al., 2009). Konieczny et al. (2016) studied the denaturation temperature of mussel (*Anodonta woodiana*) protein by differential scanning calorimetry (DSC). They found that the denaturation transition temperature of mussel protein was between 42 and 76 °C. DSC results indicated that two denaturation transitions, one was paramyosin

and myosin at 60-61 ℃, another was actin at 69-70 ℃. For protein-starch system, as the temperature increased, MPC begun to gel and form a network structure, which could limit the diffusion of water molecules and prevent starch granules from absorbing water and expanding (Wu et al., 1985), thus increasing the pasting temperature. Wu et al. (2020) found that the pasting temperature of corn, rice, tapioca, potato starch in myofibrillar protein solution was higher than in water.

Table 17: The pasting temperature of starches (10% w/w) in water and MPC solution.

	NRS	**WRS**	**WCS**	**WPS**
Water	78.5 ± 0.3 ℃	74.5 ± 0.4 ℃	72.5 ± 0.5 ℃	61.5 ± 0.5 ℃
MPC solution	81.5 ± 0.5 ℃	76.5 ± 0.5 ℃	78.5 ± 0.2 ℃	69.5 ± 0.5 ℃

4.3.2. Viscoelastic properties

Frequency sweep measurement was used to characterize all samples' small deformation rheological properties. **Figure 15** and **Figure 16** show the storage modulus (G') and loss modulus (G'') as a function of the frequency for pure starch samples and MPC-starch samples, respectively. For strong gels, the slope of G' is almost 0 and G' is higher than G''; G'' displays the minimum value at the middle frequency (Binsi et al., 2006). From **Figure 15**, for 2.5% pure NRS, WRS, and WCS samples, both G' and G'' were very low throughout the entire frequency range, and G' was less than twice as large as G''. Thus, 2.5% pure NRS, WRS, and WCS samples may be considered a paste rather than a gel after heating. Estimating whether 2.5% pure WPS dispersion after heating formed a gel was impossible because the data was lost. In general, the heat-inducted method was used to prepare the single hydrogel of protein, and the gel strength, G', G'' of the single protein hydrogel were very low due to its porous and loose 3D gel structures (K. Liu et al., 2021). For other samples except 2.5% w/w pure starch, G' was always higher than G'' over the whole frequency range, suggesting elastic behavior, but

the ratio of G' to G'' was less than 10, showing that most samples could be seen as weak gels (**Figure 15** and **Figure 16**). G' and G'' slowly increased with increasing frequency and showed a slight frequency dependence, a typical characteristic of weak gels. It could be seen that adding various starches only improved values of G' and G'' but did not change the state of protein-starch mixtures.

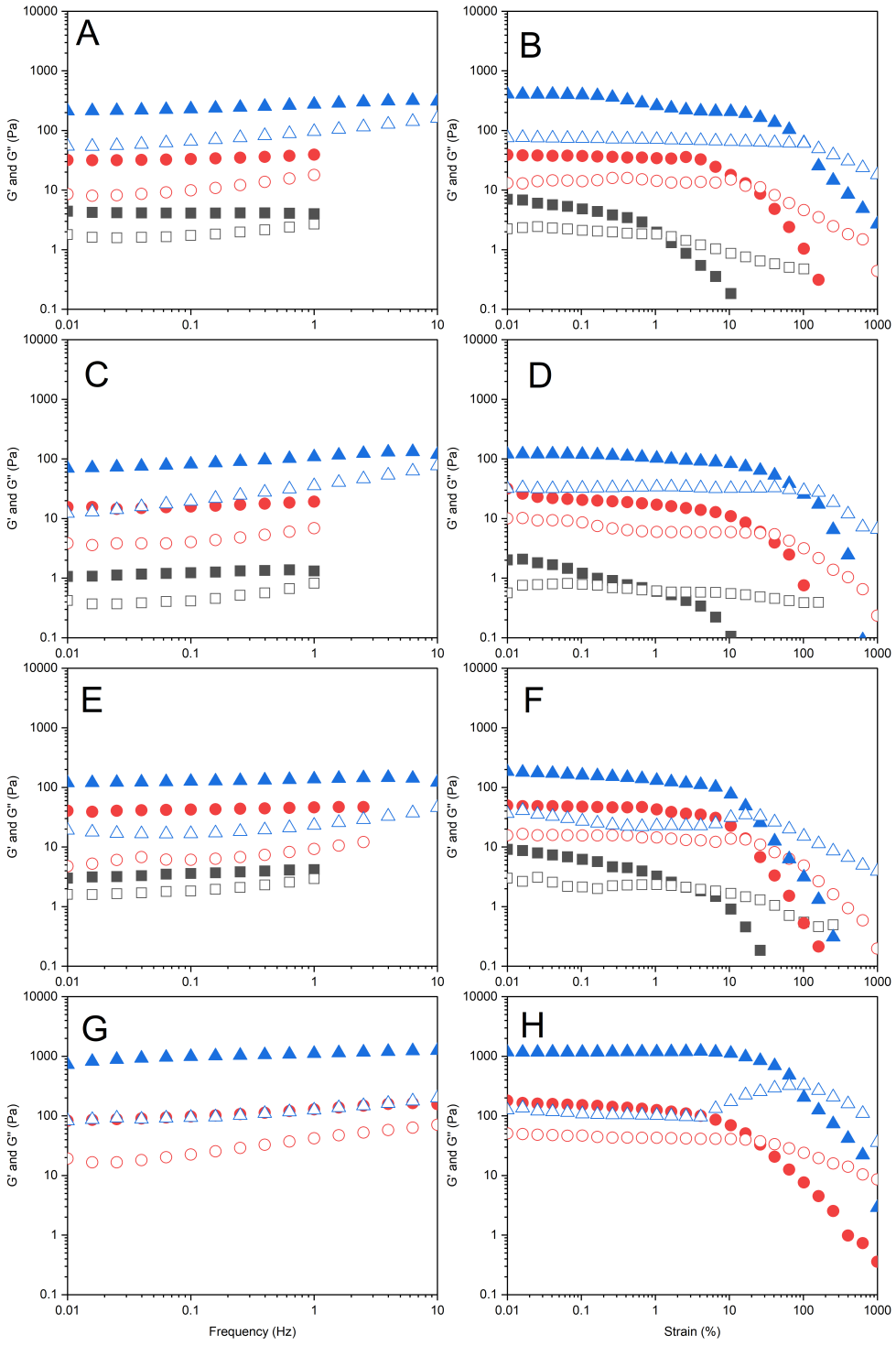


Figure 15: *G′* (solid symbols) and *G″* (open symbols) for pure starches as a function of frequency (A, C, E, G) and strain amplitude (B, D, F, H). Figures are NRS (A, B), WRS (C, D), WCS (E, F), and WPS (G, H). Symbols are 2.5% starch (■), 5% starch (●), and 10% starch (▲).

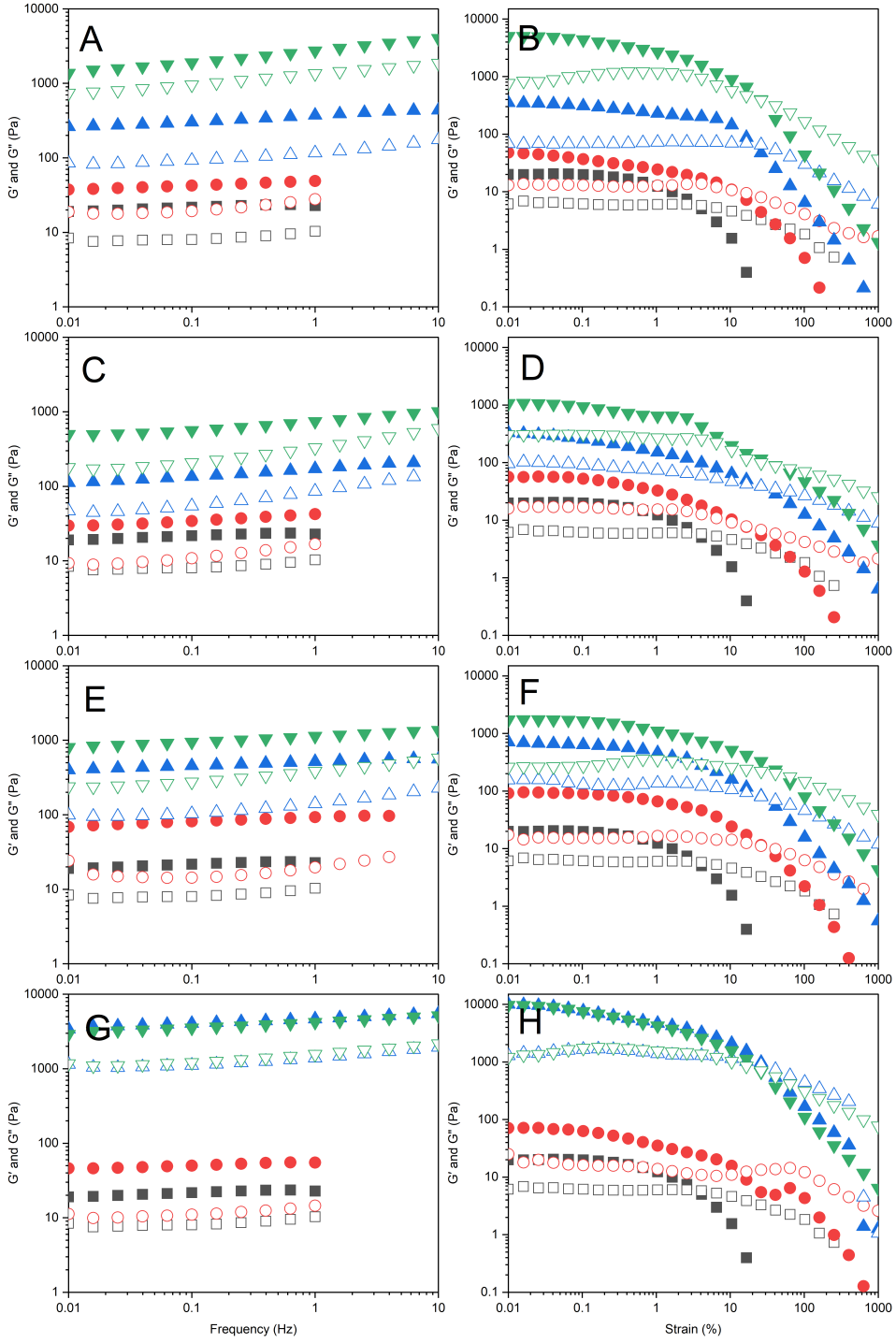


Figure 16: *G′* (solid symbols) and *G″* (open symbols) for MPC containing starches as a function of frequency (A, C, E, G) and strain amplitude (B, D, F, H). Symbols are MPC (■), MPC containing 2.5% starch (●), MPC containing 5% starch (▲), and MPC containing 10% starch (▼). Figures are MPC-NRS (A, B), MPC-WRS (C, D), MPC-WCS (E, F), and MPC-WPS (G, H).

Binary gels made from polysaccharides and proteins have been extensively researched to overcome the disadvantages of single gels, such as poor gel strength, low stability, and poor water retention ability (Yang et al., 2021). Complex gels' strength and stability are higher than pure protein and polysaccharide gels. Gubbins (1983) suggested that under ideal conditions, for protein-polysaccharide composite gels, the properties of the composite material were the sum of protein and polysaccharide if there are no intermolecular interactions between protein and polysaccharide molecules. Adding starch results in stronger protein gels for starch-protein systems since denaturation and aggregation of proteins, water absorption, and expansion of starch granules may occur simultaneously or consecutively under heating conditions. When the starch granules absorb water and swell, they are distributed throughout the protein system and exert pressure on the protein matrix, leading to a stronger and denser gel (Campo & Tovar, 2008).

To compare the gel strength of different samples and to investigate the impact of adding different types and concentrations of starches on MPC gels, G' of all samples at 1 Hz is illustrated in **Figure 17**. For all pure starch samples, G' varied depending on starch types and concentrations. G' significant increased as the starch suspension concentration increased (**Figure 17 A**). For example, when the concentration of all pure starch samples increased from 2.5% to 5%, the G' of starch samples increased from ~4 Pa to ~39.2 Pa for NRS, from ~1.3 Pa to ~19.2 Pa for WRS, from ~4.2 Pa to ~46.1 Pa for WCS, to ~128.5 Pa for WPS (2.5% data lost), respectively. All 2.5% w/w starch samples cannot be considered a gel because they looked more like a paste from the appearance. Most low-concentration starch solutions have difficulty forming gels, but starch solutions at higher concentrations have stronger intermolecular interactions and cross-linking under heating conditions, resulting in more stable gels (Ai & Jane, 2015). According to **Figure 17 A**, when the starch concentration reached 10% w/w, the G' of all starch gels was very high, at ~274 Pa for NRS, at ~108.2 Pa for WRS, at ~138.2 Pa for WCS, at ~1109.2 Pa for WPS. During the gelatinization process, WPS had the largest G' and excellent viscosity. This was because WPS had larger granules and a

lower pasting temperature. The swelling power of WPS was much higher than that of other starches because of a higher content of phosphate groups on amylopectin, making it easier to absorb free water (Dereje, 2021; Tako & Hizukuri, 2002). Compared to WPS, other starches had smaller granules and the gel strength was much lower than WPS. Native rice starch and waxy rice starch had different amylose content and granular structure. According to Lu et al. (2011), waxy rice starch was difficult to form a gel matrix because amylose played an important role when formed network structures.

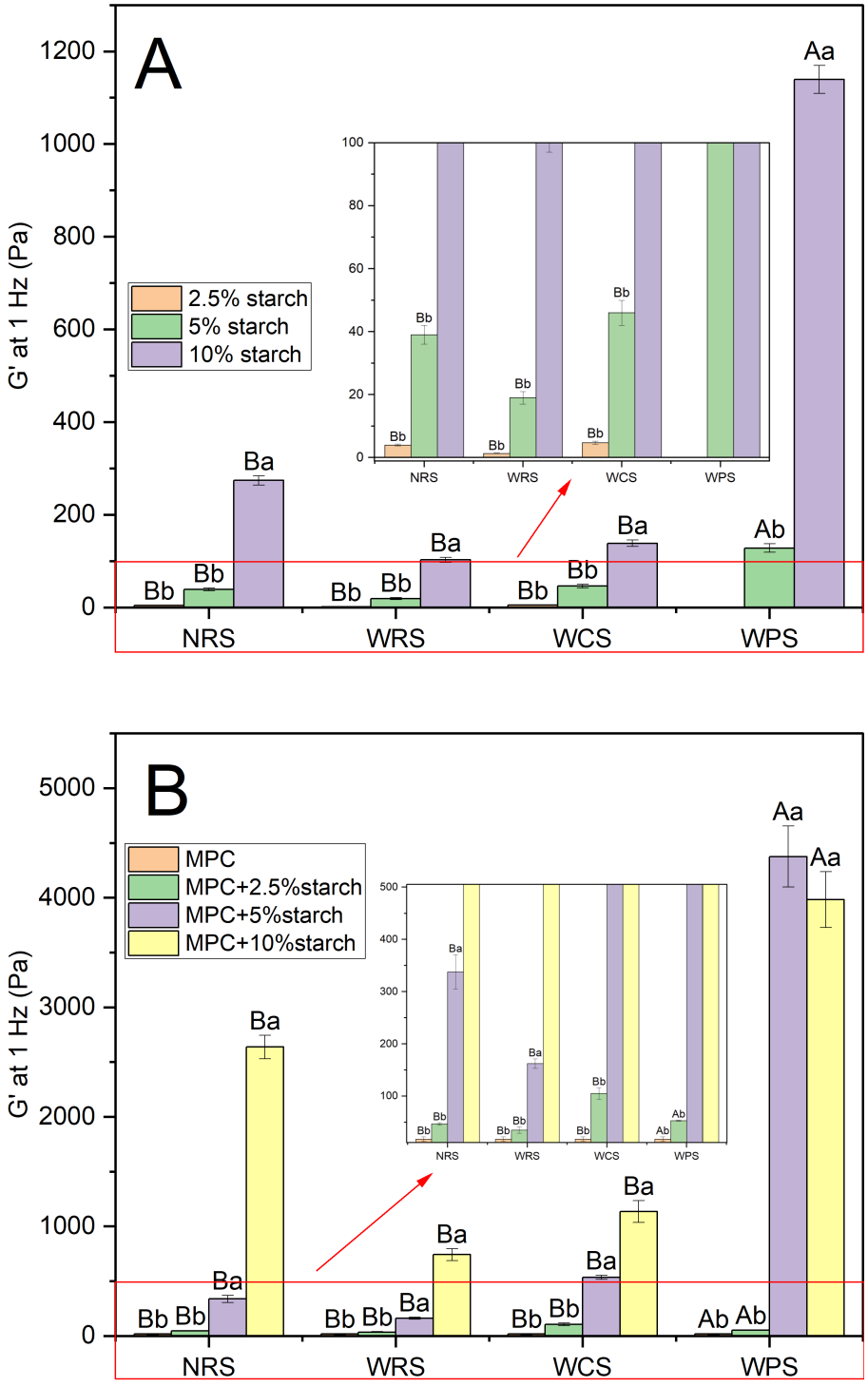


Figure 17: *G'* at 1 Hz for pure starch (A) and MPC-starch samples (B), respectively. A significant difference (P<0.05) in starch type and starch concentration is shown by different capital and lowercase letters above the columns, respectively.

The strength of MPC gels containing starches was higher than that of the control. When different concentrations (2.5%-10% w/w) of various starches (NRS, WRS, WCS, WPS)

were added into 10% w/w MPC dispersion respectively, the gel strength of all MPC-starch gels increased significantly (**Figure 17 B**). The increase in starch concentration in the protein-starch system can significantly increase the G' of MPC gels. For example, for MPC-NRS system, as the NRS concentration increased from 0 to 2.5%, 5%, and 10%, the G' of MPC-NRS gel increased from ~22.8 Pa to ~48.9 Pa, ~372.4 Pa, ~2744.3 Pa, respectively. MPC-WRS and MPC-WCS gels indicated the same trend. However, for MPC gels containing WPS, the G' of the MPC sample containing 5% WPS was the highest, with ~4654.7 Pa; but the G' decreased slightly to ~4206.8 Pa when the WPS concentration increased to 10%. The amount of starch added should be controlled to prevent it from compressing the protein matrix and destroying the gel network structure, which would reduce the gel strength (Zhang et al., 2024). WPS had a substantially greater filling impact on protein gels than other starches did, because WPS squeezed the protein matrix more strongly, so the gel strength would decrease if the WPS concentration was further raised. High-concentration WPS may compete with protein for water. WPS pasting temperature was low, swelling capacity was strong, and water was likely to gather around starch granules, thus affecting protein gelation. In the presence of 5% WPS, the water competition between protein and starch was small, and they could interact better, thus forming a stronger network structure (Luo et al., 2020). Luo et al. (2020) studied the influence of adding 0-20% potato starch on the gel performance of hairtail surimi. The strength of surimi gels improved with the increasing starch concentration, reaching the maximum value when the starch concentration was 16% and then decreased when the concentration increased to 20%. Furthermore, the type of added starches greatly influenced the gel strength of the protein-starch system. For example, when MPC-starch system contained 10% w/w starch, MPC-WPS had the highest G' at ~4654.7 Pa among all MPC-starch gels, followed by MPC-NRS at ~2744.3 Pa and MPC-WCS at ~1135 Pa, MPC-WRS showed the smallest G' at ~742.7 Pa. Compared to 10% w/w pure MPC system, G' increased ~120, ~32, ~50, ~185 times for MPC-NRS, MPC-WRS, MPC-WCS, MPC-WPS. The G' of the protein-starch mixture was much larger than the linear sum of G' of pure starch and protein at the same concentration.

Huang et al. (2024) studied the effect of 0-14% tapioca starch on the quality of *Nemipterus virgatus* surimi gels. They found that after adding 12% tapioca starch, the hardness, gel strength, WHC of surimi gels improved by ~24 N, ~17.48 N, ~89.01%, respectively. Other studies also proved that adding starches could improve the heat-induced protein gels. In a particular range, as the added starch concentration increased, the gel strength also increased compared to pure protein gels. Mi et al. (2021) added 30, 60, 90, and 120 g/kg of different kinds of corn starches into hairtail (*Trichiurus haumela*) myosin solution to prepare gels; the results indicated that the WHC and strength of myosin-corn starch gel were considerably more significant than those of pure myosin gel. When the concentration of corn starch added was higher, the gel network formed was denser, and the gel strength was larger. They concluded that adding corn starch could cause a large amount of myosin aggregation and promote the self-assembly process of myosin at low temperatures. Starch granules were filled in the myosin network, absorbed water, and swelled up to exert great squeezing pressure on the protein network during starch gelatinization, thus enhancing the gel strength. Campo and Tovar (2008) investigated the influence of the wheat starch concentration (7%, 11%, 15%) on the rheological properties of Alaska Pollock and Pacific Whiting surimi gels. They found a large growth in complex modulus G^* as the wheat starch content increased. They also concluded that the filling properties of starch led to a growth in the gel strength of surimi. When the concentration of starch in the protein-starch system was low, water could enter gel pores with great freedom and speed because the starch did not completely fill the protein gel network and gel pores were large. However, as the starch content was increased, the protein gel network containing starch became denser. This resulted in free water being trapped inside the network, which was difficult to move and converted into bound water, thereby increasing the gel strength (Luo et al., 2020).

Strain sweep measurement was used to characterize the large deformation rheological properties of MPC samples containing various starches. **Figure 16** shows G' and G'' as

a function of the strain. For all samples, they showed similar trends. G' and G'' did not change with the increasing applied strain in the low strain amplitude range, and G' was always higher than G'', showing elastic behavior. However, when the applied strain reached a critical value defined as the linear viscoelastic region, once beyond this region, G' and G'' decreased significantly, G' decreased more rapidly until G' intersected G'', the strain and stress corresponding to this point (G'=G'') were defined as the breaking strain and breaking stress, respectively. Beyond this point, G'' was greater than G', indicating that the gel structure was severely damaged and began to flow. To better compare the large deformation rheological properties of 10% MPC gels containing different starches, **Figure 18** shows the dependence between the breaking strain, breaking stress, and the addition of starches in MPC gels. The breaking strain and breaking stress increased with the increase in starch concentration, and they were dependent on the type of starch. Overall, the trend of the breaking strain and breaking stress with added starch concentration was consistent with that of G' at 1Hz with added starch concentration during the frequency sweep measurement.

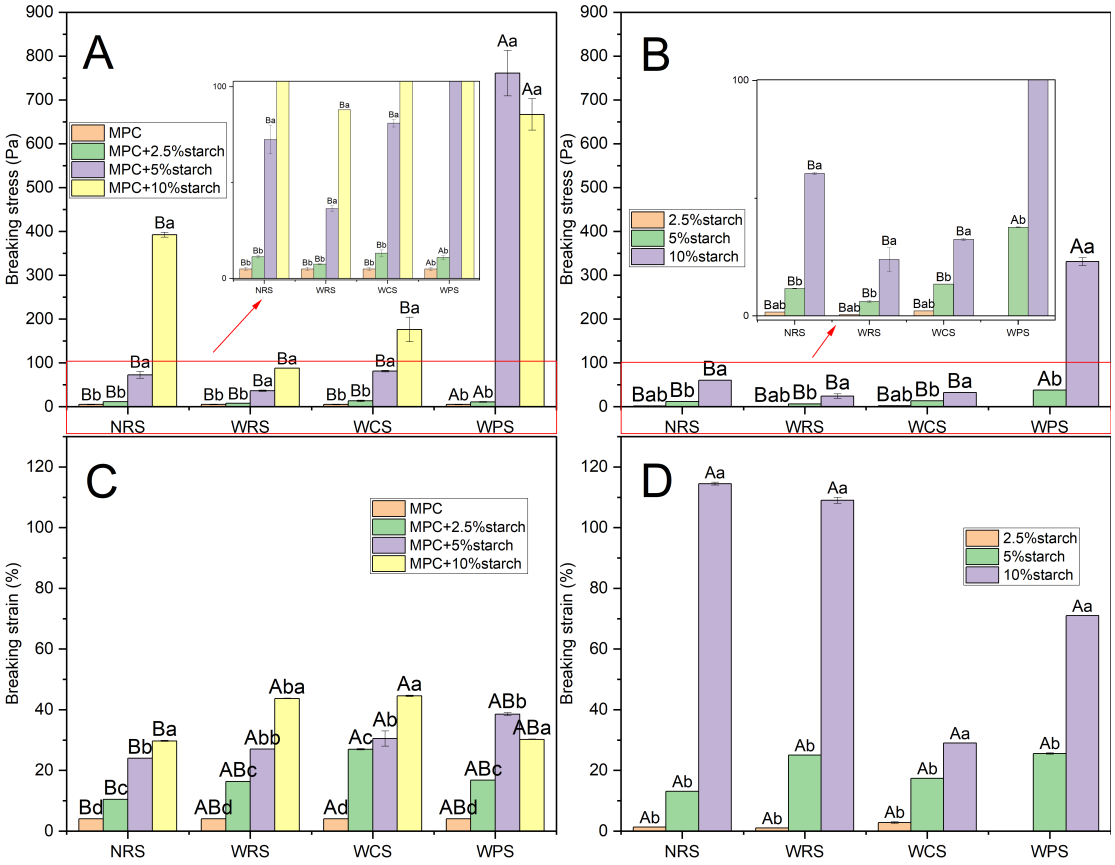


Figure 18: Breaking stress (A, B) and strain (C, D) for pure starch and MPC-starch samples, respectively. A significant difference (P<0.05) in starch type and starch concentration is shown by different capital and lowercase letters above the columns, respectively.

4.3.3. Microstructures of MPC-starch mixture as revealed by CLSM

Confocal laser scanning microscopy (CLSM) was used to observe and compare the microstructural characteristics of the starch-protein mixtures. **Figure 19** shows CLSM images of MPC suspensions containing 5% w/w different starches, including NRS, WRS, WCS, and WPS, before (sol) and after (gel) heat treatment. Proteins stained with fast green appears as green, while the starches-rich zones and voids in between the protein particles appear the dark. CLSM images indicated that 10% w/w pure MPC solution cannot form a gel after heating. Konieczny et al. (2021) studied gelation of freshwater mussel (*Sinanodonta woodiana*) protein, they thought that the protein

concentration affected significantly on the gelling property of mussel proteins. They found that 10% was the least gelation concentration for freshwater mussel, dispersions lower than 10% cannot form gels under heating conditions. In this research, 10% w/w MPC dispersion cannot form a gel after heating, which may because the concentration was lower. Gelation requires minimum protein concentration, gel formation usually requires polymerization and cross-linking between protein molecules (covalent bonds, hydrogen bonds, hydrophobic interactions). When the protein concentration is too low, the interactions between molecules are not enough to form a continuous 3D network structure (Konieczny et al., 2021). According to **Figure 19**, all MPC dispersions containing various starches formed stable and dense protein network structure gels after heating at 90 ℃ for 30 min. Although all MPC gels containing starches were observed under heating conditions, the microstructure of the formed gel networks was still different. MPC gels containing 5% w/w WPS showed the densest green areas with tiny dark voids, indicating the densest protein network structure and the most substantial gel strength. However, for MPC-NRS gel and MPC-WRS gel, the protein network structures were loose, and the void was large. When the MPC solution containing starch was heated to form a gel, the process involved protein denaturation, aggregation, and starch gelatinization. Starch granules were embedded in the protein network structure, absorbed water, expanded, and acted as a filler to squeeze the protein network structure, increasing gel strength (Mi et al., 2021).

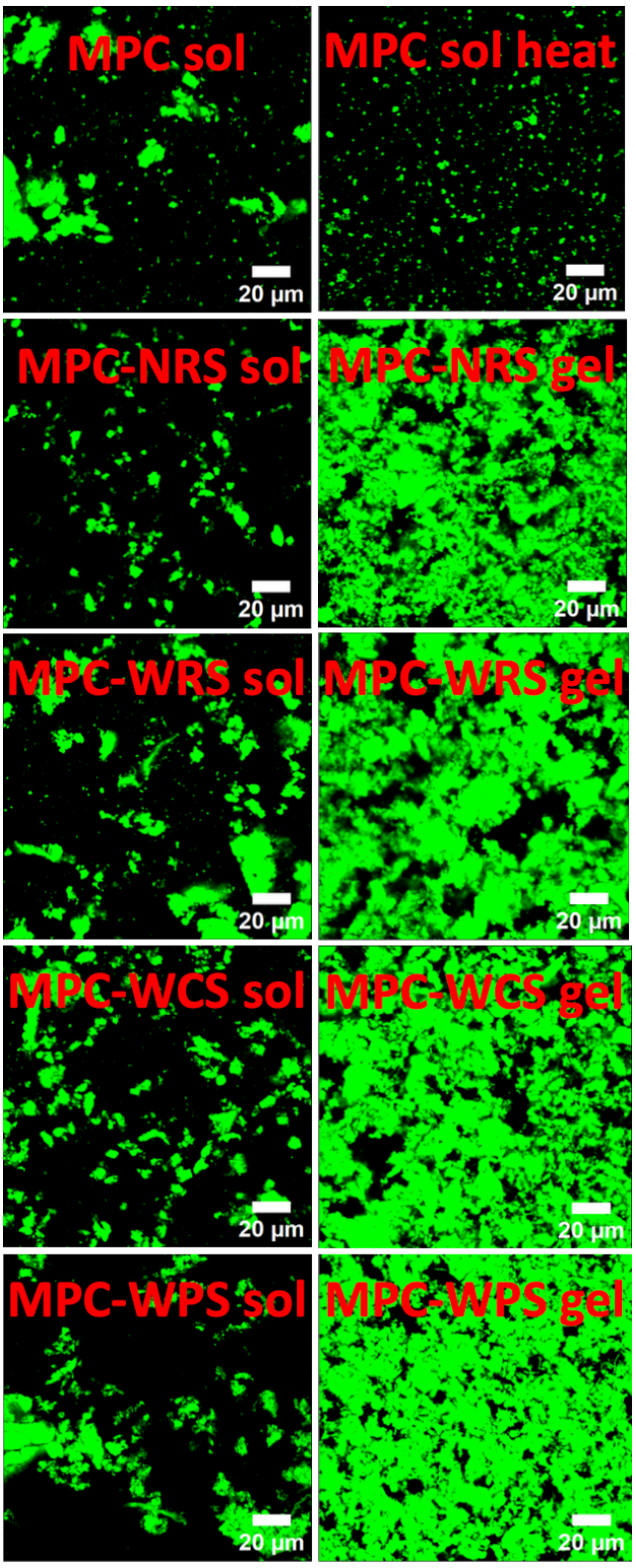


Figure 19: CLSM images of 10% w/w MPC containing 5% w/w different starches (NRS, WRS, WCS, WPS) before and after heat treatment (90 °C for 30 min).

4.4. Conclusion

This study investigated the viscoelastic properties and microstructures of 10% w/w MPC gels with varying amounts (0%-10% w/w) of different starches, such as NRS, WRS, WCS, and WPS. The addition of all types of starches greatly enhanced the strength of MPC gels, as evidenced by the increase in G' and G''. In MPC-starch gels, while starch content increased, the strength of most of the MPC gels increased except MPC-10%WPS gel slightly decreased in comparison with MPC-5%WPS gel. This can be explained by the fact that 10% w/w WPS may compress the protein matrix and destroy the gel network structure, leading to a reduction in gel strength. Furthermore, the type of starches also influenced the microstructure and strength of MPC gel. WPS significantly enhanced the strength of MPC gel. The G' of MPC-WPS gel was vastly higher than other MPC-starch gels. MPC-WPS gel appeared the densest network structure on CLSM images. Furthermore, the gels formed by a mixture of MPC and starch showed greater gel strength than the combined strength of the individual pure MPC and pure starch samples. However, there is a need for an in-depth study of the interactions between MPC and starches, and further experiments such as determining particle size and water holding capacity and conducting textural profile analysis should be carried out in future research. In summary, the study's findings could be pivotal in creating food products with optimal gel strength by utilising MPC and certain starches.

5. Chapter 5. Conclusion and future work

This study was focused on the New Zealand green-lipped mussel protein and the potential applications of the defatted residual mussel powder from its oil extraction. It is mainly divided into two parts: one is about the characterization of the physicochemical and functional properties of defatted mussel protein concentrates after desalting, and the other is about the determination of the heat-induced gel of defatted mussel protein concentrate incorporated with starch.

Desalted mussel powder was obtained by screening and filtration, centrifugation eight times, and followed with freeze-drying to remove its large particles and salt content. 5% w/w desalted MPC dispersions at different pH (3, 5, 7, 9) were treated with ultrasonication for 15 min. Protein structure, physicochemical, and functional properties were studied at different pH values before and after ultrasound treatment. SDS-PAGE results showed that ultrasound treatment and pH did not change the primary structure of desalted MPC. Sonicated MPC had smaller particle size, higher solubility, and absolute zeta potential value than untreated MPC. 10% heat-induced MPC gels were observed after heating at 90 ℃ for 30 min. Unlike the conclusion of most studies that ultrasound treatment could enhance the gel properties of proteins, this study found that ultrasound treatment reduced the gel strength of 10% MPC. Heat-induced untreated MPC gels at pH 3 and pH 9 had the highest G', at ~1291.5 Pa and ~1999.7 Pa, respectively. Emulsions cannot be stabilized by untreated MPC at all pH due to large particles and poor emulsification. Sonicated MPC could form stable O/W emulsions (oil volume fraction = 70%). Emulsion at pH 5 showed the largest oil droplets and the worst rheological property due to less net charge on the protein surface and lower solubility when close to the isoelectric point.

In addition, this project studied the effect of starch on heat-induced MPC gels. In this part, 10% w/w defatted MPC cannot form a gel after heating at 90 ℃ for 30 min.

Confocal laser scanning microscopy (CLSM) images and rheological measurements indicated that adding starch increased the strength of MPC gels. Dense 3D network structures were observed under CLSM after adding high-concentration (5%) starches. Compared to 10% MPC without starch (control), when MPC samples contained 10% starches, the G' of MPC-NRS, MPC-WRS, MPC-WCS, MPC-WPS gels increased ~120, ~32, ~50, ~185 times, respectively. MPC containing WPS showed the highest G' among all MPC-starch gels at all concentrations due to lower pasting temperature and higher swelling capacity of WPS.

According to the results of this study, the future direction is proposed as below.

- Further investigation is needed to fully understand the effect of pH and ultrasound treatment on the change of MPC structure. This study only focused on the change of the primary structure by conducting SDS-PAGE. The secondary and tertiary structure changes can be characterized by FTIR and protein surface hydrophobicity, respectively.

- This study investigated the effect of pH and ultrasound treatment on the emulsifying and gelling properties of MPC. Adding salt may change the structure and solubility of proteins, and salt ions can affect the adsorption of proteins at the oil-water interface, thus influencing the stability of emulsions. In the future, the effect of salt addition on these properties can be studied combined with pH and ultrasound treatment.

- This project studied the addition of starch to heat-induced MPC gelation and only conducted rheological measurements and CLSM to reflect the effect of starch on MPC gel properties. For a more comprehensive understanding of adding starch to heat-induced MPC gelation, future research should include measurements of the gel texture, water holding capacity, hardness, and chewability. This will provide a more complete reflection of the influence of starch on MPC gels.

- Polysaccharides like xanthan gum and guar gum may change MPC gel properties. In the future, the effects of different concentrations of xanthan gum and guar gum on heat-induced MPC gels can be studied.

- For emulsions stabilized by sonicated MPC, the effects of different oil volume fractions on the rheological properties and storage stability of emulsions at different pH can be studied.

- This study investigated the influence of ultrasound treatment on MPC dispersions. Other non-heat treatments, such as HPH, can also change the structure of proteins and improve solubility, gelation, and emulsification. HPH can be applied to change protein structures and compared with ultrasound treatment.

6. References

Abshirini, M. (2022). *Effect of New Zealand Greenshell™ mussel on osteoarthritis biomarkers and inflammation in healthy postmenopausal women : a thesis presented in partial fulfilment of the requirements for the degree of Doctor of Philosophy in Nutritional Science, School of Health Sciences, Massey University, Palmerston North, New Zealand.*

Ai, Y., & Jane, J. L. (2015). Gelatinization and rheological properties of starch. *Starch-Stärke*, *67*(3-4), 213-224.

Alberts, B. (2015). *Molecular biology of the cell* (Sixth edition ed.). Garland Science, Taylor and Francis Group.

Alfaro, A. C. (2006). Population dynamics of the green-lipped mussel, Perna canaliculus, at various spatial and temporal scales in northern New Zealand. *Journal of Experimental Marine Biology & Ecology*, *334*(2), 294-315.

Alfaro, A. C., Jeffs, A. G., & Hooker, S. H. (2001). Reproductive behavior of the green-lipped mussel, Perna canaliculus, in northern New Zealand. *Bulletin of Marine Science*, *69*(3), 1095-1108.

Amiri, A., Sharifian, P., & Soltanizadeh, N. (2018). Application of ultrasound treatment for improving the physicochemical, functional and rheological properties of myofibrillar proteins. *International Journal of Biological Macromolecules*, *111*, 139-147.

Arakawa, T., & Timasheff, S. N. (1984). Mechanism of protein salting in and salting out by divalent cation salts: balance between hydration and salt binding. *Biochemistry*, *23*(25), 5912-5923.

Bangar, S. P., Esua, O. J., Sharma, N., & Thirumdas, R. (2022). Ultrasound-assisted modification of gelation properties of proteins: A review. *Journal of Texture Studies*, *53*(6), 763-774.

Bangar, S. P., Singh, A., Ashogbon, A. O., & Bobade, H. (2023). Ball-milling: A sustainable and green approach for starch modification. *International Journal of Biological Macromolecules*, *237*, 124069.

Benjakul, S., Visessanguan, W., Ishizaki, S., & Tanaka, M. (2001). Differences in gelation characteristics of natural actomyosin from two species of bigeye snapper, Priacanthus tayenus and Priacanthus macracanthus. *Journal of Food Science*, *66*(9), 1311-1318.

Berne, B. J., & Pecora, R. (1976). *Dynamic light scattering : with applications to chemistry, biology, and physics*. Wiley.

Bhargava, N., Mor, R. S., Kumar, K., & Sharanagat, V. S. (2021). Advances in application of ultrasound in food processing: A review. *Ultrasonics sonochemistry*, *70*, 105293.

Binsi, P. K., Shamasundar, B. A., & Dileep, A. O. (2006). Some physico-chemical, functional and rheological properties of actomyosin from green mussel (Perna viridis). *Food Research International*, *39*(9), 992-1001.

Boulet, M., Britten, M., & Lamarche, F. (2000). Aggregation of some food proteins in aqueous dispersions: Effects of concentration, pH and ionic strength. *Food Hydrocolloids*, *14*(2), 135-144.

Bradford, M. M. (1976). A rapid and sensitive method for the quantitation of microgram quantities of protein utilizing the principle of protein-dye binding. *Analytical Biochemistry*, *72*(1-2), 248-254.

Breternitz, N. R., Bolini, H. M. A., & Hubinger, M. D. (2017). Sensory acceptance evaluation of a new food flavoring produced by microencapsulation of a mussel (Perna perna) protein hydrolysate. *LWT-Food Science and Technology*, *83*, 141-149.

Campana, S. E., & Moksness, E. (1991). Accuracy and precision of age and hatch date estimates from otolith microstructure examination. *ICES Journal of Marine Science*, *48*(3), 303-316.

Campo, L., & Tovar, C. (2008). Influence of the starch content in the viscoelastic properties of surimi gels. *Journal of Food Engineering*, *84*(1), 140-147.

Cano-Sarmiento, C., Téllez-Medina, D. I., Viveros-Contreras, R., Cornejo-Mazón, M., Figueroa-Hernández, C. Y., García-Armenta, E., Alamilla-Beltrán, L., García, H. S., & Gutiérrez-López, G. F. (2018). Zeta Potential of Food Matrices. *Food Engineering Reviews*, *10*(3), 113-138.

Cha, Y., Shi, X., Wu, F., Zou, H., Chang, C., Guo, Y., Yuan, M., & Yu, C. (2019). Improving the stability of oil-in-water emulsions by using mussel myofibrillar proteins and lecithin as emulsifiers and high-pressure homogenization. *Journal of Food Engineering*, *258*, 1-8.

Chen, L., Remondetto, G. E., & Subirade, M. (2006). Food protein-based materials as nutraceutical delivery systems. *Trends in Food Science & Technology*, *17*(5),

272-283.

Cui, Q., Wang, X., Wang, G., Li, R., Wang, X., Chen, S., Liu, J., & Jiang, L. (2019). Effects of ultrasonic treatment on the gel properties of microbial transglutaminase crosslinked soy, whey and soy–whey proteins. *Food Science and Biotechnology*, *28*(5), 1455-1464.

Deng, X. H., Ni, X. X., Han, J. H., Yao, W. H., Fang, Y. J., Zhu, Q., & Xu, M. F. (2023). High-intensity ultrasound modified the functional properties of Neosalanx taihuensis myofibrillar protein and improved its emulsion stability. *Ultrasonics Sonochemistry*, *97*, 106458.

Dereje, B. (2021). Composition, morphology and physicochemical properties of starches derived from indigenous Ethiopian tuber crops: A review. *International Journal of Biological Macromolecules*, *187*, 911-921.

Ding, Q., Tian, G., Wang, X., Deng, W., Mao, K., & Sang, Y. (2021). Effect of ultrasonic treatment on the structure and functional properties of mantle proteins from scallops (Patinopecten yessoensis). *Ultrasonics Sonochemistry*, *79*, 105770.

Ding, Y., Liu, R., Rong, J., Liu, Y., Zhao, S., & Xiong, S. (2012). Rheological behavior of heat-induced actomyosin gels from yellowcheek carp and grass carp. *European Food Research and Technology*, *235*, 245-251.

Dong, X., Pan, Y., Zhao, W., Huang, Y., Qu, W., Pan, J., ... & Prakash, S. (2020). Impact of microbial transglutaminase on 3D printing quality of Scomberomorus niphonius surimi. *Lwt*, *124*, 109123.

Fan, M., Hu, T., Zhao, S., Xiong, S., Xie, J., & Huang, Q. (2017). Gel characteristics and microstructure of fish myofibrillar protein/cassava starch composites. *Food Chemistry*, *218*, 221-230.

Patrignani, F., & Lanciotti, R. (2016). Applications of high and ultra high pressure homogenization for food safety. *Frontiers in Microbiology*, *7*, 1132.

Fukuda, N., Fujiura, M., Kimura, M., Nozawa, H., & Seki, N. (2006). Thermally induced gelation of paramyosin from scallop adductor muscle. *Fisheries Science*, *72*(6), 1261-1268.

Gallo, M., Ferrara, L., & Naviglio, D. (2018). Application of ultrasound in food science and technology: A perspective. *Foods*, *7*(10), 164.

Gao, X., Yongsawatdigul, J., Wu, R., You, J., Xiong, S., Du, H., & Liu, R. (2021). Effect of ultrasound pre-treatment modes on gelation properties of silver carp

surimi. *Lwt*, *150*, 111945.

Gao, Y., Fukushima, H., Deng, S., Jia, R., Osako, K., & Okazaki, E. (2018). Effect of pH and heating conditions on the properties of Alaska pollock (Theragra chalcogramma) surimi gel fortified with fish oil. *Journal of texture studies*, *49*(6), 595-603.

Gawel, J. P. F., Aldridge, D. C., & Willer, D. F. (2023). Barriers and drivers to increasing sustainable bivalve seafood consumption in a mass market economy. *Food Frontiers*, *4*(3), 1257-1269.

Gebauer, W. (2001). Protein quantitation: Bradford method. *eLS*.

Glazer, A. N., & Gould, H. (1976). *Chemical modification of proteins*. North-Holland.

Grecco Zanotti, M. A., & Gonçalves dos Santos, R. (2019). Thixotropic Behavior of Oil-in-Water Emulsions Stabilized with Ethoxylated Amines at Low Shear Rates. *Chemical Engineering and Technology*, *42*(2), 432-443.

Grienke, U., Silke, J., & Tasdemir, D. (2014). Bioactive compounds from marine mussels and their effects on human health. *Food Chemistry*, *142*, 48-60.

Grisham, D. R., & Nanda, V. (2020). Zeta potential prediction from protein structure in general aqueous electrolyte solutions. *Langmuir*, *36*(46), 13799-13803.

Grossmann, L., & McClements, D. J. (2023). Current insights into protein solubility: A review of its importance for alternative proteins. *Food Hydrocolloids*, *137*, 108416.

Gubbins, K. E. (1983). Classical thermodynamics of nonelectrolyte solutions, H. C. Van Ness and M. M. Abbott, McGraw-Hill 1982. *AIChE Journal*, *29*(2), 349.

Han, G., & Li, Y. (2024). A review of inhibition mechanisms of surimi protein hydrolysis by different exogenous additives and their application in improving surimi gel quality. *Food Chemistry*, 140002.

He, M., Zhang, M., Gao, T., Chen, L., Liu, Y., Huang, Y., ... & Li, Y. (2024). Assembly of soy protein-corn starch composite gels by thermal induction: Structure, and properties. *Food Chemistry*, *434*, 137433.

Hong, Z., Kong, Y., Guo, R., & Huang, Q. (2024). Stabilizing effect of silver carp myofibrillar protein modified by high intensity ultrasound on high internal phase emulsions: Protein denaturation, interfacial adsorption and reconfiguration. *International Journal of Biological Macromolecules*, *265*,

130896.

Hsieh, C.-F., Liu, W., Whaley, J. K., & Shi, Y.-C. (2019). Structure and functional properties of waxy starches. *Food Hydrocolloids*, *94*, 238-254.

Hu, Y., Cheng, L., Lee, S. J., & Yang, Z. (2023). Formation and characterisation of concentrated emulsion gels stabilised by faba bean protein isolate and its applications for 3D food printing. *Colloids and Surfaces A: Physicochemical and Engineering Aspects*, *671*, 131622.

Huang, X., Liu, Q., Wang, P., Song, C., Ma, H., Hong, P., & Zhou, C. (2024). Tapioca starch improves the quality of Virgatus nemipterus surimi gel by enhancing molecular interaction in the gel system. *Foods*, *13*(1), 169.

Hunt, A., Getty, K. J., & Park, J. W. (2010). Development of temperature tolerant surimi gels using starch–protein interactions. *Journal of Food Quality*, *33*, 119-136.

Hunt, A., Getty, K. J. K., & Park, J. W. (2009). Roles of Starch in Surimi Seafood: A Review. *Food Reviews International*, *25*(4), 299-312.

Jafarpour, A., & Gorczyca, E. M. (2009). Characteristics of sarcoplasmic proteins and their interaction with surimi and kamaboko gel. *Journal of Food Science*, *74*(1), N16-N22.

Jambrak, A. R., Mason, T. J., Lelas, V., Herceg, Z., & Herceg, I. L. (2008). Effect of ultrasound treatment on solubility and foaming properties of whey protein suspensions. *Journal of Food Engineering*, *86*(2), 281-287.

Janssen, S. W., Pouvreau, L., & de Vries, R. J. (2024). Commercial plant protein isolates: The effect of insoluble particles on gelation properties. *Food Hydrocolloids*, *154*, 110049.

Jayaprakash, R., & Perera, C. O. (2020). Partial purification and characterization of bioactive peptides from cooked New Zealand green-lipped mussel (Perna canaliculus) protein hydrolyzates. *Foods*, *9*(7), 879.

José, M., Leidy Indira, H.-C., Cristina, B., Lucía, S., Ester, B., & Noelia, B. (2020). High Homogenization Pressures to Improve Food Quality, Functionality and Sustainability. *Molecules*, *25*(14), 3305.

Juliano, C., Manconi, P., & Cossu, M. (2016). Characterisation of commercial Perna canaliculus samples and development of extemporaneous oral veterinary paste formulations containing Perna. *Natural Product Research*, *30*(18), 2041-2048.

Karabulut, G., Kapoor, R., Yemis, O., & Feng, H. (2024). Manothermosonication, high-pressure homogenization, and their combinations with pH-shifting improve the techno-functionality and digestibility of hemp protein. *Food Hydrocolloids*, *150*, 109661.

Khokhlov, A. R., & Osada, Y. (2002). *Polymer gels and networks*. Marcel Dekker.

Klunklin, W., & Savage, G. (2018). Addition of defatted green-lipped mussel powder and mixed spices to wheat–purple rice flour biscuits: Physicochemical, in vitro digestibility and sensory evaluation. *Food Science and Nutrition*, *6*(7), 1839-1847.

Kong, W., Zhang, T., Feng, D., Xue, Y., Wang, Y., Li, Z., Yang, W., & Xue, C. (2016). Effects of modified starches on the gel properties of Alaska Pollock surimi subjected to different temperature treatments. *Food Hydrocolloids*, *56*, 20-28.

Konieczny, P., Andrzejewski, W., Yang, T., Urbańska, M., Stangierski, J., Tomczyk, Ł., & Mikołajczak, B. (2021). Selected quality attributes of freshwater mussel powder as a promising ingredient for pet food. *Animals*, *12*(1), 90.

Konieczny, P., Tomaszewska-Gras, J., Andrzejewski, W., Mikołajczak, B., Urbańska, M., Mazurkiewicz, J., & Stangierski, J. (2016). DSC and electrophoretic studies on protein denaturation of Anodonta woodiana (Lea, 1834). *Journal of Thermal Analysis and Calorimetry: An International Forum for Thermal Studies*, *126*(1), 69-75.

Kumar, L., Brennan, M. A., Mason, S. L., Zheng, H., & Brennan, C. S. (2017). Rheological, pasting and microstructural studies of dairy protein–starch interactions and their application in extrusion-based products: A review. *Starch-Stärke*, *69*(1-2), 1600273.

Laidlaw, S. A., Grosvenor, M., & Kopple, J. D. (1990). The Taurine Content of Common Foodstuffs. *Journal of Parenteral and Enteral Nutrition*, *14*(2), 183-188.

Lam, R. S. H., & Nickerson, M. T. (2013). Food proteins: A review on their emulsifying properties using a structure–function approach. *Food Chemistry*, *141*(2), 975-984.

Leloup, V. M., Colonna, P., & Buleon, A. (1991). Influence of amylose-amylopectin ratio on gel properties. *Journal of Cereal Science*, *13*(1), 1-13.

Li, G., Li, J., & Li, D. (2010). Seasonal variation in nutrient composition of Mytilus coruscus from China. *Journal of agricultural and food chemistry*, *58*(13), 7831-

7837.

Li, J., Dai, Z., Chen, Z., Hao, Y., Wang, S., & Mao, X. (2023). Improved gelling and emulsifying properties of myofibrillar protein from frozen shrimp (Litopenaeus vannamei) by high-intensity ultrasound. *Food Hydrocolloids*, *135*, 108188.

Li, N., Zhang, K. X., Du, J. Y., Tan, Z. F., Xu, Y. P., Liu, X. Y., ... & Li, D. Y. (2022). High-intensity ultrasound improved the physicochemical and gelling properties of Litopenaeus vannamei myofibrillar protein. *Ultrasonics Sonochemistry*, *90*, 106217.

Li, Y., Zeng, Q. H., Liu, G., Chen, X., Zhu, Y., Liu, H., ... & Wang, J. J. (2020). Food-grade emulsions stabilized by marine Antarctic krill (Euphausia superba) proteins with long-term physico-chemical stability. *Lwt*, *128*, 109492.

Liaset, B., Lied, E., & Espe, M. (2000). Enzymatic hydrolysis of by-products from the fish-filleting industry; chemical characterisation and nutritional evaluation. *Journal of the Science of Food and Agriculture*, *80*(5), 581-589.

Liu, B., Wu, Y., Liang, Q. Y., & Zheng, H. (2024). Effects of high-intensity ultrasound on physicochemical and gel properties of myofibrillar proteins from the bay scallop (Argopecten irradians). *Ultrasonics Sonochemistry*, 106935.

Liu, C., Fan, L., Yang, Y., Jiang, Q., Xu, Y., & Xia, W. (2021). Characterization of surimi particles stabilized novel pickering emulsions: Effect of particles concentration, pH and NaCl levels. *Food Hydrocolloids*, *117*, 106731.

Liu, C., Zhou, H., Su, Y. C., Li, Y., & Li, J. (2009). Chemical compositions and functional properties of protein isolated from by-product of triangle shell pearl mussel hyriopsis cumingii. *Journal of Aquatic Food Product Technology*, *18*(3), 193-208.

Liu, H., Nie, Y., & Chen, H. (2014). Effect of Different Starches on Colors and Textural Properties of Surimi-Starch Gels. *International Journal of Food Properties*, *17*(7), 1439-1448.

Liu, K., Chen, Y. Y., Zha, X. Q., Li, Q. M., Pan, L. H., & Luo, J. P. (2021). Research progress on polysaccharide/protein hydrogels: Preparation method, functional property and application as delivery systems for bioactive ingredients. *Food Research International*, *147*, 110542.

Liu, X., Sun, X., Wei, Y., Ma, Y., Sun, P., & Li, X. (2022). Effects of ultrasonic treatment on physico-chemical properties and structure of tuna (Thunnus tonggol) myofibrillar proteins. *Journal of Food Composition and Analysis*, *108*, 104438.

López, J. L., Marina, A., Vázquez, J., & Alvarez, G. (2002). A proteomic approach to the study of the marine mussels Mytilus edulis and M. galloprovincialis. *Marine biology*, *141*, 217-223.

Lu, S., Chen, Y. K., Chen, J. J., Lii, C. Y., Lai, P., & Chen, H. H. (2011). Water mobility, rheological and textural properties of rice starch gel. *Journal of Cereal Science*, *53*(1), 31-36.

Lunardi, C. N., Gomes, A. J., Rocha, F. S., De Tommaso, J., & Patience, G. S. (2021). Experimental methods in chemical engineering: Zeta potential. *Canadian Journal of Chemical Engineering*, *99*(3), 627-639.

Luo, H., Guo, C., Lin, L., Si, Y., Gao, X., Xu, D., ... & Yang, W. (2020). Combined use of rheology, LF-NMR, and MRI for characterizing the gel properties of hairtail surimi with potato starch. *Food and Bioprocess Technology*, *13*, 637-647.

Luo, L., Zhang, R., Palmer, J., Hemar, Y., & Yang, Z. (2021). Impact of High Hydrostatic Pressure on the Gelation Behavior and Microstructure of Quinoa Protein Isolate Dispersions. *ACS Food Science & Technology*, *1*(11), 2144-2151.

Ma, W., Wang, J., Xu, X., Qin, L., Wu, C., & Du, M. (2019). Ultrasound treatment improved the physicochemical characteristics of cod protein and enhanced the stability of oil-in-water emulsion. *Food Research International*, *121*, 247-256.

Malek, M. N. F. A., Hussin, N. M., Embong, N. H., Bhuyar, P., Rahim, M. H. A., Govindan, N., & Maniam, G. P. (2023). Ultrasonication: a process intensification tool for methyl ester synthesis: a mini review. *Biomass Conversion and Biorefinery: Processing of Biogenic Material for Energy and Chemistry*, *13*(2), 1457-1467.

Martínez-Monteagudo, S. I., Yan, B., & Balasubramaniam, V. M. (2016). Engineering Process Characterization of High-Pressure Homogenization—from Laboratory to Industrial Scale. *Food Engineering Reviews*, 1-27.

Miller, M. R., Abshirini, M., Wolber, F. M., Tuterangiwhiu, T. R., & Kruger, M. C. (2023). Greenshell mussel products: a comprehensive review of sustainability, traditional use, and efficacy. *Sustainability*, *15*(5), 3912.

McClements, D. J. (2004). *Food emulsions: principles, practices, and techniques*. CRC press.

McGevin, L. E. (2010). *Mussels: Anatomy, habitat and environmental impact*. Nova Science.

Menut, P., Seiffert, S., Sprakel, J., & Weitz, D. A. (2012). Does size matter? Elasticity of compressed suspensions of colloidal-and granular-scale microgels. *Soft matter*, *8*(1), 156-164.

Mi, H., Liang, S., Li, Z., Yi, S., Chen, J., Li, X., & Li, J. (2021). Effect of corn starch on the structure, physicochemical and gel properties of hairtail (Trichiurus haumela) myosin. *International Journal of Food Science and Technology*, *56*(6), 2843-2852.

Miller, M. R., & Tian, H. (2018). Changes in proximate composition, lipid class and fatty acid profile in Greenshell™ mussels (Perna canaliculus) over an annual cycle. *Aquaculture Research*, *49*(3), 1153-1165.

Miller, M. R., Abshirini, M., Wolber, F. M., Tuterangiwhiu, T. R., & Kruger, M. C. (2023). Greenshell mussel products: a comprehensive review of sustainability, traditional use, and efficacy. *Sustainability*, *15*(5), 3912.

Minkyung, B., Kainat, A., & Jung-Eun, Y. (2022). Beneficial Effects of Taurine on Metabolic Parameters in Animals and Humans. *Journal of Obesity & Metabolic Syndrome*, *31*(2), 134-146.

Mirmoghtadaie, L., Shojaee Aliabadi, S., & Hosseini, S. M. (2016). Recent approaches in physical modification of protein functionality. *Food Chemistry*, *199*, 619-627.

Moshrefi, A., & Nabki, F. (2021, August). An efficient method to enhance the quality of ultrasound medical images. In *2021 IEEE International Midwest Symposium on Circuits and Systems (MWSCAS)* (pp. 267-270). IEEE.

Murphy, K. J., Mann, N. J., & Sinclair, A. J. (2003). Fatty acid and sterol composition of frozen and freeze-dried New Zealand Green Lipped Mussel (Perna canaliculus) from three sites in New Zealand. *Asia Pacific Journal of Clinical Nutrition*, *12*(1), 50-60.

Naik, A. S., & Hayes, M. (2019). Bioprocessing of mussel by-products for value added ingredients. *Trends in food science & technology*, *92*, 111-121.

Nazari, B., Mohammadifar, M. A., Shojaee-Aliabadi, S., Feizollahi, E., & Mirmoghtadaie, L. (2018). Effect of ultrasound treatments on functional properties and structure of millet protein concentrate. *Ultrasonics Sonochemistry*, *41*, 382-388.

Noisuwan, A., Wilkinson, B., Hemar, Y., & Bronlund, J. E. (2009). Dynamic rheological and microstructural properties of normal and waxy rice starch gels

containing milk protein ingredients. *Starch/Staerke*, *61*(3-4), 214-227.

Noisuwan, A., Wilkinson, B., Hemar, Y., Bronlund, J. E., & Williams, M. A. K. (2007). Viscosity, swelling and starch leaching during the early stages of pasting of normal and waxy rice starch suspensions containing different milk protein ingredients. *Starch/Staerke*, *59*(8), 379-387.

Nollet, L. M., & Toldrá, F. (Eds.). (2009). *Handbook of seafood and seafood products analysis*. CRC Press.

Noman, A., Xu, Y., Al-Bukhaiti, W. Q., Abed, S. M., Ali, A. H., Ramadhan, A. H., & Xia, W. (2018). Influence of enzymatic hydrolysis conditions on the degree of hydrolysis and functional properties of protein hydrolysate obtained from Chinese sturgeon (Acipenser sinensis) by using papain enzyme. *Process Biochemistry*, *67*, 19-28.

Oldroyd, J. G. (1953). The Elastic and Viscous Properties of Emulsions and Suspensions. *Proceedings of the Royal Society of London. Series A, Mathematical and Physical Sciences*, *218*(1132), 122-132.

Park, J. W. (2014). *Surimi and surimi seafood* (Third edition ed.). CRC Press.

Petsko, G. A., & Ringe, D. (2003). *Protein structure and function*. New Science.

Powanda, M. C., Rainsford, K. D., & Whitehouse, M. W. (2015). *Novel natural products : therapeutic effects in pain, arthritis and gastro-intestinal diseases*. Springer.

Qaderi, F., Tamadoni, A., & Banisheikholeslami, A. (2024). Cost estimation for application of ultrasonication–ozonation hybrid process in remediation of PAH-contaminated soil. *Environment, Development & Sustainability*, *26*(5), 12441-12466.

Rajasekaran, B., Singh, A., Ponnusamy, A., Patil, U., Zhang, B., Hong, H., & Benjakul, S. (2023). Ultrasound treated fish myofibrillar protein: Physicochemical properties and its stabilizing effect on shrimp oil-in-water emulsion. *Ultrasonics Sonochemistry*, *98*, 106513.

Ratnayake, W. S., & Jackson, D. S. (2008). Chapter 5 starch gelatinization. *Advances in Food & Nutrition Research*, *55*, 221-268.

Schirmer, M., Jekle, M., & Becker, T. (2015). Starch gelatinization and its complexity for analysis. *Starch-Starke*, *67*(1-2), 30-41.

Shim, J., & Mulvaney, S. J. (2001). Effect of heating temperature, pH, concentration and starch/whey protein ratio on the viscoelastic properties of corn starch/whey protein mixed gels. *Journal of the Science of Food and Agriculture*, *81*(8), 706-717.

Singh, N., Singh, J., Kaur, L., Singh Sodhi, N., & Singh Gill, B. (2003). Morphological, thermal and rheological properties of starches from different botanical sources. *Food Chemistry*, *81*(2), 219-231.

Stenton-Dozey, J. M., Heath, P., Ren, J. S., & Zamora, L. N. (2021). New Zealand aquaculture industry: research, opportunities and constraints for integrative multitrophic farming. *New Zealand Journal of Marine and Freshwater Research*, *55*(2), 265-285.

Stewart, R. J. C., Coad, J., Reynolds, G. W., & Pedley, K. C. (2012). New Zealand green-lipped mussels (Perna canaliculus) enhance non-haem iron absorption in vitro. *British Journal of Nutrition*, *108*(6), 949-952.

Strayer, D. L. (2008). *Freshwater mussel ecology: a multifactor approach to distribution and abundance*. University of California Press.

Sun, X. D., & Holley, R. A. (2011). Factors influencing gel formation by myofibrillar proteins in muscle foods. *Comprehensive reviews in food science and food safety*, *10*(1), 33-51.

Surasani, V. K. R., Mandal, A., & Pandey, A. (2018). Utilization of freshwater mussel (Lamellidens marginalis) for the isolation of proteins through pH shift processing: characterization of isolates. *Environmental Science and Pollution Research*, *25*(31), 31497-31507.

Surh, J., Decker, E. A., & McClements, D. J. (2006). Properties and stability of oil-in-water emulsions stabilized by fish gelatin. *Food Hydrocolloids*, *20*(5), 596-606.

Tadpitchayangkoon, P., Yongsawatdigul, J., & Park, J. W. (2010). Conformational changes and dynamic rheological properties of fish sarcoplasmic proteins treated at various pHs. *Food Chemistry*, *121*(4), 1046-1052.

Tako, M., & Hizukuri, S. (2002). Gelatinization mechanism of potato starch. *Carbohydrate Polymers*, *48*(4), 397-401.

Tang, C.-H. (2007). Functional properties and in vitro digestibility of buckwheat protein products: Influence of processing. *Journal of Food Engineering*, *82*(4), 568-576.

Tao, Y., & Sun, D. W. (2015). Enhancement of food processes by ultrasound: a

review. *Critical reviews in food science and nutrition*, *55*(4), 570-594.

Thawornchinsombut, S., & Park, J. W. (2004). Role of pH in solubility and conformational changes of Pacific whiting muscle proteins. *Journal of Food Biochemistry*, *28*(2), 135-154.

Trivedi, D. (2006). *Effect of starch addition on rheological properties of processed cheese : a thesis presented in partial fulfilment of the requirements for the degree of Master of Technology in Food Technology at Massey University, Palmerston North, New Zealand*.

Ulbricht, C., Chao, W., Costa, D., Nguyen, Y., Seamon, E., & Weissner, W. (2009). An evidence-based systematic review of green-lipped mussel (Perna canaliculus) by the Natural Standard Research Collaboration. *Journal of Dietary Supplements*, *6*(1), 54-90.

Vareltzis, P. K., & Undeland, I. (2012). Protein isolation from blue mussels (Mytilus edulis) using an acid and alkaline solubilisation technique-process characteristics and functionality of the isolates. *Journal of the Science of Food and Agriculture*, *92*(15), 3055-3064.

Viacheslav, K. (2012). *Scanning Electron Microscopy*. InTech.

Vijaykrishnaraj, M., Bharath Kumar, S., & Prabhasankar, P. (2015). Green mussel (Perna canaliculus) as a marine ingredient to enrich gluten free pasta: product quality, microstructure and biofunctional evaluation. *Journal of Food Measurement and Characterization*, *9*(1), 76-85.

Vijaykrishnaraj, M., Roopa, B. S., & Prabhasankar, P. (2016). Preparation of gluten free bread enriched with green mussel (Perna canaliculus) protein hydrolysates and characterization of peptides responsible for mussel flavour. *Food Chemistry*, *211*, 715-725.

Wang, W., & Roberts, C. J. (2018). Protein aggregation - Mechanisms, detection, and control. *International Journal of Pharmaceutics*, *550*(1-2), 251-268.

Wang, Z., Chang, S., Li, Y., Kong, L., Wu, D., Qin, L., Yu, C., Wu, C., & Du, M. (2018). Effects of ball milling treatment on physicochemical properties and digestibility of Pacific oyster (Crassostrea gigas) protein powder. *Food Science and Nutrition*, *6*(6), 1582-1590.

Wen, Q. H., Tu, Z. C., Zhang, L., Wang, H., & Chang, H. X. (2017). Effect of high intensity ultrasound on the gel and structural properties of Ctenopharyngodon idellus myofibrillar protein. *Journal of food biochemistry*, *41*(1), e12288.

Wu, Shi, X., Zou, H., Zhang, T., Dong, X., Zhu, R., & Yu, C. (2019). Effects of high-pressure homogenization on physicochemical, rheological and emulsifying properties of myofibrillar protein. *Journal of Food Engineering*, *263*, 272-279.

Wu, G. (2013). Functional amino acids in nutrition and health. *Amino Acids: The Forum for Amino Acid, Peptide and Protein Research*, *45*(3), 407-411.

Wu, M., Wang, J., Hu, J., Li, Z., Liu, R., Liu, Y., Cao, Y., Ge, Q., & Yu, H. (2020). Effect of typical starch on the rheological properties and NMR characterization of myofibrillar protein gel. *Journal of the Science of Food and Agriculture*, *100*(1), 258-267.

Wu, M. C., Lanier, T. C., & Hamann, D. D. (1985). Thermal Transitions of Admixed Starch/Fish Protein Systems During Heating. *Journal of Food Science*, *50*(1), 20-25.

Wu, Y., Xiang, H., Chen, S., Zhao, Y., Cai, Q., Lin, W., ... & Wang, Y. (2023). Characterization of the aggregation behavior of sea bass (Lateolabrax japonicus) myofibrillar proteins mediated by different ionic strengths: protein structures, gel properties, and emulsion stabilities. *LWT*, *189*, 115483.

Xie, D., Tang, Y., & Dong, G. (2024). Various factors affecting the gel properties of surimi: A review. *Journal of Texture Studies*, *55*(3), e12847.

Xue, S., Xu, X., Shan, H., Wang, H., Yang, J., & Zhou, G. (2018). Effects of high-intensity ultrasound, high-pressure processing, and high-pressure homogenization on the physicochemical and functional properties of myofibrillar proteins. *Innovative Food Science and Emerging Technologies*, *45*, 354-360.

Yada, R. Y. (2018). *Proteins in food processing* (Second edition ed.). Woodhead Publishing.

Yan, H., Zou, H., Li, S., Sun, S., Xu, Q., & Yu, C. (2022). Modification of functional properties of mussel actomyosin by ultrasound treatment and the appplication at O/W emulsion. *Lwt*, *170*, 114086.

Yang, X., Li, A., Li, D., Guo, Y., & Sun, L. (2021). Applications of mixed polysaccharide-protein systems in fabricating multi-structures of binary food gels—A review. *Trends in Food Science & Technology*, *109*, 197-210.

Yang, Z., & Cheng, L. (2024). Impact of ultrasound emulsification on the physicochemical properties of emulsions stabilised by quinoa protein isolates at

different pHs. *Food Biophysics*, *19*(1), 160-171.

Yang, Z., de Campo, L., Gilbert, E. P., Knott, R., Cheng, L., Storer, B., ... & Hemar, Y. (2022). Effect of NaCl and CaCl2 concentration on the rheological and structural characteristics of thermally-induced quinoa protein gels. *Food Hydrocolloids*, *124*, 107350.

Yu, C., Cha, Y., Wu, F., Fan, W., Xu, X., & Du, M. (2018). Effects of ball-milling treatment on mussel (Mytilus edulis) protein: structure, functional properties and in vitro digestibility. *International Journal of Food Science and Technology*, *53*(3), 683-691.

Yu, C., Cha, Y., Wu, F., Xu, X., Qin, Y., Li, X., & Du, M. (2018). Effects of high-pressure homogenisation on structural and functional properties of mussel (Mytilus edulis) protein isolate. *International Journal of Food Science and Technology*, *53*(5), 1157-1165.

Yu, C., Li, S., Sun, S., Yan, H., & Zou, H. (2022). Modification of emulsifying properties of mussel myofibrillar proteins by high-intensity ultrasonication treatment and the stability of O/W emulsion. *Colloids and Surfaces A: Physicochemical and Engineering Aspects*, *641*, 128511.

Yu, C., Sun, S., Li, S., Yan, H., & Zou, H. (2022). Scallops as a new source of food protein: high-intensity ultrasonication improved stability of oil-in-water emulsion stabilised by myofibrillar protein. *International Journal of Food Science and Technology*, *57*(2), 1173-1185.

Yu, C., Wu, F., Cha, Y., Qin, Y., & Du, M. (2018). Effects of ultrasound on structure and functional properties of mussel (Mytilus edulis) protein isolates. *Journal of Food Processing and Preservation*, *42*(8).

Zhang, C., Liu, H., Xia, X., Sun, F., & Kong, B. (2021). Effect of ultrasound-assisted immersion thawing on emulsifying and gelling properties of chicken myofibrillar protein. *Lwt*, *142*, 111016.

Zhang, H., Xia, W. S., Xu, Y. S., Jiang, Q. X., Wang, C. X., & Wang, W. J. (2013). Effects of spray-drying operational parameters on the quality of freshwater mussel powder. *Food and Bioproducts Processing*, *91*(3), 242-248.

Zhang, S., Zhang, L., Yin, T., You, J., Liu, R., Wang, L., Huang, Q., Wang, W., & Ma, H. (2024). Exploring the versatility of carbohydrates in surimi and surimi products: novel applications and future perspectives. *Journal of the Science of Food & Agriculture*, *104*(4), 1874-1883.

Zhang, T., Chen, S., Xu, X., Zhuang, X., Chen, Y., Xue, Y., ... & Jiang, N. (2023). Effects of konjac glucomannan on physical properties and microstructure of fish myofibrillar protein gel: Phase behaviours involved. *Food Hydrocolloids*, *134*, 108034.

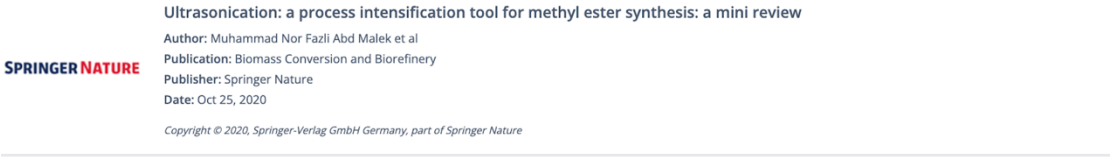
Zhang, Y., & Chang, S. K. (2023). Microbial transglutaminase cross-linking enhances the textural and rheological properties of the surimi-like gels made from alkali-extracted protein isolate from catfish byproducts and the role of disulfide bonds in gelling. *Foods*, *12*(10), 2029.

Zhao, Q., Xiong, H., Selomulya, C., Chen, X. D., Huang, S., Ruan, X., Zhou, Q., & Sun, W. (2013). Effects of Spray Drying and Freeze Drying on the Properties of Protein Isolate from Rice Dreg Protein. *Food and Bioprocess Technology: An International Journal*, *6*(7), 1759-1769.

Zou, H., Zhao, N., Sun, S., Dong, X., & Yu, C. (2020). High-intensity ultrasonication treatment improved physicochemical and functional properties of mussel sarcoplasmic proteins and enhanced the stability of oil-in-water emulsion. *Colloids and Surfaces A: Physicochemical and Engineering Aspects*, *589*, 124463.

Zou, Y., Lu, F., Yang, B., Ma, J., Yang, J., Li, C., Wang, X., Wang, D., & Xu, W. (2021). Effect of ultrasound assisted konjac glucomannan treatment on properties of chicken plasma protein gelation. *Ultrasonics Sonochemistry*, *80*, 105821.

7. Appendices



Ultrasonication: a process intensification tool for methyl ester synthesis: a mini review

Author: Muhammad Nor Fazli Abd Malek et al
Publication: Biomass Conversion and Biorefinery
Publisher: Springer Nature
Date: Oct 25, 2020

Copyright © 2020, Springer-Verlag GmbH Germany, part of Springer Nature

Order Completed

Thank you for your order.

This Agreement between Jingying Lin ("You") and Springer Nature ("Springer Nature") consists of your order details and the terms and conditions provided by Springer Nature and Copyright Clearance Center.

License number	Reference confirmation email for license number
License date	Jul 28, 2024

Licensed Content

Licensed Content Publisher	Springer Nature
Licensed Content Publication	Biomass Conversion and Biorefinery
Licensed Content Title	Ultrasonication: a process intensification tool for methyl ester synthesis: a mini review
Licensed Content Author	Muhammad Nor Fazli Abd Malek et al
Licensed Content Date	Oct 25, 2020

About Your Work

Title of new work	A study on the physicochemical properties of defatted New Zealand green-lipped mussel protein concentrates (MPC) dispersions
Institution name	Massey University
Expected presentation date	Jul 2024

Requestor Location

Requestor Location	Jingying Lin Massey University Auckland, 0632 New Zealand Attn: Jingying Lin

Billing Information

Billing Type	Invoice
Billing address	Jingying Lin Massey University Auckland, New Zealand 0632 Attn: Jingying Lin

Order Details

Type of Use	Thesis/Dissertation
Requestor type	academic/university or research institute
Format	print and electronic
Portion	figures/tables/illustrations
Number of figures/tables/illustrations	1
Will you be translating?	no
Circulation/distribution	500 - 999
Author of this Springer Nature content	no

Additional Data

Portions	Figure 4 (probe ultrasonicator)
The Requesting Person / Organization to Appear on the License	Jingying Lin

Tax Details



Various factors affecting the gel properties of surimi: A review

Author: Gua Dong, Yu Tang, Dongfei Xie
Publication: Journal of Texture Studies
Publisher: John Wiley and Sons
Date: Jun 25, 2024

© 2024 Wiley Periodicals LLC.

Order Completed

Thank you for your order.

This Agreement between Jingying Lin ("You") and John Wiley and Sons ("John Wiley and Sons") consists of your license details and the terms and conditions provided by John Wiley and Sons and Copyright Clearance Center.

Your confirmation email will contain your order number for future reference.

License Number	5837560226783
License date	Jul 28, 2024

Licensed Content

Licensed Content Publisher	John Wiley and Sons
Licensed Content Publication	Journal of Texture Studies
Licensed Content Title	Various factors affecting the gel properties of surimi: A review
Licensed Content Author	Gua Dong, Yu Tang, Dongfei Xie
Licensed Content Date	Jun 25, 2024
Licensed Content Volume	55
Licensed Content Issue	3
Licensed Content Pages	10

About Your Work

Title of new work	A study on the physicochemical properties of defatted New Zealand green-lipped mussel protein concentrates (MPC) dispersions
Institution name	Massey University
Expected presentation date	Jul 2024

Requestor Location

Requestor Location	Jingying Lin Massey University Auckland, 0632 New Zealand Attn: Jingying Lin

Order Details

Type of use	Dissertation/Thesis
Requestor type	University/Academic
Format	Print and electronic
Portion	Figure/table
Number of figures/tables	1
Will you be translating?	No

Additional Data

Portions	Figure 2
The Requesting Person / Organization to Appear on the License	Jingying Lin

Tax Details

Publisher Tax ID	EU826007151